

AERODYNAMIC PARAMETER ESTIMATION USING FLIGHT TEST
DATA

A THESIS SUBMITTED TO
THE GRADUATE SCHOOL OF NATURAL AND APPLIED SCIENCES
OF
MIDDLE EAST TECHNICAL UNIVERSITY

BY

ÜMİT KUTLUAY

IN PARTIAL FULLFILLMENT OF THE REQUIREMENTS
FOR
THE DEGREE OF DOCTOR OF PHILOSOPHY
IN
MECHANICAL ENGINEERING

SEPTEMBER 2011

Approval of the thesis:

**AERODYNAMIC PARAMETER ESTIMATION USING FLIGHT
TEST DATA**

submitted by **ÜMIT KUTLUAY** in partial fulfillment of the requirements for the degree of **Doctor of Philosophy in Mechanical Engineering Department, Middle East Technical University** by,

Prof. Dr. Canan Özgen
Dean, Graduate School of **Natural and Applied Sciences** _____

Prof. Dr. Suha Oral
Head of Department, **Mechanical Engineering** _____

Prof. Dr. Bülent E. Platin
Supervisor, **Mechanical Engineering Dept., METU** _____

Dr. Gökmen Mahmutyazıcıoğlu
Co-Supervisor, **TÜBİTAK - SAGE** _____

Examining Committee Members:

Prof. Dr. M. Kemal Özgören
Mechanical Engineering Dept., METU _____

Prof. Dr. Bülent E. Platin
Mechanical Engineering Dept., METU _____

Prof. Dr. Serkan Özgen
Aerospace Engineering Dept., METU _____

Asst. Prof. Dr. Yakup Özkazanç
Electrical and Electronics Engineering Dept.,
Hacettepe University _____

Asst. Prof. Dr. Yiğit Yazıcıoğlu
Mechanical Engineering Dept., METU _____

Date: 16.09.2011

I hereby declare that all information in this document has been obtained and presented in accordance with academic rules and ethical conduct. I also declare that, as required by these rules and conduct, I have fully cited and referenced all material and results that are not original to this work.

Name, Last Name: Ümit KUTLUAY

Signature :

ABSTRACT

AERODYNAMIC PARAMETER ESTIMATION USING FLIGHT TEST DATA

Kutluay, Ümit

Ph.D., Department of Mechanical Engineering

Supervisor: Prof. Dr. Bülent E. Platin

Co-Supervisor: Dr. Gökmen Mahmutyazıcıoğlu

September 2011, 205 pages

This doctoral study aims to develop a methodology for use in determining aerodynamic models and parameters from actual flight test data for different types of autonomous flight vehicles.

The stepwise regression method and equation error method are utilized for the aerodynamic model identification and parameter estimation.

A closed loop aerodynamic parameter estimation approach is also applied in this study which can be used to fine tune the model

parameters. Genetic algorithm is used as the optimization kernel for this purpose. In the optimization scheme, an input error cost function is used together with a final position penalty as opposed to widely utilized output error cost function.

Available methods in the literature are developed for and mostly applied to the aerodynamic system identification problem of piloted aircraft; a very limited number of studies on autonomous vehicles are available in the open literature. This doctoral study shows the applicability of the existing methods to aerodynamic model identification and parameter estimation problem of autonomous vehicles. Also practical considerations for the application of model structure determination methods to autonomous vehicles are not well defined in the literature and this study serves as a guide to these considerations.

Keywords: System identification, parameter estimation, aerodynamics, aerodynamic model, equation error method, stepwise regression, closed loop optimization, genetic algorithm, flight test, flight test data.

ÖZ

UÇUŞ TEST VERİLERİNİ KULLANARAK AERODİNAMİK PARAMETRE KESTİRİMİ

Kutluay, Ümit

Doktora, Makina Mühendisliği Bölümü

Tez Yöneticisi : Prof. Dr. Bülent E. Platin

Ortak Tez Yöneticisi: Dr. Gökmen Mahmutyazıcıoğlu

Eylül 2011, 205 Sayfa

Bu doktora çalışmasının amacı, otonom uçuş araçları için aerodinamik model belirlenmesi ve parametre kestiriminde kullanılacak bir yöntem ortaya koymaktır.

Aerodinamik model tanınması ve parametre kestirimi için, adımsal bağlanım ve denklem hatası yöntemleri kullanılmaktadır.

Bu çalışmada ayrıca kapalı döngüde aerodinamik parametre kestirimi yapmak amaçlı bir yaklaşım da denenmiştir. Bu yaklaşım ile aerodinamik model parametrelerinin değerlerine ince ayar yapmak mümkün olacaktır. Yaklaşımın eniyileme yöntemi olarak genetik algoritma kullanılmaktadır. Eniyileme döngüsünde bedel

fonksiyonu olarak, literatürde çoğunlukla kullanılan çıktı hatası yerine, son konum cezası ile birlikte giridi hatası kullanılmaktadır.

Literatürde halihazırda kullanılan yöntemler, pilotlu uçakların aerodinamik sistem tanılması probleminin çözümü için geliştirilmişlerdir; otonom uçuş araçları üzerinde yapılan uygulamalara ilişkin açık kaynaklardaki referanslar kısıtlıdır. Bu doktora çalışmasında, halihazırdaki yöntemlerin otonom araçların aerodinamik model tanılması ve parametre kestirimi probleminin çözümünde kullanılabileceği gösterilmiştir. Ayrıca, aerodinamik model tanılması ve parametre kestirimi yöntemlerinin otonom uçuş araçlarına uygulanması konularında literatürde yeterince inceleme yapılmadığı görüldüğünden, bu doktora çalışması bir rehber olmayı amaçlamaktadır.

Anahtar Kelimeler: Sistem tanılama, parametre kestirimi, aerodinamik, aerodinamik model, denklem hatası yöntemi, adımsal bağlanım, kapalı döngüde eniyileme, genetik algoritma, uçuş testi, uçuş test verisi.

To all who has ever taught me...

ACKNOWLEDGEMENTS

Completion of this study could not been possible without the help, support, patience, and understanding of many people that I respect, care about, and love.

First of all, it is my debt of gratitude to acknowledge my supervisor, Prof. Dr. Bülent E. Platin, whose belief in me was the biggest motivation of all during the course of this study. I am forever grateful for his patience, guidance and understanding.

I would like to extend my deepest acknowledgments to my co-supervisor Dr. Gökmen Mahmutyazıcıođlu, who has been more than a guide and mentor for me for the past 10 years. I have always felt his support and belief in me during the entire course of my graduate studies and professional career.

This study was supported by TÜBİTAK – SAGE. I firmly believe that, if it was not for them, I would not be the engineer that I am today. I would like to acknowledge my division chief and my dear friend Mrs. Sevsay Aytar Ortaç for supporting my decision to pursue a doctoral degree and standing by me whenever I needed. My group coordinator Mr. Koray Dayanç is also acknowledged for his support during this study. My special thanks go to my colleagues and friends Mr. İbrahim Murat Karbancıođlu for his discussions on the subject,

and Mr. Şamil Korkmaz for his support on Matlab and Simulink and also for his ideas about the philosophy of engineering. I would like to extend my thanks to my dear friends and colleagues Dr. Umut Durak and Dr. Emrah Tufan, with whom we have “suffered” from academia together during the “best years of our lives”.

I would like to thank to the thesis committee members Prof. Dr. M. Kemal Özgören and Prof. Dr. Serkan Özgen, for their invaluable comments and discussions during thesis review meetings.

I would like to acknowledge my first grade teacher Mrs. Firuze Yaman, who set me up into this road some 26 years ago. I am also grateful to all my teachers and professors and I am forever proud to be a member of Middle East Technical University, where I learned to think and speak freely, to ask questions and to strive for the better.

I am as always grateful to my mother Ümran Kutluay and my father Mehmet Kamil Kutluay. I would also like to express my gratitude to my dear brother Emir Kutluay. My grandmother Emine Tüfekçi, my aunt Ülker Gürman and my mother in-law Fatma Tiryaki are acknowledged for their support, good wishes and prayers. I am thankful to all my family members, who tolerated my endless complaints about how busy I was and still stood by me.

My dear wife Kadriye Kutluay, who sometimes had to cope with one of the grumpiest man on earth, gets the deepest gratitude for her love and support. I am grateful to her for being together with me during this adventure.

TABLE OF CONTENTS

ABSTRACT	iv
ÖZ	vi
ACKNOWLEDGEMENTS	ix
TABLE OF CONTENTS	xii
LIST OF TABLES	xv
LIST OF FIGURES.....	xvii
NOMENCLATURE AND LIST OF SYMBOLS	xxii
CHAPTERS	
1. AN OVERVIEW OF SYSTEM IDENTIFICATION AND PARAMETER ESTIMATION IN AEROSPACE APPLICATIONS	1
1.1 Problem Definition	4
1.2 State of the Art in System Identification and Parameter Estimation for Aerospace Applications.....	6
1.3 Scope, Originality and Contributions of the Doctoral Study.....	11
2. AERODYNAMIC MODELING.....	14
3. MODEL STRUCTURE DETERMINATION	27
3.1 Stepwise Regression	28
3.2 Equation Error Method	34

3.3	Delta Coefficient Approach to Model Structure Determination	37
3.4	Practical Considerations for Model Structure Determination of Autonomous Flight Vehicles	40
3.4.1	Flight Test Data Processing and Dealing with Low Quality Flight Test Data	40
3.4.2	Complexity of the Model, Selection and Automated Generation of Regressors/Parameters.....	55
3.4.3	Selection of Run Parameters and Stopping Rules	59
3.4.4	Compensating for Non-Standard Conditions of Flight Test	67
4.	CLOSED LOOP AERODYNAMIC PARAMETER ESTIMATION USING GENETIC ALGORITHM	76
4.1	Output Error Method	76
4.2	Closed Loop Optimization to Minimize Control Input Errors	80
4.3	Run Parameters and Cost Function	83
5.	TEST CASES.....	90
5.1	Test Cases for Model Structure Determination	90
5.1.1	Simulated Flight Test Data for Guided FV.....	92
5.1.2	Simulated Flight Test Data for Guided FV with Maneuvers	104
5.1.3	Actual Flight Test Data for Guided FV	116
5.1.4	Actual Flight Test Data for Freefall Separation Model	133
5.2	Test Cases for Closed Loop Parameter Estimation	146
5.2.1	Simulated Flight Test Data for Guided FV.....	146

5.2.2	Simulated Flight Test Data for Guided FV with Maneuvers	157
5.2.3	Actual Flight Test Data for Guided FV	172
6.	DISCUSSION, CONCLUSION AND FUTURE WORK.....	193
	REFERENCES.....	198
	CURRICULUM VITAE.....	202

LIST OF TABLES

TABLES

Table 1. Aerodynamic coefficients and associated flight variables	56
Table 2. Original aerodynamic model of the guided FV (forces) ..	95
Table 3. Original aerodynamic model of the guided FV (moments)	95
Table 4. Identified model and parameter estimates for C_x	97
Table 5. Identified model and parameter estimates for C_y	97
Table 6. Identified model and parameter estimates for C_z	97
Table 7. Identified model and parameter estimates for C_l	98
Table 8. Identified model and parameter estimates for C_n	98
Table 9. Identified model and parameter estimates for C_x	108
Table 10. Identified model and parameter estimates for C_y	108
Table 11. Identified model and parameter estimates for C_z	108
Table 12. Identified model and parameter estimates for C_l	108
Table 13. Identified model and parameter estimates for C_m	109
Table 14. Identified model and parameter estimates for C_n	109
Table 15. Identified model and parameter estimates for C_x	125
Table 16. Identified model and parameter estimates for C_y	125
Table 17. Identified model and parameter estimates for C_z	125
Table 18. Identified model and parameter estimates for C_l	126

Table 19. Identified model and parameter estimates for C_m	126
Table 20. Identified model and parameter estimates for C_n	126
Table 21. Identified model and parameter estimates for C_x	136
Table 22. Identified model and parameter estimates for C_y	137
Table 23. Identified model and parameter estimates for C_z	137
Table 24. Identified model and parameter estimates for C_l	138
Table 25. Identified model and parameter estimates for C_m	138
Table 26. Identified model and parameter estimates for C_n	139
Table 27. Selected dominant parameters for attempt 2.....	184
Table 28. Estimated values for dominant parameters C_x	190
Table 29. Estimated values for dominant parameters C_y	190
Table 30. Estimated values for dominant parameters C_z	191
Table 31. Estimated values for dominant parameters C_l	191
Table 32. Estimated values for dominant parameters C_m	192
Table 33. Estimated values for dominant parameters C_n	192

LIST OF FIGURES

FIGURES

Figure 1. PSD for longitudinal motion (pitching)	43
Figure 2. PSD for lateral motion (rolling).....	44
Figure 3. Typical flight test maneuver data, [20].....	46
Figure 4. Flight test data for an autonomous flight vehicle (4 different flights).....	48
Figure 5. Augmented FTD for an autonomous flight vehicle.	50
Figure 6. Fourier sine series coefficients plotted versus frequency	52
Figure 7. Rolling rate – smoothed, original signal and noise estimate	54
Figure 8. Flow chart of automated regressor generation.....	59
Figure 9. Comparison of different search window selecting functions and scale factors	62
Figure 10. Flow chart of model structure determination and parameter estimation	66
Figure 11. 3d view of Karapınar Proving Ground wind conditions during test run H32_s8_a2.....	70
Figure 12. Body rates with and without correction for meteorological conditions.....	72
Figure 13. Cartesian velocities with and without correction for meteorological conditions.....	73
Figure 14. Flight angles with and without correction for meteorological conditions.....	74

Figure 15. Total velocity, Mach number and dynamic pressure with and without correction for meteorological conditions	75
Figure 16. Flowchart of Output Error Method	79
Figure 17. Flowchart of the Proposed Estimation Method	81
Figure 18. Simulated flight test data 1 flight parameters	93
Figure 19. Simulated flight test data 1 rates	94
Figure 20. Estimated response vs data - C_x	99
Figure 21. Estimated response vs data - C_y	100
Figure 22. Estimated response vs data - C_z	101
Figure 23. Estimated response vs data - C_l	102
Figure 24. Estimated response vs data - C_n	103
Figure 25. Simulated flight test data 2 flight parameters	105
Figure 26. Simulated flight test data 2 rates	106
Figure 27. Estimated response vs data - C_x	110
Figure 28. Estimated response vs data - C_y	111
Figure 29. Estimated response vs data - C_z	112
Figure 30. Estimated response vs data - C_l	113
Figure 31. Estimated response vs data - C_m	114
Figure 32. Estimated response vs data - C_n	115
Figure 33. Actual flight test data 1 flight parameters	117
Figure 34. Actual flight test data 1 rates	118
Figure 35. Difference of in-flight aerodynamics from the database (with respect to angle of attack)	119
Figure 36. Difference of in-flight aerodynamics from the database (with respect to angle of sideslip)	120

Figure 37. PSD Estimates for the in-flight aerodynamics	122
Figure 38. PSD Estimates for the delta aerodynamics	123
Figure 39. Estimated response vs data - C_x	127
Figure 40. Estimated response vs data - C_y	128
Figure 41. Estimated response vs data - C_z	129
Figure 42. Estimated response vs data - C_l	130
Figure 43. Estimated response vs data - C_m	131
Figure 44. Estimated response vs data - C_n	132
Figure 45. Actual flight test data 4 flight parameters	134
Figure 46. Actual flight test data 4 rates	135
Figure 47. Estimated response vs data - C_x	140
Figure 48. Estimated response vs data - C_y	141
Figure 49. Estimated response vs data - C_z	142
Figure 50. Estimated response vs data - C_l	143
Figure 51. Estimated response vs data - C_m	144
Figure 52. Estimated response vs data - C_n	145
Figure 53. Deflections for test case 1	147
Figure 54. Flight parameters for test case 1	148
Figure 55. Rates for test case 1	149
Figure 56. Estimation result for C_x - test case 1	151
Figure 57. Estimation result for C_y - test case 1	152
Figure 58. Estimation result for C_z - test case 1	153
Figure 59. Estimation result for C_l - test case 1	154
Figure 60. Estimation result for C_m - test case 1	155

Figure 61. Estimation result for C_n – test case 1.....	156
Figure 62. Simulated flight test data 1 flight parameters.....	158
Figure 63. Simulated flight test data 1 rates.....	159
Figure 64. Deflections for test case 2.....	161
Figure 65. Error in deflections for test case 2.....	162
Figure 66. Flight parameters for test case 2	163
Figure 67. Rates for test case 2	164
Figure 68. Estimation result for C_x – test case 2.....	166
Figure 69. Estimation result for C_y – test case 2.....	167
Figure 70. Estimation result for C_z – test case 2.....	168
Figure 71. Estimation result for C_l – test case 2	169
Figure 72. Estimation result for C_m – test case 2.....	170
Figure 73. Estimation result for C_n – test case 2.....	171
Figure 74. Deflections for test case 3 (attempt 1)	173
Figure 75. Error in deflections for test case 3 (attempt 1)	174
Figure 76. Flight parameters for test case 3 (attempt 1)	175
Figure 77. Rates for test case 3 (attempt 1)	176
Figure 78. Dominant terms for C_x – test case 3	178
Figure 79. Dominant terms for C_y – test case 3.....	179
Figure 80. Dominant terms for C_z – test case 3	180
Figure 81. Dominant terms for C_l – test case 3	181
Figure 82. Dominant terms for C_m – test case 3.....	182
Figure 83. Dominant terms for C_n – test case 3.....	183
Figure 84. Deflections for test case 3 (attempt 2)	186

Figure 85. Error in deflections for test case 3 (attempt 2)	187
Figure 86. Flight parameters for test case 3 (attempt 2)	188
Figure 87. Rates for test case 3 (attempt 2)	189

NOMENCLATURE AND LIST OF SYMBOLS

AFCS	Automatic Flight Control System
ALV	Air Launched Vehicle
C_D	Drag Coefficient
C_L	Lift Coefficient
C_l	Rolling Moment Coefficient
C_m	Pitching Moment Coefficient
C_n	Yawing Moment Coefficient
C_x	Axial Force Coefficient
C_y	Side Force Coefficient
C_z	Normal Force Coefficient
CFD	Computational Fluid Dynamics
dof	Degree of Freedom
EKF	Extended Kalman Filtering
FAS	Fin Actuation System
FTD	Flight Test Data

FV	Flight Vehicle
L	Total Aerodynamic Moment Around X axis
M	Total Aerodynamic Moment Around Y axis, Mach Number
ML	Maximum Likelihood
MM5	Fifth-Generation NCAR / Penn State Mesoscale Model
N	Total Aerodynamic Moment Around Z axis
p	Body Angular Rate Around X axis (Roll Rate)
PE	Parameter Estimation
PSD	Power Spectral Density Estimates
PSE	Predicted Square Error
q	Body Angular Rate Around Y axis (Pitch Rate)
r	Body Angular Rate Around Z axis (Yaw Rate)
R_i	Regressor
R^2	Coefficient of Determination
S	Reference Area
SI	System Identification
SIDPAC	System Identification Programs for Aircraft

u	Body Linear Velocity in X direction
UAV	Unmanned Air Vehicle
UTC	Universal Time Coordinated
V	Flight Velocity
v	Body Linear Velocity in Y direction
w	Body Linear Velocity in Z direction
X	Total Aerodynamic Force Acting in X direction
Y	Total Aerodynamic Force Acting in Y direction
Z	Total Aerodynamic Force Acting in Z direction
α	Angle of attack
β	Sideslip Angle
δ	Control Deflection Angle
δ_a	Aileron Deflection Angle
δ_e	Elevator Deflection Angle
δ_r	Rudder Deflection Angle
ρ	Density of Air
Δ	Difference Operator

CHAPTER 1

AN OVERVIEW OF SYSTEM IDENTIFICATION AND PARAMETER ESTIMATION IN AEROSPACE APPLICATIONS

It is the very basic instinct of an engineer to try to understand the governing laws of any phenomena that he/she faces by analyzing the observable outcomes. Thus, engineering is inherently based on the effort of solving inverse problems in order to innovate, improve or even avoid the phenomena faced in life.

From a literal point of view, the term "system identification" (SI) is defined as "... a scientific discipline that provides answers to the age-old inverse problem of obtaining a description in some suitable form for a system, given its behavior as a set of observations." by Hamel and Jategaonkar, [1]. Parameter estimation (PE) problems are, in fact, a subset of system identification problems, where the purpose is to obtain the "parameters" of the model identified.

The three dimensional (3D) dynamics of any rigid flight vehicle is governed by six nonlinear ordinary differential equations which

consist of three force equations and three moment equations in which time appears as the independent variable. These equations involve the four fundamental classes of forces/moments acting on the body; namely,

- Aerodynamic forces/moments
- Inertial forces/moments
- Gravitational forces
- Propulsive forces

It is rather easy to obtain some accurate estimates for the gravitational, inertial, and even propulsive forces by some measurements and/or calculations. However, it is neither that easy, nor straight forward to obtain aerodynamic forces and moments. Although, throughout the design cycle of a flight vehicle, a number of different approaches (calculations, analysis, tests, etc.) are used to obtain aerodynamic forces and moments, the final aerodynamic estimates still contain some discrepancies and/or errors due to the shortcomings of the methods utilized.

An initial model for the aerodynamic forces and moments along with a database which contain the parameter values of this model for an air vehicle is usually generated by using either a semi-empirical tool (like DATCOM) or an analytical tool (like Vortex Lattice Method) at the early stages of preliminary design.

Although, theoretical and empirical aerodynamics provide aerodynamic force and moment coefficients and stability and control derivatives with relatively high computational speed and acceptable accuracy, they fail to give satisfactory results when new and complex geometries are considered.

As the design evolves, some higher fidelity methods such as computational fluid dynamics (CFD) are required and used for the data generation. Although the CFD methods are becoming more and more reliable and faster with the advances in computer technology, they still may fail to predict the complex dynamics occasionally.

Wind tunnels are in use by aerospace engineers for over a hundred years and it is common to update aerodynamic models and databases using the results of wind tunnel tests once the design is fixed. However, they have their own limitations such as test section sizes, scaling requirements, model surface quality effects, model-sting interference effects, and so on.

Aeroballistic ranges are alternatives to the wind tunnels with one major difference in the way the flight conditions are simulated; the model is accelerated to the desired flight velocities. Although these ranges are very useful in obtaining the aerodynamic parameters of air vehicles that fly through a wide range of Mach

numbers, such as artillery rockets or free fall bombs, they also have serious limitations like the Reynolds number mismatch, model surface quality effects and scaling requirements. However, the biggest limitation associated with the aeroballistic ranges is controlling the flight parameters such as angle of attack and angle of side slip.

As a summary, the final aerodynamic models and databases obtained at the end of the design process might be, and most of the time are, inaccurate for at least some flight conditions likely to be faced by the flight vehicle throughout its life cycle. These inaccuracies are discovered by flight testing the actual full scale system on a variety of conditions that represent the entire flight envelope. Then, it is the flight mechanist's job to deduce ways to correct the aerodynamic model and estimate the parameters using the flight test data in hand.

1.1 Problem Definition

As a matter of fact, there is no standard approach for deciding on the aerodynamic model of a flight vehicle (FV). Depending on the requirements and type of the flight vehicle, the aerodynamic model can be expressed as a linear or nonlinear function of flight variables and geometry parameters. Furthermore, these model functions can be continuous or interpolated from a look-up table.

Yet, the need to obtain an updated and better model stands regardless of the format of the aerodynamic database.

The types of flight vehicles that are of interest to this study are autonomous, one-shot flight vehicles, with polynomial aerodynamic models. In contrast to the flight test data of a piloted aircraft, the flight test data that can be obtained from the flight tests of these vehicles is heavily stripped of the necessary information for identification and estimation purposes unless a special care is taken in the flight test design. Yet, it is not always possible to design a flight test for these one-shot autonomous flight vehicles, but the flight test data for SI and PE is collected as byproduct during the flight tests conducted for the purpose of performance demonstration. This poses a question on the applicability of the methods developed for the SI and PE of piloted aircraft to the autonomous flight vehicles.

There are plenty of references in the literature on the identification of aerodynamic model and estimation of aerodynamic coefficients of an aircraft from its flight test data yet, most of the efforts spent on this subject are concentrated on the selection of estimation method for a known aerodynamic model. On the other hand, only a limited amount of literature exists for the SI and PE of autonomous flight vehicles. This is due to partly the confidentiality of the autonomous flight vehicles and partly to the fact that the small number of autonomous flight vehicles (and

therefore number of flight tests with these vehicles) as compared to piloted aircraft. These two issues raise the question of applicability of the methods developed for piloted aircraft to autonomous flight vehicles and define a need for a complete methodology for processing the flight test data for these types of vehicles.

1.2 State of the Art in System Identification and Parameter Estimation for Aerospace Applications

Although the mathematical background of system identification can be traced back to 18th century; its first applications in aerospace field were not seen until the mid 20th century [1]. Especially after the introduction of digital computers, many methods have been developed for the SI and PE purposes.

The most popular PE method in the literature nowadays is the Equation Error Method. Also known as Least Squares Estimation, the method provides unbiased, efficient, and consistent estimation in theory, [2]. Its ease of application, which is one of the main reasons of the method's popularity, comes from the simplicity of the algorithm in which no iterations are needed to estimate the parameters. The ability to merge flight test data from different maneuvers/sorties into one without much effort is also another contributing factor to its popularity. Also, the stepwise regression method, which is used for model identification utilizes equation

error method to estimate the parameters of the identified models. However, Equation Error Method have a drawback in practice, since the flight test data always contain measurement errors, which in turn cause the estimators to be neither as efficient, consistent nor unbiased. Yet, the results of the equation error method can be used as the feasible starting point of other parameter estimation methods.

The other most widely applied method is the Output Error Method which, as the name suggests, aims to arrive at the best estimates of the aerodynamic parameters by minimizing the error between the model output and the flight test data. For this purpose different optimization schemes are applied, ranging from gradient based optimization to genetic algorithm.

Other approaches to system identification include Filter Error Method, Kalman and Extended Kalman Filtering and Artificial Neural Networks.

The following paragraphs cover some of the work done in the field of aerodynamic system identification and parameter estimation as a result of a literature survey performed.

Aksteter et. al. [3] formulated the longitudinal aerodynamics model of a Harrier aircraft and employed the equation error method to estimate the nonlinear parameters. An aerodynamic model was built-up using basic theoretical relations such as parabolic drag assumption and Prandtl Galuert rule and then was divided into three parts as static, dynamic, and control. Different segments of the flight test data were used to estimate parameters for these three parts (for example, static part was estimated form the portion of the flight test data where the vehicle was flying close to the trim conditions). Although this study demonstrates a complete estimation methodology, it lacks the aerodynamic model identification process.

Özger [4] briefly summarized the aerodynamic model validation approach at EADS Military Air Systems. In that work, a correlation analysis for each flight test maneuver was run and as a result the correlated and uncorrelated parameters were discovered. Then by using 6dof equations, the flight test aerodynamic parameters (which are going to be referred as the in-flight aerodynamics throughout this dissertation) were gathered from the flight test data. This in-flight aerodynamics was later compared with the parameters foreseen by the existing aerodynamic model and linear correction model (which is going to be referred as the delta coefficient model throughout this dissertation) is obtained by calculating the difference between the two. The equation error method and output error method were both utilized for parameter estimation and results were compared. Özger's work defines a nice framework for the aerodynamic model identification and

parameter estimation problem based on the actual flight test. The methodology followed in this doctoral study is in some part inspired from his work.

Paris and Alaverdi worked on a nonlinear aerodynamic model extraction from the flight test data for the S-3B Viking aircraft using the commercial software package IDEAS (Integrated Data and Analysis System), [5]. They employed an equation error estimation technique for the early model development and an output error estimation technique for the final tuning. However, the updates to final aerodynamic model were all decided by visual comparison of the simulation output and calibrated flight data, that is, the judgment of an experienced flight mechanics engineer is essential for that study.

Song et. al. [6] examined the estimation of a full set of aerodynamic coefficients (6 component aerodynamics, i.e., C_D , C_L , C_m , C_y , C_l , C_n with 30 independent coefficients of Taylor series expansions) for an air launched missile using extended Kalman filtering (EKF) method and concluded that the parameter identification was very useful in the improvement of the predicted aerodynamic coefficients of a flight vehicle, in their case from wind tunnel tests tabulated data. Terms less than third order in the Taylor series expansion were included in the first place and then some important terms, which were selected by employing the

multidimensional algebraic algorithm were added. The rate derivatives were also added, apparently by engineering judgment.

Anderson et. al. focused on utilizing genetic algorithm and pareto genetic algorithm to aerodynamic parameter estimation of ballistic weapons ([7], [8], [9]). Yet, the aerodynamic model structures were not identified and selected as first order linear models.

Gage et. al. [10] examined the use of genetic programming for aerodynamic model structure determination of ballistic weapons. Although the trajectory of a ballistic weapon was successfully modeled as a result of the study, the identified model structures need to be worked on to become more physically relevant.

Mohammadi et. al. [11] studied the aerodynamic identification problem for an antitank guided missile and concluded that Extended Kalman Filtering (EKF) method was suitable for the estimation of time varying aerodynamic parameters, such as the parameters of the antitank missile which had a flight regime between Mach 0.2 and 0.92.

1.3 Scope, Originality and Contributions of the Doctoral Study

After reviewing the current state of the art for SI and PE applications in the field of flight mechanics, it is seen that, plenty studies were carried out on this subject and but especially for aircraft type flight vehicles. However, when it comes to the other types of flight vehicles such as tactical UAVs, cruise missiles, and guided air launched weapons, only a limited number of literature is found. Furthermore, in those studies, most of the effort was concentrated on the selection and tuning of the estimation algorithm and an engineering judgment was still widely utilized for the determination of the aerodynamic model structure.

The aim of this doctoral study is set as to develop a method which will be used for determination of aerodynamic models and parameters for different types of autonomous FVs using actual flight test data. The devised method, is expected to identify the aerodynamic model structures for six aerodynamic coefficients and estimate the parameters with a minimum intervention from the user, thus it minimizes, if not eliminates, the need for the engineering judgment of an experienced flight mechanics specialist.

The aerodynamic model sought should be based on the correlations between significant motion parameters and in-flight

calculated aerodynamics coefficients (or difference of in-flight aerodynamics from the a priori aerodynamics) using inverse six degrees of freedom (6 dof) equations of motion. The structures for each and every aerodynamic coefficient are to be obtained with a minimal intervention to automated model structure determination scheme. The model parameters are to be obtained by the utilization of the equation error method.

The fine tuning of the model parameters is done by a closed loop optimization cycle, utilizing genetic algorithm.

Practical considerations for the application of model structure determination methods to autonomous vehicles are not well defined in the literature and this doctoral study is expected to serve as a guide to these considerations. Practical considerations for the closed loop aerodynamic parameter estimation method will be defined in this study, as well. Both approaches are expected to be successfully applied to actual flight test data.

During the course of this doctoral study, three conference papers have been published. Two of them, [12], [13], explain the practical considerations in flight test data processing of autonomous flight vehicles and aerodynamic model structure determination. The third one, [14], gives preliminary results of closed loop aerodynamic parameter estimation using genetic

algorithm for simulated flight test data of an autonomous flight vehicle.

This thesis dissertation starts with an overview of system identification and parameter estimation in aerospace applications. The second chapter defines the concept of aerodynamic modeling. The methods used for aerodynamic model structure determination are given in the third chapter. The fourth chapter deals with principles of the proposed closed loop aerodynamic parameter estimation using genetic algorithm. Some test cases with simulated and actual flight test data are given in the fifth chapter and the dissertation is concluded with the discussions of results in the last chapter.

CHAPTER 2

AERODYNAMIC MODELING

The fundamental problem of science of flight mechanics is the determination of the relation between the aerodynamic properties and motion variables of a flight vehicle. This problem was stated by B. Melvill Jones and cited by Tobak and Schiff as follows, [15]:

“Given the shape of aeroplane and the properties of air through which it moves the air reactions X, Y, Z, L, M, N , depend on the motion of aeroplane relative to air; that is to say upon six variables U, V, W, P, Q, R and their rates of change with respect to time. In practice, the principle difficulty lies in determining the relationships between X, Y, \dots and U, V, \dots ”

In the expression above, $U, V,$ and W are used to denote the components of the relative velocity of the flight vehicle with respect to wind, resolved in body coordinate frame ($V_{b/w}^{(b)}$). As stated by Tobak and Schiff in their lecture in AGARD LS – 114, [15], there are two approaches to tackle this problem. First one is the “straightforward” approach in which the flow-field around the

maneuvering FV (gas dynamics equations) is solved simultaneously with the inertial equations that govern the motion of the fv (equations of motion). The shortcomings of this approach are obvious; not only a unique solution must be sought for each and every initial condition but also the computational cost of solving gas dynamics equations simultaneously with equations of motion is very high.

The need to uncouple these equations results in the modeling efforts, through which the aim is to obtain a form of aerodynamic response to some characteristic motions. This approach can be applied to a wide range of motion variables and flight conditions, so that the response to arbitrary motions can be calculated directly. Although some computational time is still required in order to obtain the aerodynamic responses to the characteristic motions, the aerodynamic model allows the engineer to solve for the arbitrary initial conditions without referring to flow-field calculations.

The foundations of the aerodynamic modeling, upon which our current notion still relies on, was laid by George H. Bryan, just eight years after the Wright Brothers' historic flight in 1903. There are two primary assumptions in Bryan's approach, [15]:

1. The instantaneous forces and moments acting on the FV only depend on the instantaneous values of motion variables.
2. The aerodynamic forces and moments vary only linearly with motion variables.

The first assumption allows defining any aerodynamic parameter as a function of time. For instance, the pitching moment coefficient can be expressed as a function of two basic motion variables angle of attack (α) and pitch control surface deflection (δ) as:

$$C_m t = C_m(\delta t, \alpha t) \quad (1)$$

The second assumption allows expanding the aerodynamic coefficient into a Taylor series up to the first order terms around some initial conditions (such as $\alpha = 0, \delta = 0$):

$$C_m t = C_{m_0} + \frac{\partial C_m}{\partial \alpha} \Big|_{\substack{\alpha=0 \\ \delta=0}} \alpha t + \frac{\partial C_m}{\partial \delta} \Big|_{\substack{\alpha=0 \\ \delta=0}} \delta t \quad (2)$$

Any of the six principle aerodynamic variables (C_X – or C_D , C_Y , C_Z – or C_L , C_I , C_m , C_n) can be written as a Taylor series expansion in related motion variables. The partial derivatives appearing in Eq. (2) are called as “dimensionless stability and control derivatives”.

Referring to Tobak and Schiff [15], the obvious problem associated with Bryan’s first assumption was discovered in the following years when the researchers in flight mechanics found out that the response of the aircraft to a change in angle of attack was greatly affected by the presence of a horizontal tail, since the downwash generated by the wing in response to a change in angle of attack required some time to be convected to the tail. Thus, the model needed to be updated to include some time dependency. This problem was solved by adding a term to the model that reflected the contribution of time rate of change of angle of attack:

$$C_m t = C_{m_0} + \frac{\partial C_m}{\partial \alpha} \alpha t + \frac{\partial C_m}{\partial \delta} \delta t + C_{m_\alpha} \alpha t \quad (3)$$

Later on, studies on the flutter phenomena and also on the aerodynamic responses of wings to step changes in motion variables (linear aerodynamic indicial responses) allowed the establishment of an underlying theoretical basis for including the time dependent term in the aerodynamic model, [15]. This

theoretical basis, called the indicial response concept, is basically expressing the aerodynamic variables in terms of linear functionals as opposed to functions given in Eq. (2). Then, the aerodynamic model includes not only the effect of the motion variables at the current time step, but of all the variables in all of the past time steps as well.

Following studies showed that, for slowly varying motions, i.e., steady aerodynamics, the indicial response and the linear stability-derivative approaches yielded equivalent results, [15]. As stated by Klein and Morelli, [16], in majority of the practical applications a quasi-steady flow assumption, i.e., neglecting the dependence on the past values of the flow variables, can be justified.

Quasi-steady flow assumption is also valid for the types of the problems considered to be in the scope of this doctoral study. The types of the flight vehicles that are of interest to this study fly around a trim condition, which is achieved by the feedback controller of the onboard automatic flight control system. Also, these vehicles are not agile, when compared to highly maneuverable fighter aircraft or flexible when compared to large transport/cargo aircraft. That is to say, unsteady conditions are not likely to be encountered during the normal operating conditions of the FVs of interest. Then, it is anticipated that the linear stability derivative approach (and sometimes its extension

to non-linear aerodynamics) is adequate for the purposes of this study.

Theoretical derivation of aerodynamic model is a well known subject and details can be found in any flight mechanics and most aerodynamic system identification books. Referring to [16] and [17], a general form for the six degrees of freedom linear aerodynamic model can be obtained as in Eq. (4) and Eq. (5):

$$\begin{aligned}
 C_D &= C_{D_0} + C_{D_V} \frac{\Delta V}{V_0} + C_{D_\alpha} \Delta\alpha + C_{D_q} \frac{qc}{2V_0} + C_{D_\delta} \Delta\delta \\
 C_L &= C_{L_0} + C_{L_V} \frac{\Delta V}{V_0} + C_{L_\alpha} \Delta\alpha + C_{L_\alpha} \frac{\alpha c}{2V_0} + C_{L_q} \frac{qc}{2V_0} \\
 &\quad + C_{L_\delta} \Delta\delta \\
 C_m &= C_{m_0} + C_{m_V} \frac{\Delta V}{V_0} + C_{m_\alpha} \Delta\alpha + C_{m_\alpha} \frac{\alpha c}{2V_0} \\
 &\quad + C_{m_q} \frac{qc}{2V_0} + C_{m_\delta} \Delta\delta
 \end{aligned} \tag{4}$$

$$\begin{aligned}
C_Y &= C_{Y_0} + C_{Y_\beta} \Delta\beta + C_{Y_p} \frac{pb}{2V_0} + C_{Y_r} \frac{rb}{2V_0} + C_{Y_\delta} \Delta\delta \\
C_l &= C_{l_0} + C_{l_\beta} \Delta\beta + C_{l_p} \frac{pb}{2V_0} + C_{l_r} \frac{rb}{2V_0} + C_{l_\delta} \Delta\delta \quad (5) \\
C_n &= C_{n_0} + C_{n_\beta} \Delta\beta + C_{n_p} \frac{pb}{2V_0} + C_{n_r} \frac{rb}{2V_0} + C_{n_\delta} \Delta\delta
\end{aligned}$$

It is possible to use C_X and C_Z instead of C_D and C_L as in Eq.(6).

$$\begin{aligned}
C_X &= C_{X_0} + C_{X_V} \frac{\Delta V}{V_0} + C_{X_\alpha} \Delta\alpha + C_{X_q} \frac{qc}{2V_0} + C_{X_\delta} \Delta\delta \\
C_Z &= C_{Z_0} + C_{Z_V} \frac{\Delta V}{V_0} + C_{Z_\alpha} \Delta\alpha + C_{Z_\alpha} \frac{\alpha c}{2V_0} + C_{Z_q} \frac{qc}{2V_0} \\
&\quad + C_{Z_\delta} \Delta\delta \quad (6) \\
C_m &= C_{m_0} + C_{m_V} \frac{\Delta V}{V_0} + C_{m_\alpha} \Delta\alpha + C_{m_\alpha} \frac{\alpha c}{2V_0} \\
&\quad + C_{m_q} \frac{qc}{2V_0} + C_{m_\delta} \Delta\delta
\end{aligned}$$

Although, theoretically works perfectly, the proposed models for C_L , C_Z and C_m in Eq. (4) and (6) have identifiability problems associated with the α and q derivatives, since in an actual flight, the data recorded for these two motion variables have very similar time histories, [16]. So it is customary to define a merged derivative for these two variables as follows:

$$\begin{aligned}
C_{Lq} &= C_{L\alpha} + C_{Lq} \\
C_{Zq} &= C_{Z\alpha} + C_{Zq} \\
C_{mq} &= C_{m\alpha} + C_{mq}
\end{aligned}
\tag{7}$$

For most of the cases, the linear model, with necessary augmentations, provides satisfactory results for the estimation of the aerodynamic response. However, in cases where there are large amplitude maneuvers or rapid divergences from the reference conditions, the aerodynamic model should be extended to include some nonlinear terms. According to Klein and Morelli, [16], there are two ways to do this.

The first approach is to include the nonlinear terms of the Taylor series expansion and define nonlinear stability derivatives. Following shows the nonlinear expansion of lift coefficient for angle of attack and pitch rate, as taken from Klein and Morelli, [16]:

$$\begin{aligned}
C_L = C_{L_0} + \frac{\partial C_L}{\partial \alpha} \Delta\alpha + \frac{\partial C_L}{\partial q} q \\
+ \frac{1}{2} \frac{\partial^2 C_L}{\partial \alpha^2} (\Delta\alpha)^2 + 2 \frac{\partial^2 C_L}{\partial \alpha \partial q} \Delta\alpha q \quad (8) \\
+ \frac{\partial^2 C_L}{\partial q^2} q^2 + \dots
\end{aligned}$$

If Eq. (8) is expressed in the stability derivative format, then Eq.(9) is obtained:

$$\begin{aligned}
C_L = C_{L_0} + C_{L\alpha} \Delta\alpha + C_{Lq} \frac{qc}{2V_0} \\
+ \frac{1}{2} C_{L\alpha^2} (\Delta\alpha)^2 + 2C_{L\alpha q} (\Delta\alpha \frac{qc}{2V_0}) \quad (9) \\
+ C_{Lq^2} (\frac{qc}{2V_0})^2 + \dots
\end{aligned}$$

The second approach, which is based on the works of Klein and Batterson, [18], combines the static terms and treat the dynamic stability and control derivatives as functions of explanatory variables, i.e., angle of attack, angle of side slip and Mach number. In the previous case of Eq.(8) and Eq.(9), the explanatory variable is angle of attack. Then the nonlinear model would be:

$$C_L = C_{L_0}(\alpha) + C_{L_q}(\alpha) \frac{qc}{2V_0} \quad (10)$$

In this second approach, four basic assumptions are made. These are outlined by Klein and Morelli, [16], as:

1. Aerodynamic coefficients do not vary with the airspeed in the subsonic region.
2. The effect of time history (rate of change of) angle of attack and angle of side slip are not explicitly introduced, but their effects are implicitly included in the rate derivatives.
3. Longitudinal and lateral coefficients are dependent on the states and the control angles as

$$C_{longitudinal} = C_{longitudinal}(\alpha, \beta, q, \delta_e) \quad (11)$$

$$C_{lateral} = C_{lateral}(\alpha, \beta, p, r, \delta_a, \delta_r)$$

4. The static term of the aerodynamic model includes the nonlinear angle of attack and angle of side slip dependencies. The second part of the model is linear in motion and control variables (p, q, r, δ) but involves derivatives that depend nonlinearly on the angle of attack, angle of side slip and Mach number.

With the assumptions given above, the six degrees of freedom aerodynamic model becomes:

$$\begin{aligned}
C_X &= C_{X_0}(\alpha, \beta, M)_{q=\delta=0} + C_{X_q}(\alpha, \beta, M) \frac{qc}{2V_0} \\
&\quad + C_{X_\delta}(\alpha, \beta, M)\delta \\
C_D &= C_{D_0}(\alpha, \beta, M)_{q=\delta=0} + C_{D_q}(\alpha, \beta, M) \frac{qc}{2V_0} \\
&\quad + C_{D_\delta}(\alpha, \beta, M)\delta \\
C_Z &= C_{Z_0}(\alpha, \beta, M)_{q=\delta=0} + C_{Z_q}(\alpha, \beta, M) \frac{qc}{2V_0} \\
&\quad + C_{Z_{\delta_e}}(\alpha, \beta, M)\delta_e \\
C_L &= C_{L_0}(\alpha, \beta, M)_{q=\delta=0} + C_{L_q}(\alpha, \beta, M) \frac{qc}{2V_0} \\
&\quad + C_{L_{\delta_e}}(\alpha, \beta, M)\delta_e \\
C_m &= C_{m_0}(\alpha, \beta, M)_{q=\delta=0} + C_{m_q}(\alpha, \beta, M) \frac{qc}{2V_0} \\
&\quad + C_{m_{\delta_e}}(\alpha, \beta, M)\delta_e
\end{aligned} \tag{12}$$

$$\begin{aligned}
C_Y &= C_{Y_0}(\alpha, \beta, M)_{p=r=\delta=0} + C_{Y_p}(\alpha, \beta, M) \frac{pb}{2V_0} \\
&\quad + C_{Y_r}(\alpha, \beta, M) \frac{rb}{2V_0} \\
&\quad + C_{Y_{\delta_a}}(\alpha, \beta, M) \delta_a \\
&\quad + C_{Y_{\delta_r}}(\alpha, \beta, M) \delta_r \\
\\
C_l &= C_{l_0}(\alpha, \beta, M)_{p=r=\delta=0} + C_{l_p}(\alpha, \beta, M) \frac{pb}{2V_0} \\
&\quad + C_{l_r}(\alpha, \beta, M) \frac{rb}{2V_0} \\
&\quad + C_{l_{\delta_a}}(\alpha, \beta, M) \delta_a \\
&\quad + C_{l_{\delta_r}}(\alpha, \beta, M) \delta_r \\
\\
C_n &= C_{n_0}(\alpha, \beta, M)_{p=r=\delta=0} + C_{n_p}(\alpha, \beta, M) \frac{pb}{2V_0} \\
&\quad + C_{n_r}(\alpha, \beta, M) \frac{rb}{2V_0} \\
&\quad + C_{n_{\delta_a}}(\alpha, \beta, M) \delta_a \\
&\quad + C_{n_{\delta_r}}(\alpha, \beta, M) \delta_r
\end{aligned} \tag{13}$$

The first terms in Eq.(12) and Eq.(13) represent the static effects, i.e., the aerodynamic response with the controls are fixed and angular rates are zero. The dynamic stability derivatives are modeled as functions of angle of attack. As stated by Klein and Batterson, [18], this is a similar form to those used in wind tunnel testing. Furthermore, the models for the aerodynamic coefficients are valid for the entire range of motion variables.

The stability derivatives of Eq.(12) - (13) can be approximated as polynomials or polynomial splines, [16], [18]. The following is an example of polynomial expression for static part of the nonlinear pitching moment term:

$$\begin{aligned}
 C_{m_0}(\alpha, \beta)_{q=\delta=0} &= \theta_0 + \theta_{01}\alpha + \theta_{02}\beta + \theta_{03}\alpha^2 \\
 &+ \theta_{04}\beta^2 + \theta_{05}\alpha\beta + \theta_{06}\alpha^3 + \theta_{07}\beta^3 \\
 &+ \theta_{08}\alpha^2\beta + \theta_{09}\alpha\beta^2 + \dots
 \end{aligned} \tag{14}$$

In Eq. (14), θ_i are called the aerodynamic parameters.

According to Klein and Morelli, [16], the aerodynamic models given in Eq.(12) and Eq.(13) are "fairly general formulations".

CHAPTER 3

MODEL STRUCTURE DETERMINATION

One of the most crucial points in system identification of flight vehicles using flight test data is the selection of an adequate aerodynamic model. Depending on the type of the FV, characteristics of the motion available in the flight test data, previous experience, and a priori knowledge – most probably through wind tunnel test or CFD runs –, the model structure as well as explanatory variables may vary.

It is important to notice that, model structure determination inherently requires the utilization of an estimation method for the parameter estimation sub problem that it includes.

A number of methods have been proposed in the past to tackle the problem of finding an adequate model based on some metric rather than pure judgment of an experienced engineer. These methods fall under the classification of regression methods.

3.1 Stepwise Regression

The most widely used of these methods is the stepwise regression due it having the advantage of both forward and backward evaluation and selection capabilities. As explained by Klein and Batterson, [18], the determination of the aerodynamic model structure using stepwise regression includes three steps:

1. Postulation of the terms which might enter the model.
2. Selection of an adequate model.
3. Verification of the model selected.

Jategaonkar, [19], states that the stepwise regression problems encountered in flight mechanics are multivariate type problems, i.e., the six aerodynamic coefficients are functions of different sets of independent variables. He suggests that these types of problems are treated separately for each of the dependent variable (aerodynamic coefficient). Klein and Morelli, [16], share Jategaonkar's point of view and further claim that it is one of the biggest advantages of stepwise regression method to be able to deal with individual aerodynamic coefficient equations one at a time.

The stepwise regression procedure can be briefly summarized in a four step procedure as, [19]:

1. A set of possible independent variables (motion variables) is defined and the correlations of each of these independent variables with the dependent variable are sought. The independent variable with the highest correlation is added to the model.
2. The independent variable from the remaining set with the highest partial correlation is added to the model.
3. Partial “goodness of fit (F) values” for all the included independent variables are calculated and those found to be below a pre-specified threshold are excluded from the model.
4. Steps 2-3 are repeated until no other independent variable is left.

Eq. (14) can be written in a more general form as Eq. (15), where y is the aerodynamic coefficient, x_i 's are the independent variables (in typical applications flight parameters such as angle of attack, angle of side slip, Mach number and control surface deflections) and θ_i 's are the aerodynamic parameters:

$$y = \theta_0 + \theta_1 x_1 + \dots + \theta_{n_q} x_{n_q} \quad (15)$$

In Eq. (15), x_i 's are called as the regressors and they can be defined as valid combinations of n flight variables up to p^{th} power, selected from a set (F) of r flight variables, Eq. (16):

$$X_i = F_j^k F_l^m \dots$$

$$j \neq l \neq \dots \quad j, l, \dots = 1, 2 \dots r \quad (16)$$

$$k, m, \dots = 1, 2, \dots p \quad k + m + \dots < p$$

The stepwise regression method starts with only the static term, θ_0 and other terms are added one by one. According to the procedure explained above, the correlation coefficients are found from the following formula, [19], where the subscript i denotes the i^{th} independent variable, y and x_i are the mean values and N is the number of data samples:

$$\rho_i = r_{yx_i} = \frac{\sum_{k=1}^N y(k) x_i(k) - y \sum_{k=1}^N x_i(k)}{\sqrt{\left(\sum_{k=1}^N y(k)^2 - N y^2 \right) \left(\sum_{k=1}^N x_i(k)^2 - N x_i^2 \right)}} \quad (17)$$

$$y = \frac{1}{N} \sum_{k=1}^N y(k)$$

$$x_i = \frac{1}{N} \sum_{k=1}^N x_i(k)$$

The correlation coefficient of Eq.(17) ranges between -1 and 1 and shows the statistical dependence of y on the independent variable x_i .

The partial correlation determines the correlation between any of the two variables if the other variables are held constant. For the case of three variables, the calculation of partial correlation is fairly simple as given by the following equation, [19]:

$$r_{yx_i*x_j} = \frac{r_{yx_i} - r_{yx_j}r_{x_ix_j}}{1 - r_{yx_j}^2 \quad 1 - r_{x_ix_j}^2} \quad (18)$$

However, when there are more than two terms in the aerodynamic model, i.e., more than two independent variables, the calculation is not as straight-forward as Eq.(18). First of all, residuals after fitting the dependent variable with the proposed model (n independent variables) are calculated. Next, the residuals after fitting the independent variable, x_j ($n+1^{\text{st}}$ variable), with the same set of independent variables are calculated. Then, correlation between these two residuals gives the desired partial correlation, [19]. Jategoankar, [19], defined this procedure mathematically as follows, where e denoting the fit error:

$$\begin{aligned} y_{-j} &= \theta_1 x_1 k + \dots + \theta_{j-1} x_{j-1} k \\ &\quad + \theta_{j+1} x_{j+1} k + \dots + \theta_{nq} x_{nq} k \\ x_j &= \theta_1 x_1 k + \dots + \theta_{j-1} x_{j-1} k + \theta_{j+1} x_{j+1} k \\ &\quad + \dots + \theta_{nq} x_{nq} k \end{aligned} \quad (19)$$

$$\begin{aligned}
& r_{yx_j^*(x_1, \dots, x_{j-1}, x_{j+1}, \dots, x_{n_q})} \\
&= \frac{\sum_{k=1}^N e^{y-j} k - e^{y(-j)} \sum_{k=1}^N e^{x_j} k - e^{x_j}}{\sqrt{\left(\sum_{k=1}^N e^{y-j} k - e^{y(-j)} \right)^2 \sum_{k=1}^N e^{x_j} k - e^{x_j}^2}} \\
& e^{y(-j)} = \frac{1}{N} \sum_{k=1}^N e^{y(-j)}(k) \\
& e^{x_j} = \frac{1}{N} \sum_{k=1}^N e^{x_j}(k)
\end{aligned}$$

To assess the “quality” of the model, some statistical metrics are employed. The first one that comes in mind is the goodness of fit, defined as Eq.(20), [19], for two independent variables case. If more than two independent variables are present then the partial correlation expression given in Eq.(19) should be employed.

$$F = \frac{r_{yx_i^*x_j}}{(1 - r_{yx_i^*x_j})} \frac{N - n_q}{n_q - 1} \quad (20)$$

The coefficient of determination, R^2 , is another useful metric to assess the goodness of fit. However, R^2 , which varies between 0 and 1, can be sometimes misleading, because its value increases with the increasing total number of independent variables in the model. So, an adjusted version is also in use, which does not necessarily increase with the increasing number of terms. Equations for R^2 and adjusted R^2 are provided as follows:

$$R^2 = \frac{\sum_{k=1}^N y_k - \bar{y}^2}{\sum_{k=1}^N y_k - \bar{y}^2} \quad (21)$$

$$AdjR^2 = 1 - (1 - R^2) \frac{N - 1}{N - n_q - 1}$$

Predicted square error (PSE) is also an important statistical metric used in stepwise regression. PSE is defined as given in Eq. (22), where p is the number of terms in the model, N is the total number of data points. As shown by Klein and Morelli, [16], PSE metric always have a single global minimum value, thus it is another good indicator for stopping the stepwise regression.

$$PSE = \frac{1}{N} (y - \hat{y})^T (y - \hat{y}) + \sigma_{max}^2 \frac{p}{N} \quad (22)$$

$$\sigma_{max}^2 = \frac{1}{N} \sum_{k=1}^N (y_k - \bar{y})^2$$

Although the stepwise regression method is highly promising in theory, it has some major deficiencies in practice. According to Jategaonkar, [19], for complex problems with large number of independent variables and complex relations, some skill and judgment are required to obtain the final model. Jategaonkar counts the most important difficulties of stepwise regression as:

- If some of the independent variables are correlated with the others, i.e., a data collinearity exists, then, the variable

selection process is inefficient and inconsistent. However, both Jategaonkar, [19], and Klein,[16], state that there are some methods to deal with the data collinearity (see Sec. 3.4.1).

- The threshold values required to eliminate some of the independent variables are case specific.

Klein and Morelli, [16], point out that the stepwise regression is mostly suitable to wind tunnel testing where the response variables are measured directly and there is only measurement noise. Although the method is not suitable to flight test data based on these aspects, still it is preferred due to being easy to implement and its ability to tackle both linear and nonlinear problems. Jategaonkar, [19], notes that, based on the deficiencies of the stepwise regression method, it is preferred to use a more general approach to modeling of aerodynamics with the a priori knowledge about modes of aircraft motion, aerodynamic effects and associated model structure. Also he suggests implementing more powerful estimation methods like output error method.

3.2 Equation Error Method

Parameter estimation methods that are not based on probability theory but rely on the laws of statistics are generally termed as the equation error methods, since they minimize a cost function

defined directly in terms of an input-output relationship, [19]. The most widely used subset of equation error methods is the least squares estimation, which allows the calculation of estimates in a one-shot procedure using matrix algebra.

The technique originates back to the end of 18th century, when C.F. Gauss invented and applied it in order to describe the planetary motion. The first great success of the technique was achieved when the asteroid Ceres was relocated precisely several months after its last observation, [19]. Today, the technique is widely applied to the aerodynamic parameter estimation problem.

There is an extensive literature available on the least squares estimation problem. Yet, a brief overview of the theory is given in this dissertation based on the work of Jategaonkar, [19].

Given N discrete data samples of a dependent variable, y , and n_q independent variables, a linear combination can be defined at each time step k as, [19]:

$$y(k) = \theta_1 x_1(k) + \dots + \theta_{n_q} x_{n_q}(k) + \epsilon(k) \quad (23)$$

In Eq. (23), θ_i 's are the unknown parameters and ϵ is the equation error representing the model discrepancies and/or noise in the dependent variable y . The form of the Eq. (23) is the same as Eq. (15), i.e., the x vector contains the motion variables such as angle of attack and control surface deflections, where θ_i 's are the aerodynamic parameters. Notice that the values of θ_i 's are not dependent on time, they are constants.

Eq.(23) can be rewritten in matrix format as follows:

$$\underline{\epsilon} = \underline{Y} k - \underline{X}\theta \quad (24)$$

The errors defined in Eq.(24) are called the residuals. It is obvious that, the difference between the dependent variable y , the "observation" and the model consisting of the independent variables x , the "regressors" or the "explanatory variables", and unknown parameters should be zero for a perfect model. Thus, to obtain the best estimates of the unknown parameters, the residuals should be minimized. This is accomplished via minimizing the following cost function:

$$\begin{aligned}
J(\theta) &= \frac{1}{2} \sum_{k=1}^N \varepsilon_k^2 = \frac{1}{2} \underline{\varepsilon}^T \underline{\varepsilon} \\
&= \frac{1}{2} \underline{Y}^T - \underline{\theta}^T \underline{X}^T \underline{Y} - \underline{X} \underline{\theta}
\end{aligned} \tag{25}$$

The sum of the square errors cost function of Eq.(25) is differentiated with respect to θ so that its minimum can be found:

$$\frac{\partial J}{\partial \theta} = -\underline{Y}^T \underline{X} + \underline{\theta}^T \underline{X}^T \underline{X} \tag{26}$$

Least squares estimates of the unknown parameters, $\underline{\theta}$, can be found by equating Eq.(26) to zero and solving for θ :

$$\underline{\theta} = \underline{X}^T \underline{X}^{-1} \underline{X}^T \underline{Y} \tag{27}$$

where $(\underline{X}^T \underline{X})^{-1} \underline{X}^T$ is often referred to as pseudo inverse.

3.3 Delta Coefficient Approach to Model Structure Determination

For every flight vehicle, an aerodynamic model already exists before proceeding to flight tests. Depending on the effort spent on

preparing this model and utilized methods, it can be high or low fidelity in one or more motion parameters. Nevertheless, this a priori information about the flight mechanics characteristics of the vehicle without doubt costs a lot of money and time to obtain and should be taken into consideration while dealing with model structure determination.

To apply the stepwise regression, the in-flight aerodynamics must be gathered in the first place. In an actual flight testing a number of sensor measurements are taken from the FV. These measurements include but not limited to the linear accelerations, angular rates and atmospheric conditions. If the vehicle is a powered one, a thrust measurement is not directly available most of the time, but the required information about the thrust is gathered from the engine model using the recorded flight conditions. Then, an inverse six degrees of freedom equation of motion can be solved to obtain the aerodynamic coefficients that lead the actual flight test behavior. These equations are pretty straight forward and detailed derivations can be found in any flight mechanics text book. The following equations for the forces and moments acting at the center of mass location are taken from Jategaonkar, [19].

$$C_x = \frac{ma_x - T \cos(\theta_T)}{qS} \quad (28)$$

$$C_Y = \frac{ma_y}{qS}$$

$$C_Z = \frac{ma_z - T \sin(\theta_T)}{qS}$$

$$C_l = \frac{I_x p - I_{xz} r - I_{xz} p q - I_y - I_z q r}{qSb}$$

$$C_m = \frac{I_y q + I_{xz}(p^2 - r^2) - I_z - I_x p r}{qSl}$$

$$C_n = \frac{I_z r - I_{xz} p + I_{xz} q r - I_x - I_y p q}{qSb}$$

Using in-flight measured motion parameters (flight angles, body angular rates, Mach number and control surface deflections), the response of the a priori aerodynamic model can be obtained. A priori aerodynamic model is an important and valuable source of information, since most of the time a considerable amount of work is done (and money is spent) to obtain it. Then, it is desirable to use the existing model as a baseline aerodynamics and design the aerodynamic parameter estimation flight tests to tune this existing model.

If the difference between the in-flight aerodynamics and aerodynamics foreseen by the existing aerodynamic model is fed into the model structure algorithm, a delta coefficient model is

obtained as given in Eq. (29), where Δ stands for the identified aerodynamic model for discrepancy:

$$C_{aero} = C_{database} + \Delta C_{identified\ model} \quad (29)$$

3.4 Practical Considerations for Model Structure Determination of Autonomous Flight Vehicles

3.4.1 Flight Test Data Processing and Dealing with Low Quality Flight Test Data

As a general practice, the flight test data (FTD) is recorded at a much higher rate than the highest natural frequency of the flight mechanics modes of the vehicle. Basically, the flight vehicles have two longitudinal and three lateral modes; namely the short period and phugoid in longitudinal, rolling, spiral and Dutch roll in lateral. All of these modes, have their natural frequencies. The well known Nyquist-Shannon sampling theorem states that the sampling rate must be at least twice the maximum frequency of interest. Thus, the sampling rate at which the FTD is recorded should be selected based on the a priori information of these modes.

However, since the aerodynamic database contain some discrepancies before the flight test, so does the natural frequencies of the flight vehicle. Thus, a sample rate, which is

higher than the one foreseen by the a priori information, is selected for data recording. However, this higher sample rate could lead to large number of samples, which in turn requires more computational power than necessary.

A direct approach to overcome this oversampling is to examine the power spectral density estimates of the FTD, so that a resampling can be performed before the estimation process. The power spectral density (PSD) estimation, which gives information about how the time series is distributed with frequency, is a very common procedure and based on the results of PSD, a proper resampling frequency can be selected.

Although the resampling approach is very effective in saving the computational power, it does not provide a solution to another fundamental problem associated with the FTD of autonomous flight vehicles. For this type of flight vehicles, it is not always possible to obtain a full set of measurements and perform flight test maneuvers specially designed for system identification/parameter estimation. Thus, sometimes the data recorded during the flight test which are not designed for estimation have to be used. Also for autonomous flight vehicles, the recorded data is almost stripped of the vehicles inherent dynamics (for example, FTD of a guided gliding flight vehicle shows that the spectral powers of the modes associated with pitching and rolling motions are very low - down to order of 10^{-7}

Watts/Hz, Figure 1 and Figure 2). As a result, the phenomenon known as data collinearity is encountered.

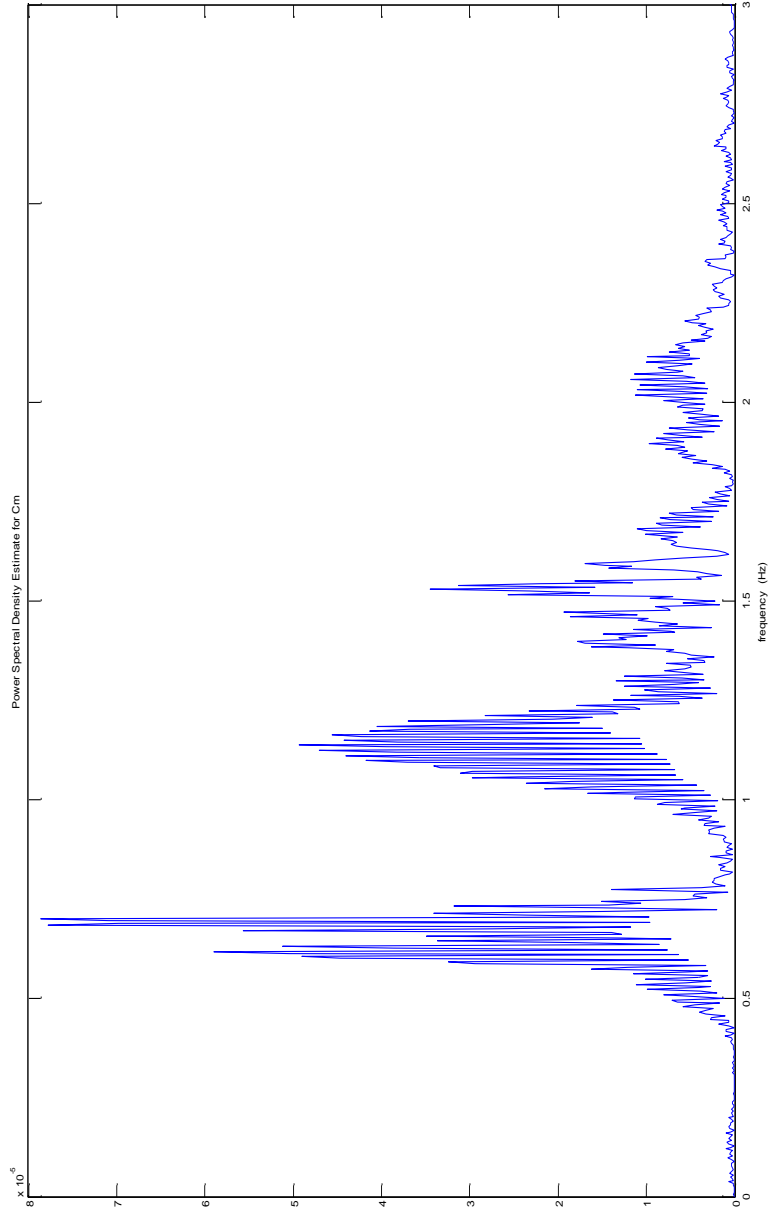


Figure 1. PSD for longitudinal motion (pitching)

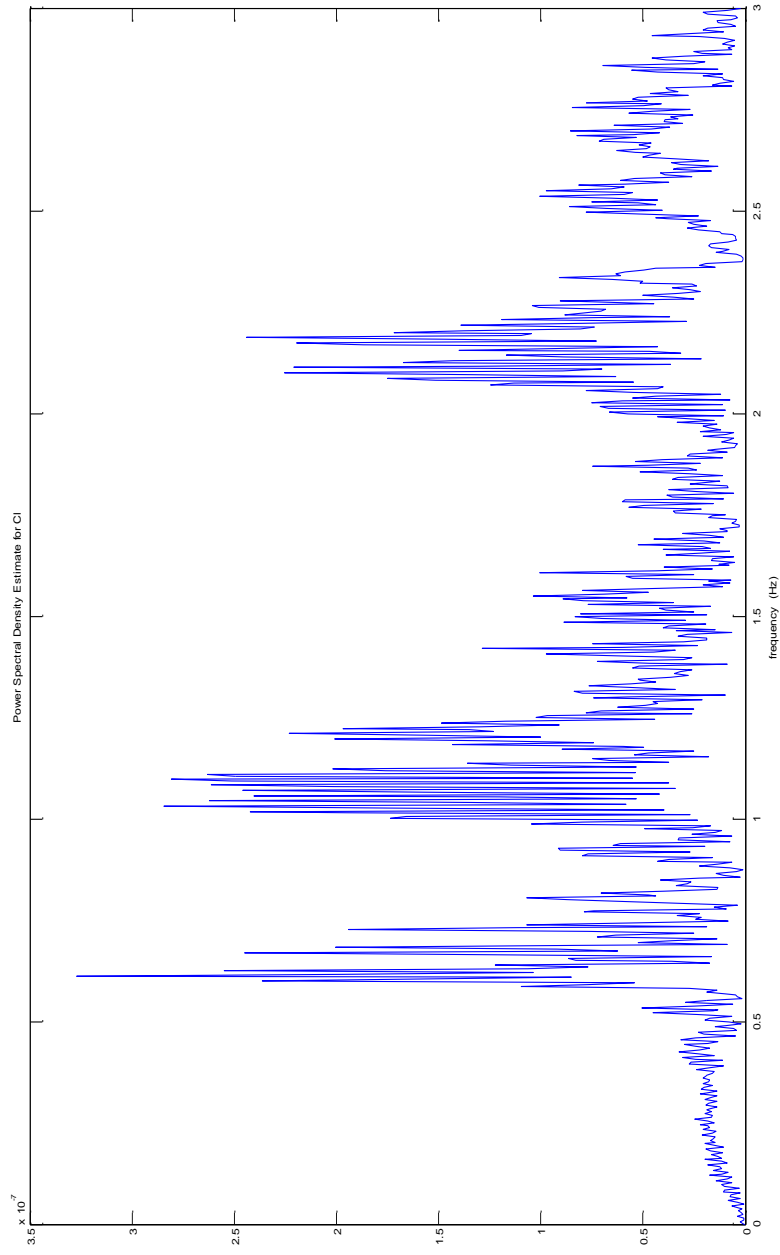


Figure 2. PSD for lateral motion (rolling)

Data collinearity is defined as *"any situation where regressors are correlated at a high enough level to cause problems in the parameter estimation"*, [16]. The main cause of data collinearity is the near-linear dependence of regressors. There are a number of possible sources of data collinearity:

1. Improper design of flight test maneuvers leads to data collinearity either due to insufficient excitation of FV modes, or changing the data of two or more regressors proportionally.
2. Constraints of the FV such as feedback control system lead to data collinearity. As Jategaonkar stated, [19], *"the controller reacts to the motion and suppresses the oscillatory and transient motion... it is detrimental to parameter estimation, because it drastically reduces the information contents required for estimating parameters"*. Also the control allocation algorithm of the flight vehicle may cause the collinearity, since some of the control surfaces are deflected proportionally based on some control mixing strategy hard coded to onboard flight computer.
3. Regressors that are small in magnitude can also cause data collinearity. If a regressor is small, then all the higher order regressors derived from it will be very small. Thus, they will be almost the same regressor, which will have an effect on the results as data collinearity.

System identification and parameter estimation of flight vehicles originally started with the need to identify the aerodynamic characteristics of the airplanes. Thus, almost all methods that are used in practice today were developed for identification of airplane problems. Figure 3 shows a typical airplane flight test maneuver history of Mach number, angle of attack, pitch rate, stabilator, leading edge and trailing edge deflections, [20]. Compared to FTD of an autonomous flight vehicle in Figure 4, the differences in the behaviors of the data sets are worth noticing. First of all, the FTD for the aircraft starts from a trim condition and throughout the maneuver, the flight parameters oscillate about the trim condition. Also notice the frequency of the oscillations; carefully designed inputs provide necessary excitation of the aircraft modes (longitudinal modes for the case of Figure 3).

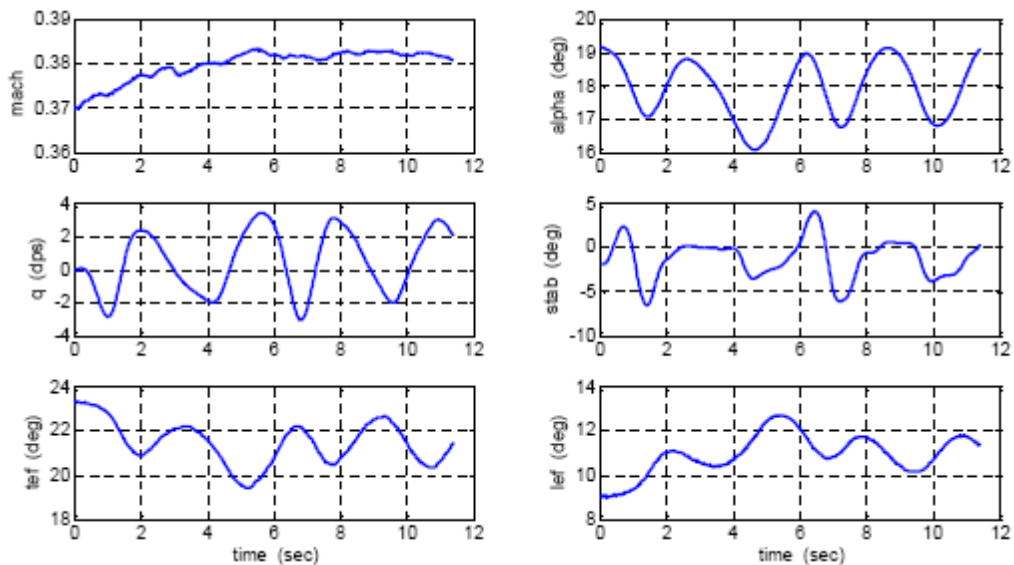


Figure 3. Typical flight test maneuver data, [20].

On the other hand, for the FTD from 4 different shots shown in Figure 4, the vehicle is always in trimmed flight, which is assured by the onboard automatic flight control system (AFCS).

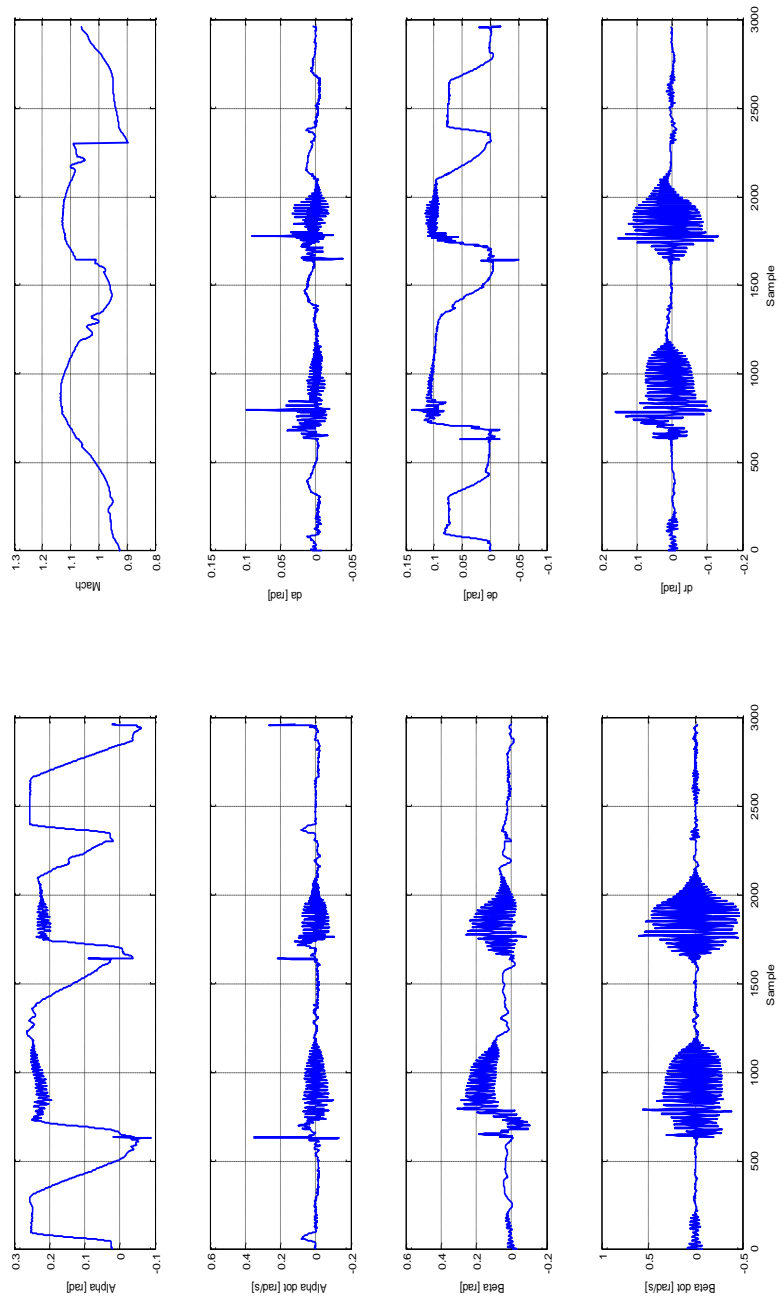


Figure 4. Flight test data for an autonomous flight vehicle (4 different flights).

Then, if the FTD of the autonomous flight vehicle can be made similar to an aircraft flight test data, the methods developed for aircraft can be applied. The easiest way to do this is to design flight test missions of the autonomous FVs to include some SI and PE maneuvers as well. Yet, this alone may not be enough since, the flight test maneuver design is based on a priori aerodynamics information and there is risk of under exciting the FV, which will result in low quality FTD or over exciting the FV, which might cause a loss of mission and the vehicle.

The stepwise regression method, which utilizes equation error method for parameter estimation, does not require the dynamics of the actual maneuver to be matched, that is it treats each data point separately. Thus, the FTD can be conditioned to look like an aircraft flight test maneuver data.

The FTD of Figure 4 inherently causes data collinearity where as this problem is solved with the conditioned FTD (Figure 5), which is obtained by trimming the original FTD (Figure 4), [12], [13].

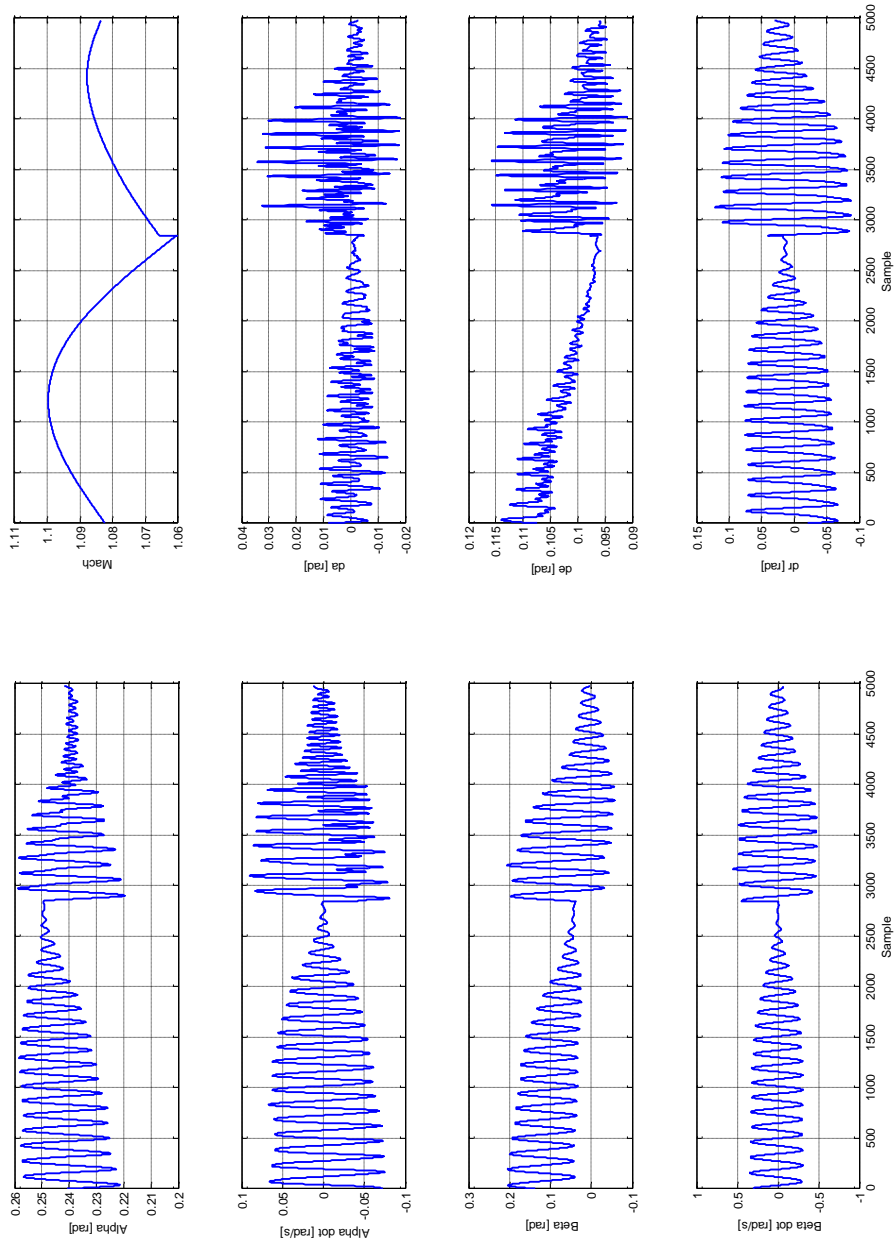


Figure 5. Augmented FTD for an autonomous flight vehicle.

3.4.1.1 Global Fourier Smoother

The equation of motion of any flight vehicle includes terms of angular accelerations. However, the onboard sensors measure the angular rates of the vehicle; thus the angular accelerations must be derived from the rates, unless opposite coupled accelerometer pairs are utilized. This causes a problem in numerical derivative operation, when the rate measurements are noisy. Similarly, time derivatives of flight angles (α , β) must be gathered from the flight angle measurements, and then the same problem is faced once again. In fact, regardless of whether the derivative of a signal is required or not, it is always preferred to work with noise free signals.

The common practice to get rid of signals is to utilize digital filters. However, filtering, if not applied correctly, can distort the system identification process since the phase and magnitude of the data are affected. Among a number of filtering methods, Global Fourier Smoothing is mostly preferred for applications of system identification with equation error method. The method is originally proposed by Morelli, [21], and application procedure can be found in Klein and Morelli, [16]. The Global Fourier Smoothing relies on the assumption that the noise signal has constant power over a wide frequency range; i.e., it is incoherent in contrast to the signal that contains the actual dynamics of the flight vehicle. Thus, the Fourier sine series coefficients associated with the noise signal will be almost constant throughout the frequency of interest where as

the Fourier sine series coefficients of the coherent signal (i.e., the actual dynamics of the FV) will rapidly decrease to zero. If, the Fourier sine series coefficients are plotted versus frequency, it is possible to discriminate between the noise and signal visually and select the cut-off frequency (Figure 6).

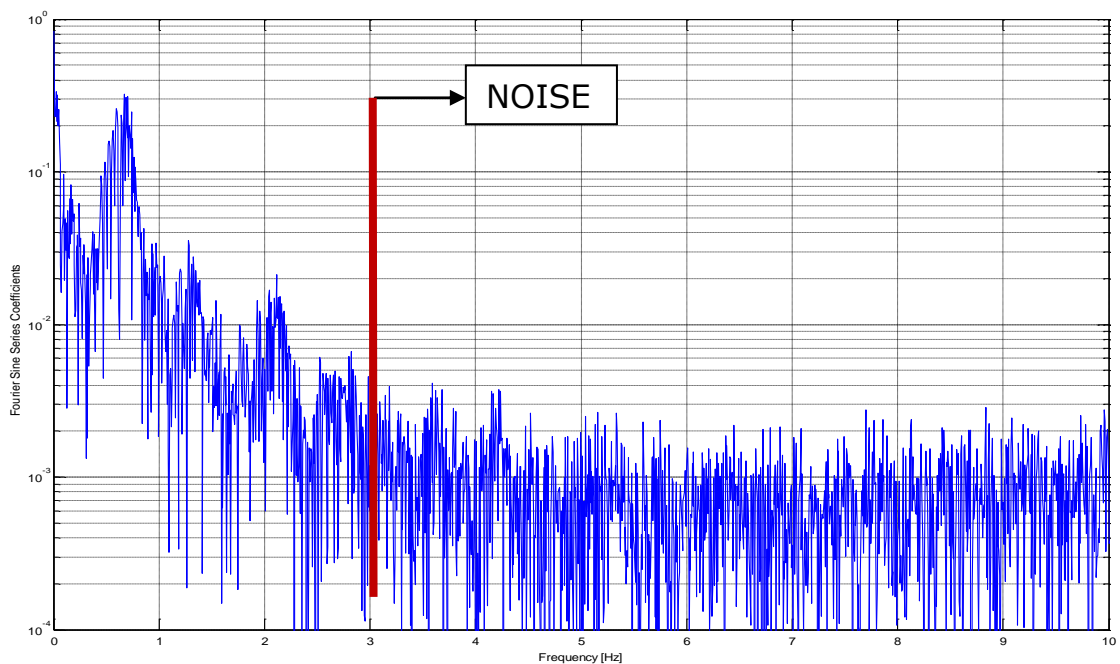


Figure 6. Fourier sine series coefficients plotted versus frequency

Once the cut-off frequency is determined, a digital filter can be designed to filter out noise. For this purpose, the Wiener filter, which was originally proposed by Norbert Wiener in 1949, is used, which is near unity at low frequencies, thus passes the Fourier

sine series components of the coherent signal and is near zero at cut-off frequency, thus removing the Fourier sine series components of the noise. Since the Fourier coefficients near the cut-off frequency is small by definition, the Wiener filter tolerates the small errors that might be done during the visual selection of the cut-off frequency. However, it is a wise idea to plot the magnitude of Fourier sine series coefficients in logarithmic scale to make the visual discrimination between signal and noise easier. Figure 7 shows an example of noisy signal, noise free signal and noise estimate.

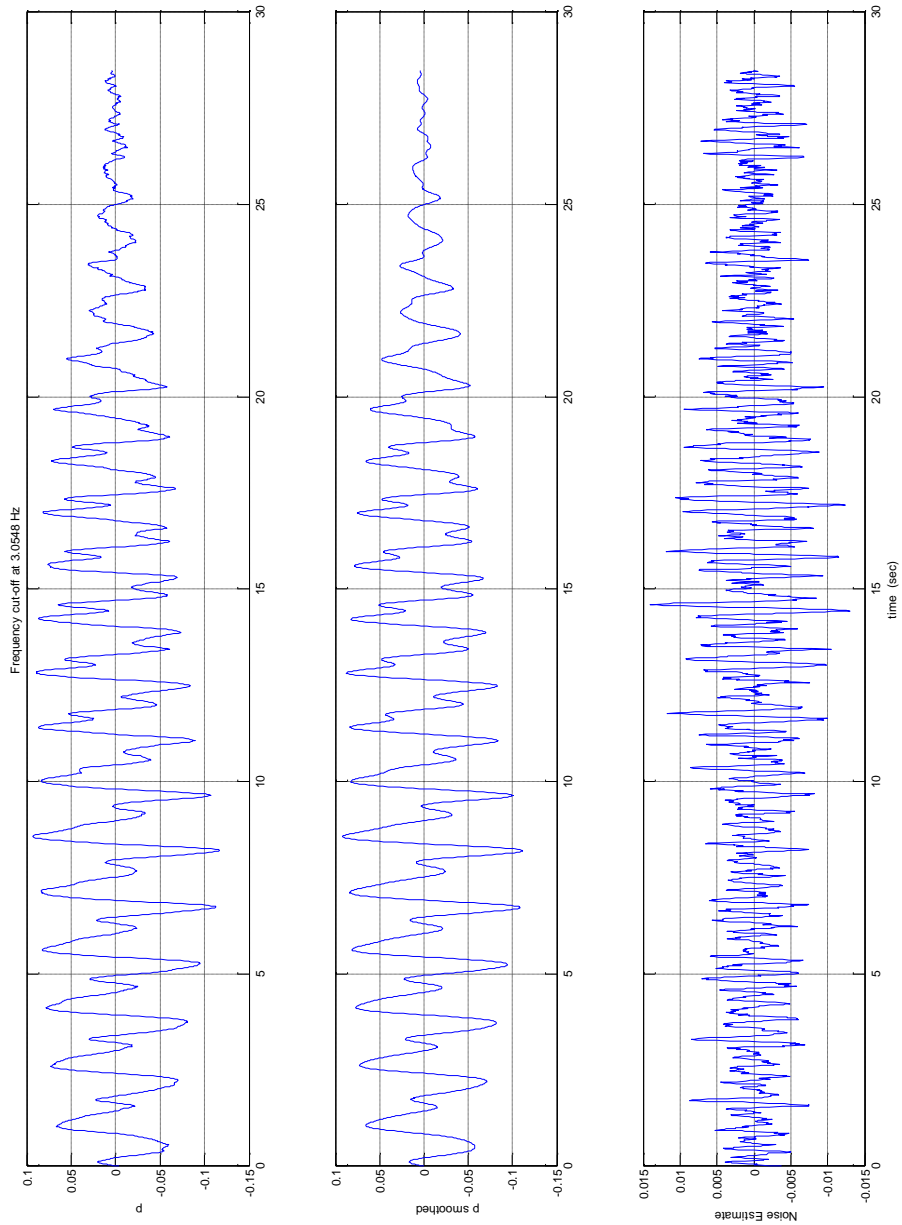


Figure 7. Rolling rate – smoothed, original signal and noise estimate

3.4.1.2 Partitioning Flight Test Data Based on the Ranges of Independent Flight Variables

Another important decision that affects the quality of the model and the accuracy of the parameter estimates is the partitioning of the FTD. For a time series with large variances in angle of attack, angle of side slip, and Mach number, it is a good idea to apply the partitioning. Although, there is no strict rule to follow, commonsense dictates that the partitions should be large enough to allow the demonstration of the underlying physics associated with motion, but short enough to allow easy correlation with the CFD or wind tunnel databases, if a priori information exists.

One straightforward approach to partitioning is to use the nodes of the a priori CFD or wind tunnel database. An update to databases is very easy for this case. However, this approach has a major drawback that, the size of the partitions are not controlled; that is there might be very large or small partitions depending on the selection of the nodes.

3.4.2 Complexity of the Model, Selection and Automated Generation of Regressors/Parameters

Maybe the most important question that needs to be asked is the following: "What should the maximum order of the model be?". In fact, this is not an easy question to answer. The order of the

aerodynamic model may change with the flight vehicle type, symmetry of the model, and flight regime.

Yet, it is a wise idea to use a-priori information while deciding on the model order. The preflight aerodynamic model, no doubt, covers at least some of the main effects of the independent variables. Whether a delta coefficient approach or a full model estimation approach is preferred, the complexity (maximum order) of the candidate models (pool of regressors/parameters) should at least be equal to the complexity of the preflight aerodynamic model. Based on the aerodynamic discussions of CHAPTER 2, an adequate pool of regressors can be assembled. Following table shows the aerodynamic coefficients and flight variables associated with them.

Table 1. Aerodynamic coefficients and associated flight variables

Coefficient	Associated Flight Parameters
C_x	M, α, β, δ
C_y	$M, \alpha, \beta, \delta_a, \delta_r, p, r$
C_z	$M, \alpha, \beta, \delta_e, q$
C_l	$M, \alpha, \beta, \delta_a, \delta_r, p, r$

Coefficient	Associated Flight Parameters
C_m	$M, \alpha, \beta, \delta_e, q$
C_n	$M, \alpha, \beta, \delta_a, \delta_r, p, r$

Notice in Table 1, C_x is associated with a coupled flight variable, δ . As shown in Eq. (30), δ is a combination of control commands (δ_a , δ_e and δ_r). The reason for the definition of a new flight parameter is the behavior of axial force with the control commands for an automated flight vehicle.

$$\delta^2 = \delta_a^2 + \delta_e^2 + \delta_r^2 \quad (30)$$

Once the decision on the model complexity is reached, the regressors themselves must be generated. This requires the utilization of an adequate combination algorithm.

A brief literature survey revealed the use of combinadic concept, which is basically a binary indexing system for combinations generated from a finite set. However, combinadic is not the cure, since not only first order combinations from a finite set are needed, but higher orders are necessary for the automated regressor generation as well.

Dr. Morelli's SIDPAC, [16], which is an open source collection of Matlab[®] scripts designed for flight test data processing, system identification and parameter estimation, utilizes an indexing system which is not binary, so that powers of every term that make up a regressor can be kept as a list. However, it is seen that, this approach to automatic regressor generation might fail to prevail when the size of the flight parameters is larger than 7, due to computational issues.

Then, a new regressor generation algorithm is devised. In this new approach, the first step is to generate the powers of independent variables. Then, the combinations of the independent variables and their powers are generated. An important step is checking for validity: A regressor is valid if its power is smaller than the maximum allowed power. The devised algorithm utilizes a two step validation check: Obviously invalid combinations are not generated in the first step and the validity of generated regressors is checked in the second step. For example, if combinations up to power 4 are sought, the combinations including more than 4 terms are not generated, since even their first order combinations have cumulative power more than 4. This algorithm (Figure 8) is tested against SIDPAC's algorithm for speed, and is almost twice faster.

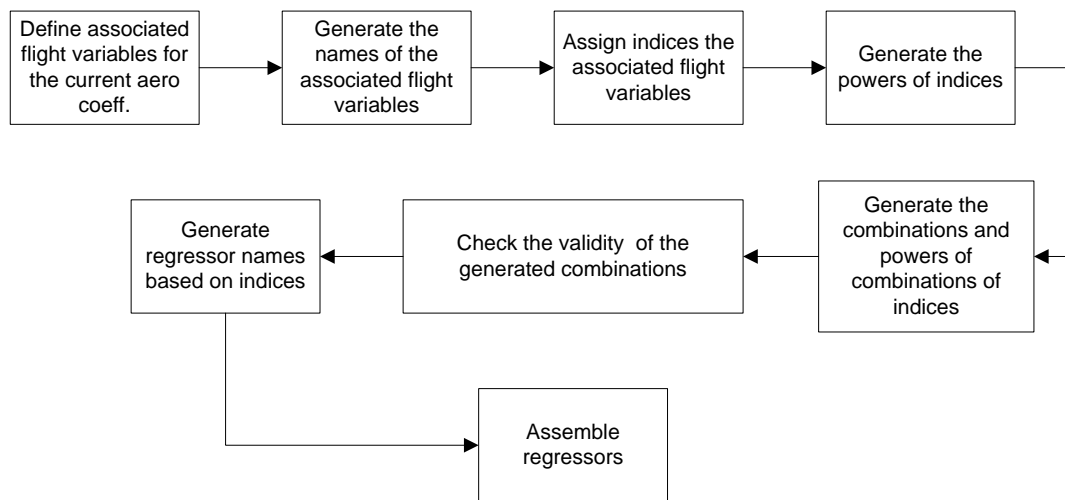


Figure 8. Flow chart of automated regressor generation

3.4.3 Selection of Run Parameters and Stopping Rules

As aforementioned in Section 1.3, one of the goals of this doctoral study is to devise a procedure that identifies the model structures and estimates the parameters with minimum intervention. From this sentence, the need for an automated selection routine for stepwise regression method is obvious.

The selection criteria given in Section 3.1 are straightforward: First select the regressor with higher correlation then add the regressor with the highest partial correlation until the stopping criterion is achieved. Yet, there are some methods to be employed in order to obtain good models.

First method is to add some physics into pure mathematics of the stepwise regression. From an engineering point of view, it is always preferred to work with simple models; i.e., a higher model complexity is not desired. Yet, it is not uncommon for stepwise regression to go for complex models if the selection criteria are left as explained before. For example, a case where the regressor with the highest partial correlation is of order 4, where as a first order regressor with slightly smaller partial correlation can exist, then the algorithm will go for the higher order one.

To employ this method and introduce physical insight into the selection scheme, it is decided to use a search window of variable height which starts from the highest correlation/partial correlation regressor and stretches downward. The height of the window shrinks, if the highest correlation/partial correlation is close to 1 and eventually it becomes zero at 1. Once the height of the window is selected, all the regressors that have correlation/partial correlations within this window are selected and sorted in ascending order with respect to their complexity. Then the regressor with the least complexity (minimum order) is selected and added to the model and the stepwise regression algorithm continues to the next step.

Different approaches can be followed in determination of the search window height. The straightforward approach is to use a

linear mapping function for this purpose. Eq. (31) shows the form of such linear mapping function, where WH denotes window height, LCL is the lowest partial correlation that is allowed in model, SF is the scale factor of the mapping and HC is the highest partial correlation in the current step of the stepwise regression:

$$WH = SF * LCL + HC - LCL * (0 - SF * LCL) / (1 - LCL) \quad (31)$$

After some trials with linear mapping, it is found out that a function which provides bigger search window sizes when the correlations are close to 1 is needed. Then, a function form, which rapidly expands the size of the search window near 1, but then gradually increases it for lower correlations is sought. The transformation functions in the form of Eq. (32) provide such a mapping, where PW is the power as integer.

$$WH = \frac{1 - HC^{1/PW}}{SF} \quad (32)$$

After some trials with the simulated and actual flight test data, a scale factor of 20 and power of 0.25 is selected as the search window sizing function, which provides sizes close to 0.5 scale factored linear mapping for low correlations and bigger window

sizes close to 1. Figure 9 shows the comparison of different window sizing functions.

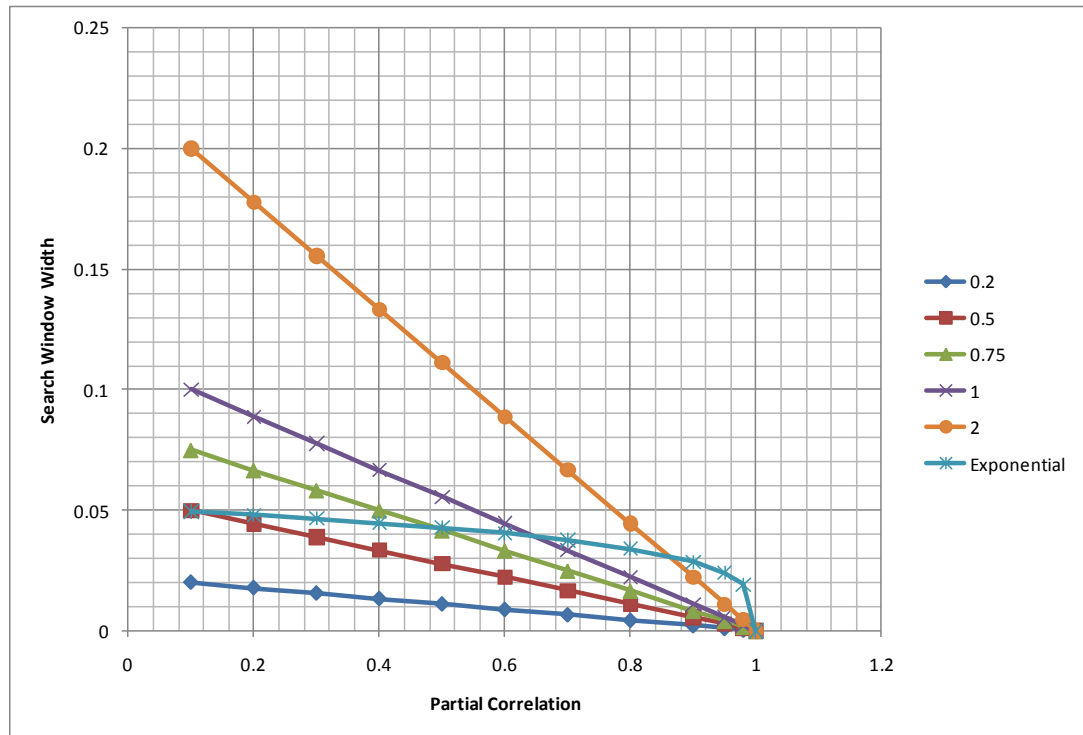


Figure 9. Comparison of different search window selecting functions and scale factors

Another method is to factor out cross correlated regressors from the selection pool. At every selection step of the stepwise regression algorithm, the parameter correlation matrix is searched for correlated regressors. If there exist some correlations between

regressors in the model, then this shows up as large elements of parameter correlation matrix. As a rule of thumb, Klein and Morelli, [16], suggested that any value larger than 0.9 is a sign of strong correlation between parameters (regressors) of the model. If this is encountered, then the regressor causing the correlation; i.e., the one added latest, is removed from the model and deleted from the pool of candidate regressors. Since the algorithm selects the parameters of the model from the pool of regressors based on their correlation/partial correlation metric, the deletion of a regressor does not introduce any complications to the estimation algorithm; parameters with higher importance have already been included! Then, the algorithm carries on searching for other regressors which might be included in the model without causing correlation with the parameters already in the model.

Although a lower limit is suggested by Klein and Morelli, [16], a value over 0.95 for parameter-to-parameter correlation limit can be used for autonomous flight vehicles of interest.

There are two fundamental stopping conditions for the stepwise regression method: The partial correlation and F-ratio limits. That is, during the stepwise regression run, if the partial correlations of the regressors outside the model are below the specified partial correlation lower limit and at the same time the F-ratios of the regressors inside the model are above the F-ratio lower limit then

the algorithm stops. Yet, these two conditions are not enough alone.

The first additional stopping condition is the predicted square error (PSE). The algorithm can carry on, as long as PSE decreases. Yet, at one stage, before the fundamental stopping criterion kicks in, PSE may start growing. This indicates that the model is becoming over parameterized; meaning that the prediction capability of the model is decreasing. So, the automated stepwise regression algorithm stops, whenever PSE starts growing.

Two other additional stopping rules are related with the goodness of fit criteria. First, a limit on goodness of fit (R^2) improvement is used. Although a limit of 1% is recommended for goodness of fit improvement in the literature as a rule of thumb, it is found that a lower limit can lead to better estimates provided that parameter-to-parameter correlations are not allowed in the model. The second stopping condition is the monotonic increase criteria for adjusted goodness of fit metric. As opposed to PSE, if the adjusted R^2 metric starts to decrease, the algorithm stops.

Finally, a convergence time limit is used as a safeguard. On rare occasions, the stepwise regression algorithm may stick in a cycle; i.e., the regressor added in the previous step is excluded in the current step and added in the next step. If such a loop occurs;

i.e., if the stepwise regression routine is not completed within the allowed convergence time limit, the automatic decision routine stops the stepwise regression algorithm. After experimenting with different desktop PC's and workstations, it is decided that 300 seconds is a reasonable convergence time limit.

Following flow chart summarizes the flow of the model structure determination and parameter estimation algorithm with implemented rules.

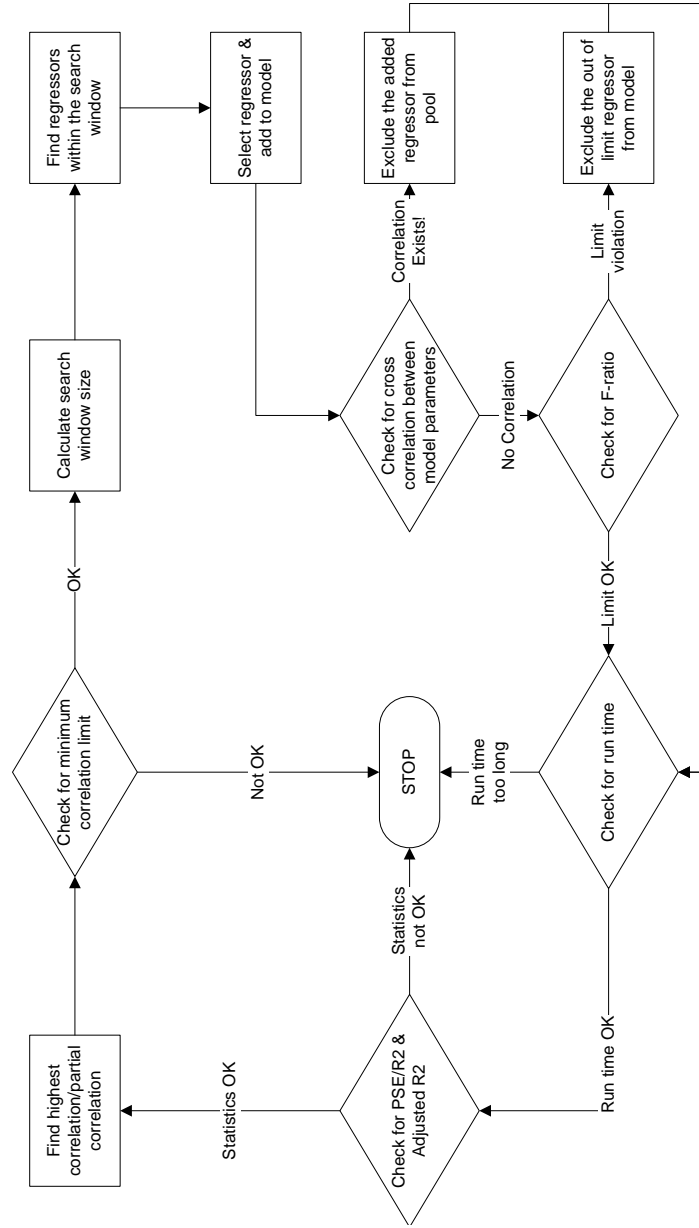


Figure 10. Flow chart of model structure determination and parameter estimation

3.4.4 Compensating for Non-Standard Conditions of Flight Test

In a sense, the atmosphere itself is the most correlated regressor of all, since it has the biggest effect on aerodynamic forces and moments. However, the atmosphere is very hard to predict and is a major error source for a flight vehicle which is not equipped with an onboard air data computer.

There are a number of different models to predict the behavior of atmosphere, and also different means of measurement to gather real time data. However, each has its own limitation. For example, flying meteorological balloons to obtain real-time density, pressure and wind information is a common practice for artillery battalions. With a relative ease of operation and low cost, this method provides a valuable information but has a limited applicability, since the motion of the balloon is not controlled and it is a matter of minutes before the balloon drifts away from the probable trajectory of the artillery shell.

It is not feasible to obtain meteorological conditions on the probable/actual trajectory (of artillery shells or any type of flight vehicles) via measurement, but still it is needed to apply corrections to incorporate the effects of non-standard conditions; i.e., deviations from the standard atmosphere. This is accomplished by the utilization of meteorological models.

One of the most preferred prediction models is the Fifth-Generation NCAR / Penn State Mesoscale Model (MM5). In Turkey, General Administration of Meteorology provides weather forecasts based on MM5. Every day, starting at 00 hours UTC, weather forecasts are run and published via internet every six hours, which are valid for a duration of 48 hours. Nevertheless they are most accurate only for the first 6 hours. However, due to run time of weather forecast code, delays occur between start of run and publishing of forecast. It is possible to obtain meteorological report for a desired region within whole Turkey based on MM5 data.

The meteorological forecast data is required at a number of points located on a uniform or non-uniform grid about the trajectory of the flight vehicle. For each grid point, the temperature, pressure density, wind direction, and wind speed were forecasted as a function of the height above sea level and time (in UTC).

As first step to obtain predicted meteorological conditions on a trajectory, the computer meteorological report at each grid node must be interpolated in time to obtain meteorological conditions at the time of flight test at each node. It is assumed that, meteorological conditions vary linearly within an hour time.

At the second step of the algorithm, it is necessary to perform an interpolation in spatial dimensions. The meteorological data is provided as uniform planes above sea level, so that it is possible to interpolate them on height. A linear interpolation is performed at every met node with flight vehicle's height from sea level as input. It is suggested that, pressure does not vary linearly but its logarithm, [22]. However, it is noticed that, density also exhibits a similar behavior, so a linear interpolation is performed for the logarithms of these two variables and then inverse logarithms are taken.

Next, for every point of flight vehicles trajectory, a 2D (planar) distance calculation is performed to obtain distances between met nodes and trajectory. These distances are normalized, so that their sum is equal to 1 and the smallest distance has the biggest weighting coefficient. Next, a weighted sum approach is followed to find the forecasted meteorological conditions on the trajectory.

Figure 11 shows the met nodes, trajectory of a flight vehicle and interpolated wind information during one of the test runs.

Interpolated Wind Directions and Velocities During Test Run of H34_s8_a2 at 1342 (using MMS Meteorological Report Data)

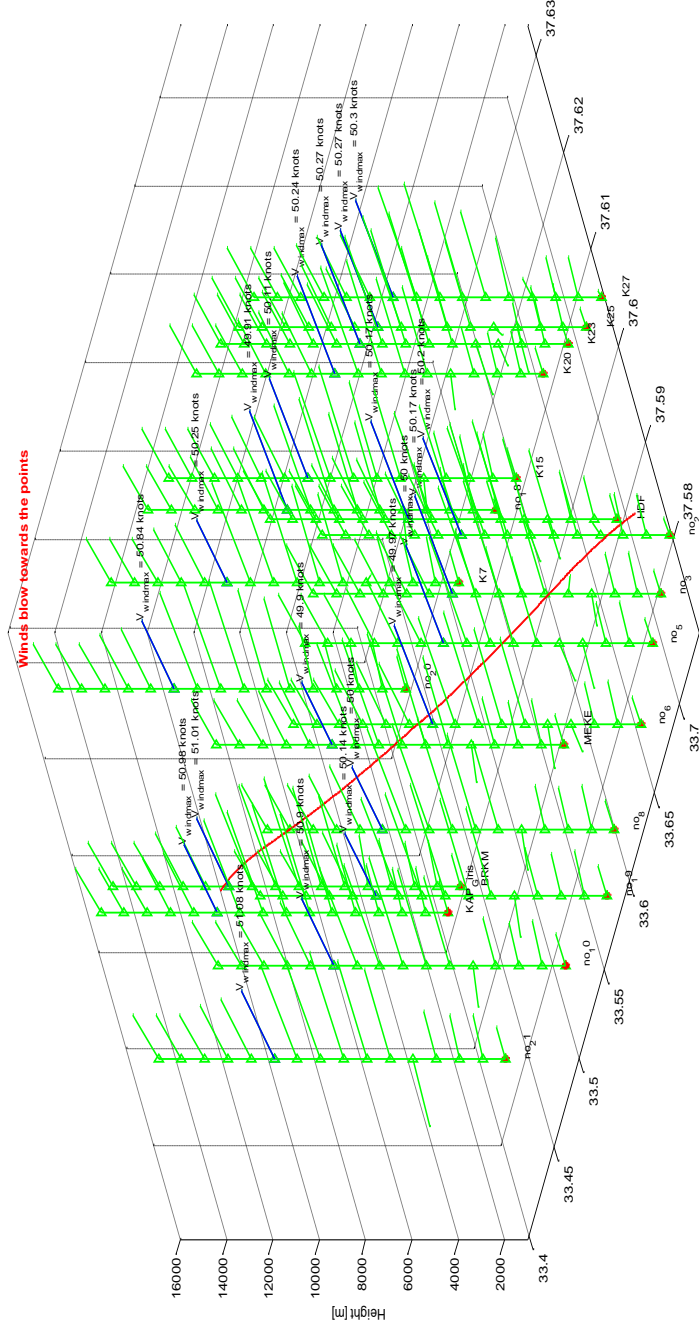


Figure 1.1. 3d view of Karapinar Proving Ground wind conditions during test run H32_s8_a2

When meteorological conditions on every point of the flight test trajectory are known, it is possible to correct the following variables for the effects of non-standard conditions:

- Body linear rates ($V_{\text{north}}, V_{\text{east}}, V_{\text{down}}, u, v, w$)
- Flight angles (α, β)
- Mach number (M)
- Dynamic pressure (q)

Figure 12 through Figure 15 show the measured/calculated values of some flight parameters versus their corrected values for the forecasted meteorological conditions.

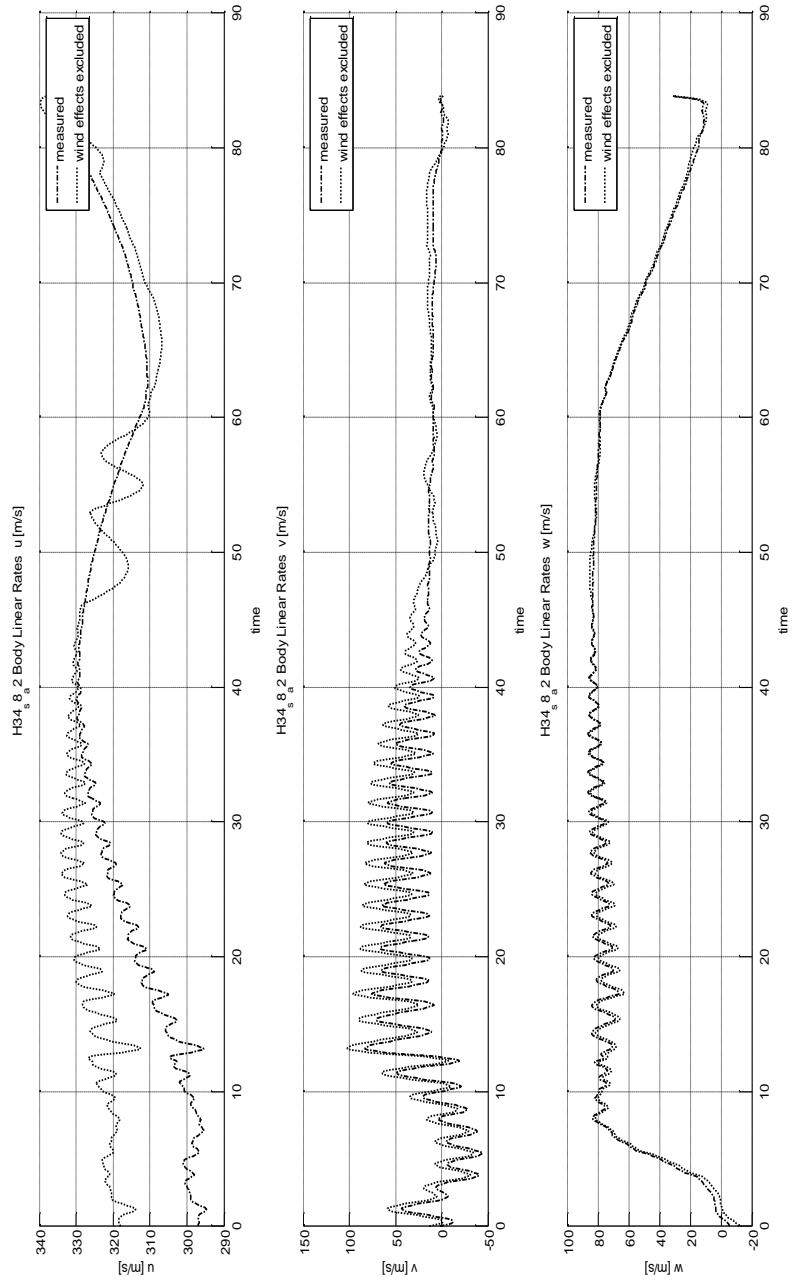


Figure 12. Body rates with and without correction for meteorological conditions

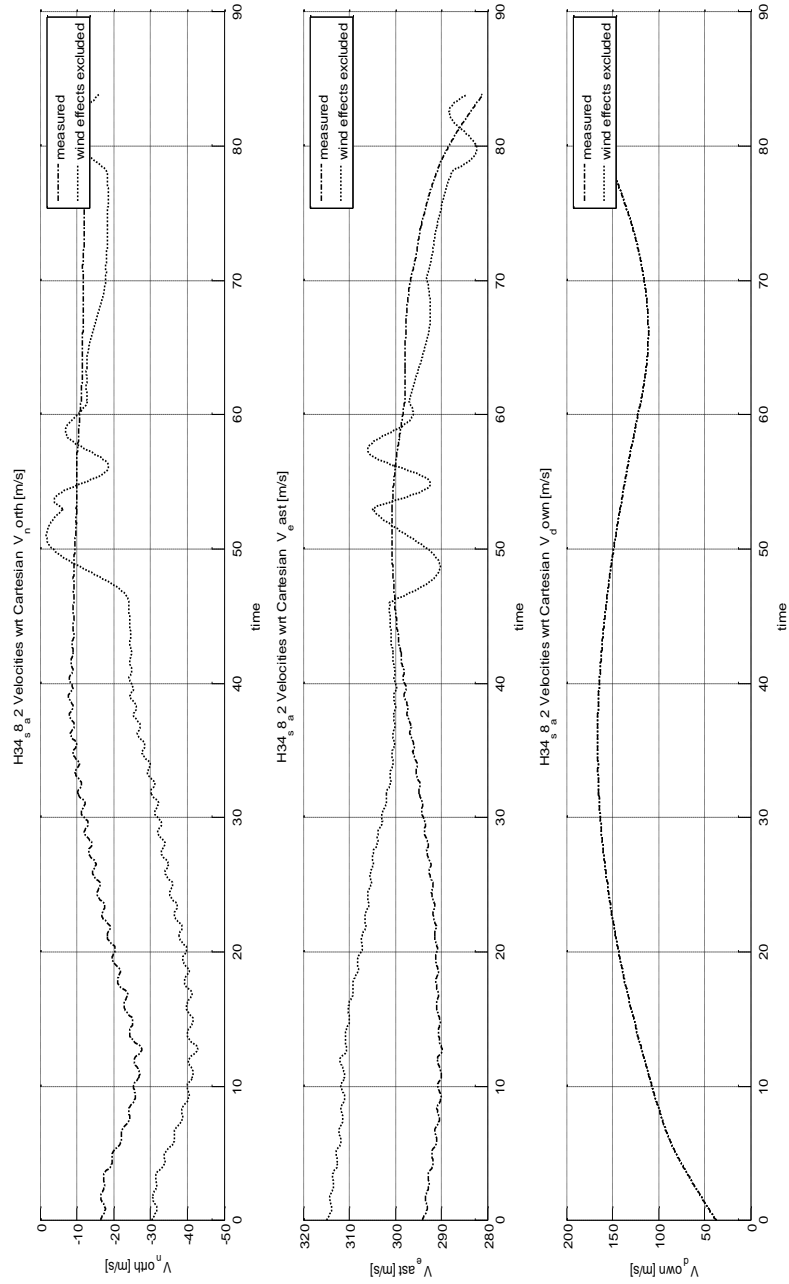


Figure 13. Cartesian velocities with and without correction for meteorological conditions

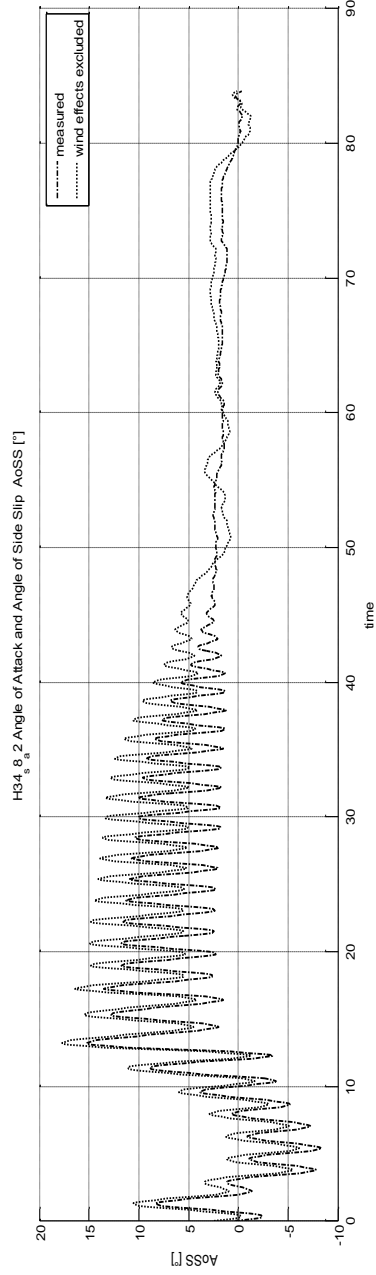
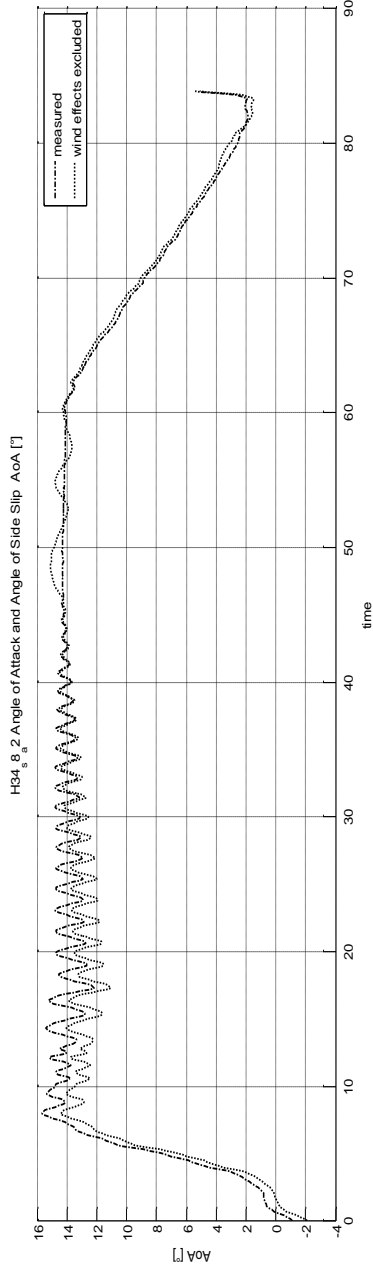


Figure 14. Flight angles with and without correction for meteorological conditions

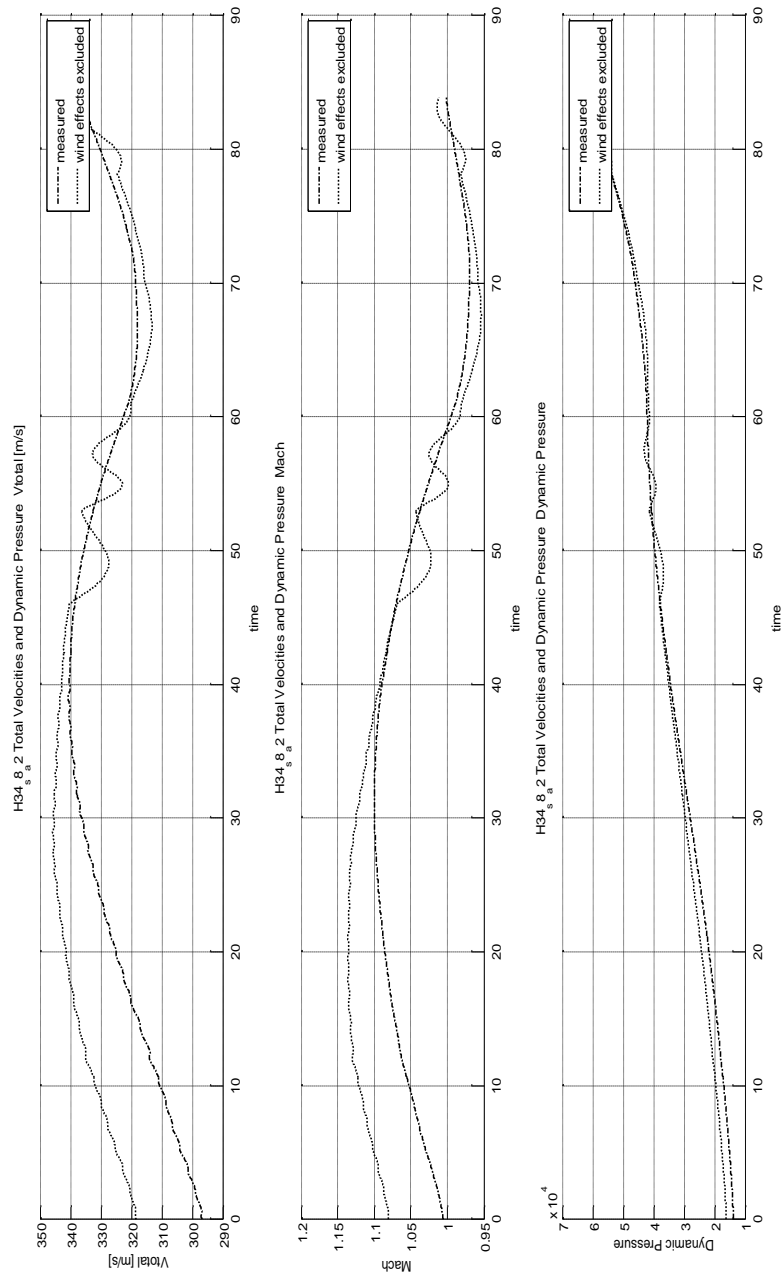


Figure 15. Total velocity, Mach number and dynamic pressure with and without correction for meteorological conditions

CHAPTER 4

CLOSED LOOP AERODYNAMIC PARAMETER ESTIMATION USING GENETIC ALGORITHM

The equation error method explained in CHAPTER 3 is a powerful tool to determine the model structure. Yet, as stated by Morelli and Klein [2], the parameter estimates of the equation error method for an actual flight test data are not as efficient and consistent as the theory states. Then, the estimates of the equation error method serve as the starting point of more complex parameter estimation methods.

This chapter deals with the optimization based parameter estimation methods and proposes a new approach to the aerodynamic parameter estimation problem using flight test data.

4.1 Output Error Method

One of the most widely used methods in practice is the output error method (OEM). It basically minimizes the error between the

actual (measured) vehicle variables and simulated ones. This is performed in an iterative manner, by employing optimization techniques. Yet, there are a number of different approaches to the output error method, which vary mostly on the method of optimization used.

As Jategaonkar states [19], the theoretical foundations of the method rely on the maximum likelihood principle. The method has been in practice since 1960s and successfully applied to many identification problems of different flight vehicles. The name maximum likelihood (ML) comes from the fact that the method produces the estimates for the parameters for which the measured data is most likely to occur. In its general form, the ML method can be used for the parameter estimation of both linear and nonlinear dynamic systems with some measurement noise. It is an advantage of the method that it assumes some known inputs and noisy measured aircraft motion variables, which are consistent with typical flight test measurements. If the model for which the parameters are sought is free of errors, then the parameter estimates of ML are "*consistent, unbiased, and efficient*", [2].

The OEM method relies on a number of assumptions as listed below. However, as Dr. Jategaonkar states, the basic rule of system identification/parameter estimation is still valid: "*If it is not in the data, it cannot be estimated*", [19]:

1. The input sequence is independent of FV response.
2. The measurement errors at different discrete time points are statistically independent and distributed with zero mean.
3. The FV response is corrupted by measurement noise only. Yet, if the vehicle encounters turbulence or wind gusts during the flight, then there will be additional disturbances on the measurements. However, if such a situation occurs during the flight tests, the data collected is discarded and not used for estimation.
4. Control inputs are sufficiently and adequately (in both magnitude and frequency) varied to excite dynamic modes of the FV.

Although the flow chart of the method is straightforward (Figure 16), the implementation varies especially in the selected optimization routine.

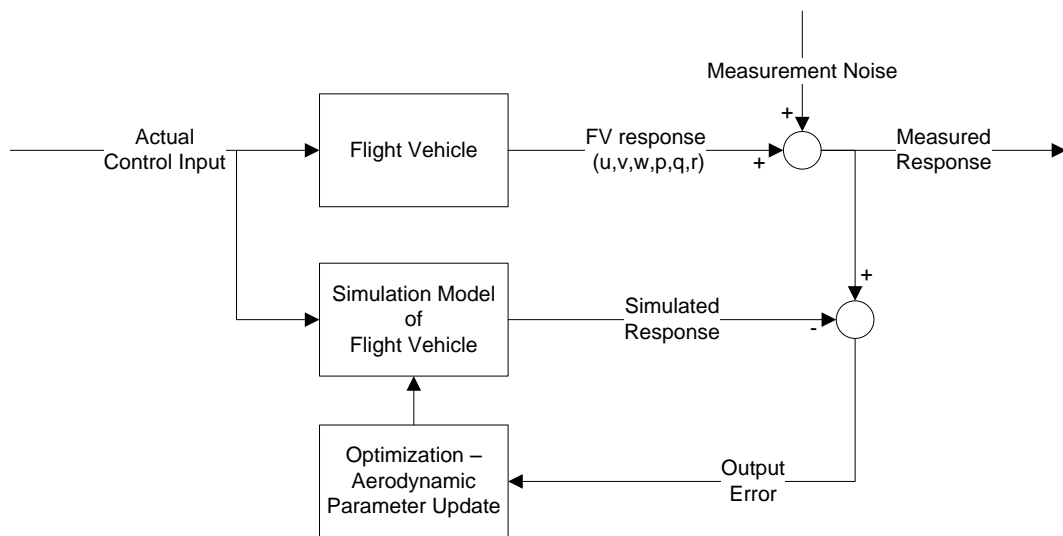


Figure 16. Flowchart of Output Error Method

The classical implementation of OEM has some shortcomings in practice. These shortcomings are mostly associated with the simulation model. If the starting aerodynamic model is not adequate enough, or the parameters are not close enough to actual values, or the parameters are not physically relevant (as might be encountered if the optimization routine is selected as genetic algorithm), there is a risk of crashing the simulation run. To avoid this problem, a common practice is to move along in time during optimization: The optimization starts with a small segment of the data. As the convergence is achieved the segment grows until it covers the entire range of the FTD. Although this workaround is successfully realized, it lengthens the computational time.

4.2 Closed Loop Optimization to Minimize Control Input Errors

Another workaround to potential simulation crashing problem is providing some robustness in the simulation model. This can be obtained if the simulation is run in a closed loop manner, thus utilizing the actual guidance law and autopilot in simulation model.

This process is known as “closed loop system identification” in the literature and as stated by Whorton, [23], [24], it is “the identification of the open-loop plant given closed-loop response data and knowledge of the compensator dynamics”. In the literature, the closed loop system identification is mostly used for controller design and tuning, [25], [26], [27], and when it is used for plant model identification, the output error is used as the cost function, [24], [28], [29].

In an application of closed loop system identification (which will be termed as closed loop optimization from here on) approach to aerodynamic parameter estimation, as an alternative to using the error in response of the actual FV and simulated FV (error in output), the error in actual control input and simulated control input can also be used. This proposed input error approach has an advantage over the traditional OEM: Control inputs can be obtained free of measurement errors during the flight test, since they are the outputs from the onboard digital computer, where as

the actual flight vehicle responses are measured with noise or calculated from noisy measurements.

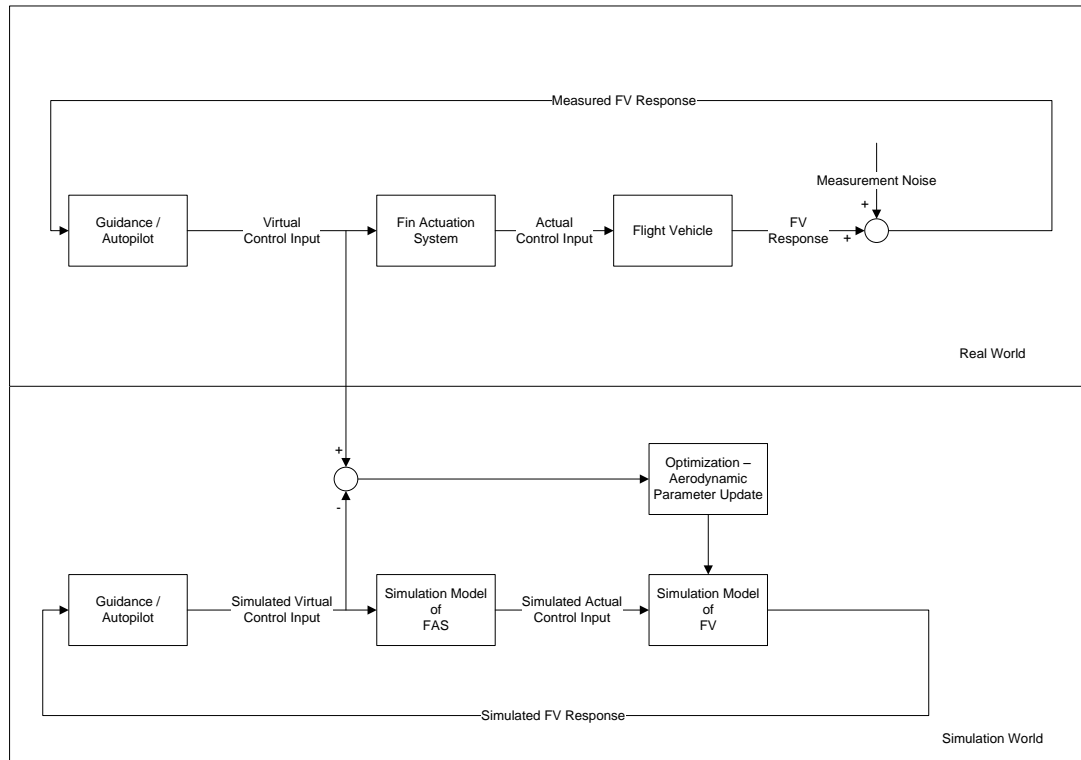


Figure 17. Flowchart of the Proposed Estimation Method

Yet, in the closed loop optimization, not only the use of actual guidance law and autopilot is necessary but it is also crucial to implement a realistic fin actuation system (FAS) model. However, the FAS model might itself contain some modeling errors. This might be overcome by applying an estimation run on the FAS model before the actual estimation run for aerodynamic

parameters; otherwise, errors due to inaccurate modeling of FAS will also be compensated by aerodynamic parameters.

Of many different optimization algorithms used for aerodynamic parameter estimation,[16],[23],[19], genetic algorithm is selected for use with the proposed closed loop optimization with input error approach.

The main reason behind this choice is the major advantage of genetic algorithms over the traditional optimization algorithms: Genetic algorithms do not require feasible initial estimates to reach a global extremum of the solution, thus the optimality of the solution is guaranteed. However, the time required to reach the solution is longer than the traditional methods.

The genetic algorithms and their applications are hot topics in engineering and many references as well as textbooks are available in the literature. Yet, very briefly summarizing, genetic algorithms are mathematical methods for global search and optimization that are based on the mechanics of natural selection and science of genetics. According to the Darwinian theory of evolution, the members of a population that have the best characteristics to survive prevail, while the rest are eliminated. This is known as the survival of the fittest. Genetic algorithms work on the following basic principle: The members with best

scores with respect to some cost function prevail and given enough time a best member is obtained.

A genetic algorithm starts by creating an initial population. The fitness value for each individual of the population is calculated and the individuals with the best fitness values, called as elites, are carried on to the next generation. The rest of the next generation is generated via mutation of a single parent or crossover of two parents from the initial population. The procedure is repeated until the stopping criteria are reached.

The mechanisms of biological and computational steps of natural selection are explained in detail by Whorton [23],[24] and practical considerations for application can be found in Matlab[®] Optimization Toolbox Manual, [30].

4.3 Run Parameters and Cost Function

The genetic algorithm selected to use is a readily available software package from Mathworks, which is built-in to Matlab[®] via the (Global) Optimization Toolbox. The parameters that should be tuned in a genetic algorithm run of Matlab[®] to obtain good results are listed, [30], with their proposed values as follows:

- **Initial Range:** Diversity is the average distance between the individuals. Despite a widespread information genetic algorithm cannot find the global minimum if the population is not diverse enough. On the other hand if it is too diverse it takes a lot of time to converge. Diversity is not directly controlled but based on the initial range used to generate the initial population and amount of mutation. That is, the initial range is a crucial parameter for the convergence and success of Matlab's genetic algorithm. A very large initial range will prevent the algorithm from converging, while a small range has the risk of missing the optimal point. For the aerodynamic estimation problem in hand, the initial population range should be selected based on the prior knowledge, either from CFD analyses or wind tunnel test results or equation error method estimations.
- **Population Size:** Population size is the number of individuals present in each generation of the genetic algorithm run. The larger the population size is, the more available search points are, thus better the final result is. However, as the population size gets larger, the computational time grows. Thus, a fine balance must be maintained between the run time and population size. The minimum requirement is that, the population size must not be smaller than the number of parameters. However, based on many runs with simulated and actual flight test data during the course of this doctoral study, it is observed that a population size of at least three times the number of parameters is required for aerodynamic parameter estimation.

- **Maximum Number of Generations:** Maximum number of generations is another important parameter of the algorithm which affects the outcome directly. Selecting a small number for the maximum number of generations causes the genetic algorithm to terminate prematurely, while a big number is inefficient way of spending computational time. However, the decision on the maximum number of generations should be made together with the method of mutation.
- **Hybrid Function:** The genetic algorithm takes quite long (run times of about 15 days on desktop PC's (Intel Core2 Quad and alike) and workstations (AMD Opteron 128 and alike) are typical for a flight test data of 60 seconds) to converge, and as the population gets closer to the optimal point, the rate of improvement decays. Then, it is a wise idea to utilize classical gradient based optimization to obtain the final parameters, once the genetic algorithm converges around the optimal. This approach unites the bests of both worlds; a global optimum in a relatively short time. The Matlab[®] Optimization Toolbox, [31], provides useful gradient based built-in optimization functions which can be used as hybrid functions. The aerodynamic parameter estimation problem is a constrained type optimization problem, since the parameters are bounded around an initial estimate (prior information based). Then the selected hybrid function for this purpose is the fmincon, constrained minimization function of Matlab[®] Optimization Toolbox.
- **Mutation Function:** In any population, there are three ways for the reproduction. First the elites are passed on the next

generation. The second mechanism is the crossover, which is the mating of two individuals in the current generation in order to obtain a child. Thus, genes from different individuals are combined into a new individual. Then, the remaining children are generated by the mechanism which is called the mutation. Mutation is randomly changing an individual's parameters in the current generation to obtain a child. Thus, mutation adds to the diversity of a population and increases the likelihood that the algorithm will generate individuals with better fitness values. Matlab[®] genetic algorithm has two different ways of generating mutation. The default is called the Gaussian mutation, which is adding a random number, chosen from a Gaussian distribution, to each entry of the parent vector. The alternative is to use adaptive feasible mutation, which randomly generates directions that are adaptive with respect to the last successful or unsuccessful generation. Based on genetic algorithm runs with simulated and actual flight test data during the course of this doctoral study, it is advised that the minimum number of generations must be at least 100 for mutation function adaptive feasible and 150 for Gaussian, in order to obtain feasible start points for hybrid function run. Yet, it is safe to run with more than 150 and 200 generations respectively. Also, if the shrink parameter, which is a control flag for rate of decay of mutation as the population evolves through generations, is set to zero, then the minimum number of generations must be higher than 250. Because of this situation, the duration advantage of Gaussian mutation over adaptive feasible diminishes

(Gaussian mutation ignores bounds on the optimization states, where as adaptive feasible regards them, thus optimization with Gaussian mutation evolves faster than optimization with Adaptive Feasible).

- Cost function: The proposed methodology is based on minimizing the error in the input. Thus, the cost function should be constructed such that, it minimizes the error between the actual in-flight recorded control inputs and simulated ones in a least squares sense, Eq. (33):

$$f_{obj} = \sum_{t=0}^{t_f} \sum_{i=1}^4 \frac{\delta_{i_{flight}}(t) - \delta_{i_{sim}}(t)}{2} \quad (33)$$

Yet, the cost function definition given in Eq. (33) is itself is not sufficient for a stable optimization. Since, there is no constraint on the number of data samples (that is the length of simulated trajectory), the generation evolves to physically meaningless parameters that tend to terminate the trajectory in relatively short times, rather than following the actual flight test trajectory.

To overcome this problem, two alternative approaches are possible. In the first approach, a final position penalty is included in the cost function. Thus, the simulation runs that terminate farther away from the actual hit point receive

higher penalties, which in turn force the evolution towards the parameters that result trajectories closer to the actual flight test run. Eq. (34), shows the updated (and equally weighted) cost function with such a final position penalty. Notice that, to avoid the dominance of any objective over the other, the fin deflections are scaled with their maximum and minimum values that occur in the flight to 0-1 range and the final position penalty is scaled such that the individual trajectories that terminate within 500 meters of actual trajectory end point receive penalties less than 1.

$$\begin{aligned}
 f_{obj} &= \int_{t=0}^{t_f} \sum_{i=1}^4 \frac{\delta_{i_{flight}}(t) - \delta_{i_{sim}}(t)}{2} \\
 &+ \frac{x_{flight} - x_{sim}}{500}^2 + \frac{y_{flight} - y_{sim}}{500}^2 + \frac{(z_{flight} - z_{sim})^2}{500}
 \end{aligned} \tag{34}$$

An alternative approach for implementing a final position penalty is to force the simulation to run longer, by scaling the data length in the cost function, Eq. (35). If the trajectory terminates in a short time, the data length of the simulated fin deflection will be a small number, thus the cost function will be a higher value; and if the trajectory terminates in a longer time vice a versa.

$$f_{obj} = \frac{\sum_{t=0}^{t_f} \sum_{i=1}^4 \overline{\delta_{i_{flight}}(t) - \delta_{i_{sim}}(t)}^2}{length(\delta_{1_{sim}})} \quad (35)$$

* 1000

The two cost functions are compared with a number of optimization runs on simulated and actual flight test data. It is seen that final position penalty (coupled with Adaptation Feasible type of mutation) gives better results.

CHAPTER 5

TEST CASES

The methods defined in the previous chapters are applied to flight test data of two different air launched flight vehicles. The first vehicle is an autonomous (onboard closed loop feedback controlled) flight vehicle, where as the second vehicle is a freefall separation model (uncontrolled).

5.1 Test Cases for Model Structure Determination

The methods for model structure determination are tested on four different test cases. The first two of these cases are simulated flight test data of the guided FV, which are obtained through a high fidelity 6 dof simulation. The third test case is the actual flight test data of the guided FV, which was gathered during performance demonstration flight tests of the FV. Thus, the data for the third test case is not specifically designed for system identification/parameter estimation purposes, yet, it is the only set of actual flight test data for guided FV available. This flight test data includes measurements for:

- Altitude
- Velocities
- Body angular rates
- Body linear accelerations
- Control surface deflections

Using these parameters, the following are calculated during post processing the data:

- Angle of attack
- Angle of side slip
- Mach number

The fourth test case is the actual flight test data of the freefall separation model. Only two sets of measurements are included in the actual flight test data; namely linear accelerations and angular rates. Using these measurements, the following are calculated during post processing of the data (thus the data is prone to possible integration errors in the post process):

- Angle of attack
- Angle of side slip
- Mach number

5.1.1 Simulated Flight Test Data for Guided FV

The first test case is a standard trajectory for the autonomous flight vehicle. No specific care is taken for maneuver design, i.e., excitation of modes of the vehicle for system identification purposes is not performed. As can be seen from the time history of the flight data in Figure 18 and Figure 19, the vehicle rapidly suppresses the effects of the initial conditions (initial angular rates are assumed on the vehicle to simulate the effects of separation from the parent aircraft) and smoothly flies the rest of the trajectory until the desired final point.

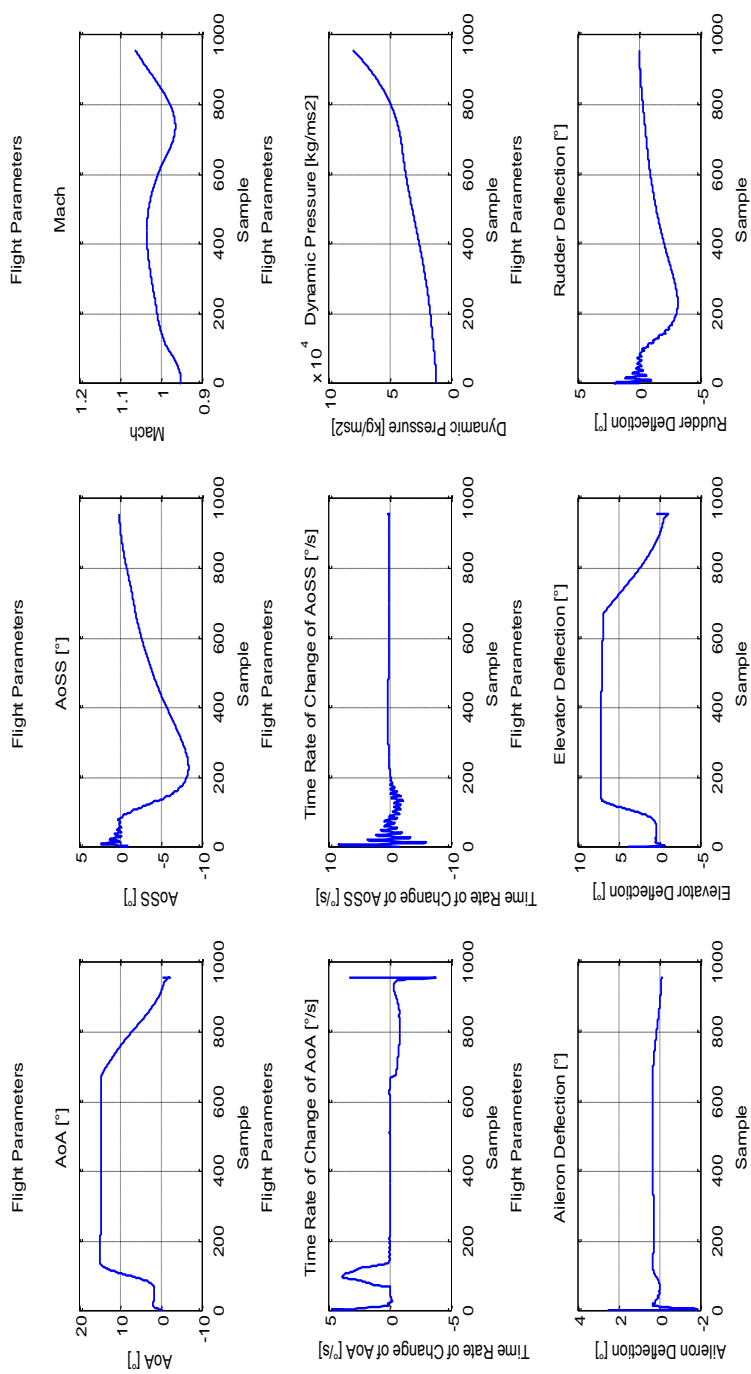


Figure 18. Simulated flight test data 1 flight parameters

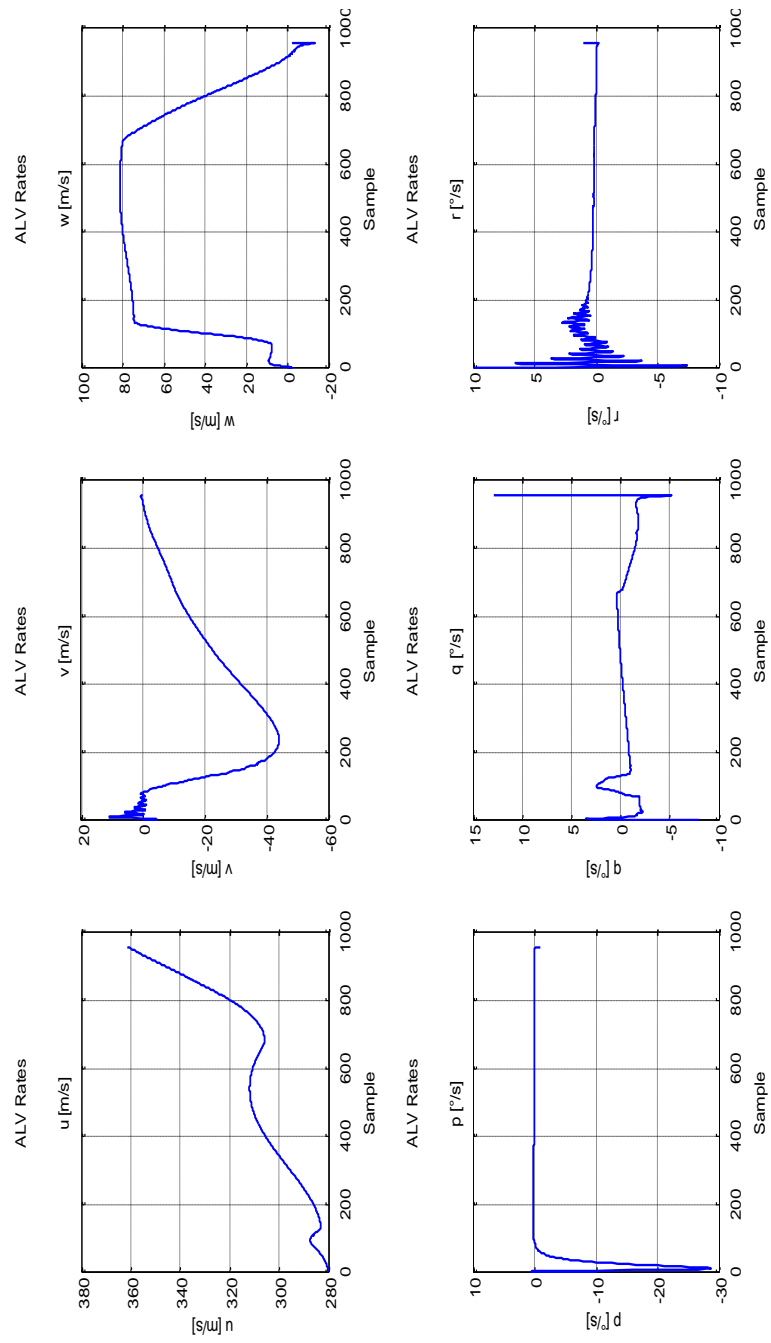


Figure 19. Simulated flight test data 1 rates

The original aerodynamic model of the flight vehicle is given in Table 2 and Table 3.

Table 2. Original aerodynamic model of the guided FV (forces)

Coefficients	C_x		C_y		C_z	
Model Parameters	Static Term	2.0445	Static Term	-0.0009	Static Term	0.0169
	alpha2	-4.3192	beta3	-40.3350	alpha3	-35.7140
	beta4	11.5640	beta2	0.0058	alpha2	0.0590
	beta3	-0.0457	beta	-6.0397	alpha	-6.1664
	beta2	-1.1341	r	-17.1996	beta	0.1425
	beta	0.0300	Machr	31.6010	q	17.1996
	Mach2	1.5909	dr	5.0365	Machq	-31.6010
	Mach	-3.8605	alpha2dr	-2.4669	de	5.0365
			alphadr	0.0433	beta2de	-2.4669
			Machdr	-1.5251	betade	0.0433
				Machde	-1.5251	

Table 3. Original aerodynamic model of the guided FV (moments)

Coefficients	C_l		C_m		C_n	
Model Parameters	Static Term	0.0015	Static Term	0.0564	Static Term	-0.0144
	alpha	-0.0328	alpha3	-33.1320	beta3	33.5710
	beta3	-0.3315	alpha2	0.3809	beta2	1.0681
	beta2	0.2492	alpha	-5.2489	beta	4.6446
	beta	0.0416	q	119.4666	r	119.4666
	p	-0.4586	Machq	-157.6500	Machr	-157.6500
	Machp	-0.8159	de	20.4878	dr	-20.4878
	da	9.9776	beta2de	-12.6650	alpha2dr	12.6650
	alpha2da	1.9753	betade	0.3407	alphadr	-0.3407
	beta2da	4.1906	Machde	-5.5976	Machdr	5.5976
	betada	0.1166				
	Mach3da	-9.3903				
	Mach2da	28.1970				
	Machda	-27.5090				

Table 4 - Table 8 show the identified models and parameter estimates (with predicted errors). Figure 20 through Figure 24 show the response of the estimated model and residuals for each aerodynamic coefficient. Although most of the identified model responses seem to agree well with the simulated flight test data, a comparison of parameters between the original aerodynamic models and the identified ones reveals that the obtained models are not relevant. For example, a dependency on the control surface deflections is identified in axial force, where as the original model is independent of deflections. Also, a model for the pitching moment coefficient (C_m) could not be identified. Of all the identified models for the five aerodynamic coefficients, only the model for the side force coefficient (C_Y) seems to capture the dominant parameters and their values acceptably, yet there are still unrelated parameters such as the square of rudder deflection in the identified model. Then, it is without a doubt that at first attempt, the model structure identification algorithms failed to identify adequate models for the guided FV. The main reason behind this failure is the insufficient information content of the simulated FTD: The simulation did not include any maneuvers for system identification and the atmospheric conditions were perfect (no winds, standard day temperatures and pressures). Under these circumstances, the autopilot did a pretty job and suppressed the vehicles dynamical responses, thus, not enough valuable information left in the FTD for the model identification algorithms to succeed.

Table 4. Identified model and parameter estimates for C_x

CX	Parameter Estimate	Standard Error	Percent Error	95% Confidence LB	95% Confidence UB
Mach	-0.6380	0.0596	9.3500	-0.7573	-0.5187
delta	-1.2430	0.1399	11.2516	-1.5227	-0.9633
alpha3	-8.5061	0.9898	11.6358	-10.4857	-6.5266
static term	0.4222	0.0600	14.2008	0.3023	0.5421

Table 5. Identified model and parameter estimates for C_y

CY	Parameter Estimate	Standard Error	Percent Error	95% Confidence LB	95% Confidence UB
beta	-5.8169	0.0432	0.7418	-5.9032	-5.7306
dr	3.1463	0.0707	2.2473	3.0049	3.2878
dr2	48.4342	2.0228	4.1764	44.3886	52.4799
static term	-0.0019	0.0011	57.7392	-0.0040	0.0003

Table 6. Identified model and parameter estimates for C_z

CZ	Parameter Estimate	Standard Error	Percent Error	95% Confidence LB	95% Confidence UB
de	-13.5862	0.1207	0.8886	-13.8276	-13.3447
static term	-0.0570	0.0108	18.9173	-0.0786	-0.0354

Table 7. Identified model and parameter estimates for C_I

CI	Parameter Estimate	Standard Error	Percent Error	95% Confidence LB	95% Confidence UB
dap	-4591.1438	113.5047	2.4723	-4818.1532	-4364.1344
static term	0.0001	0.0001	66.6298	0.0000	0.0003

Table 8. Identified model and parameter estimates for C_n

Cn	Parameter Estimate	Standard Error	Percent Error	95% Confidence LB	95% Confidence UB
betap	-10540.6233	2031.0955	19.2692	-14602.8144	-6478.4322
drp	42641.0939	3925.5223	9.2060	34790.0494	50492.1385
drda2	-8607.9217	548.4078	6.3710	-9704.7372	-7511.1062
static term	-0.0063	0.0021	33.3606	-0.0104	-0.0021

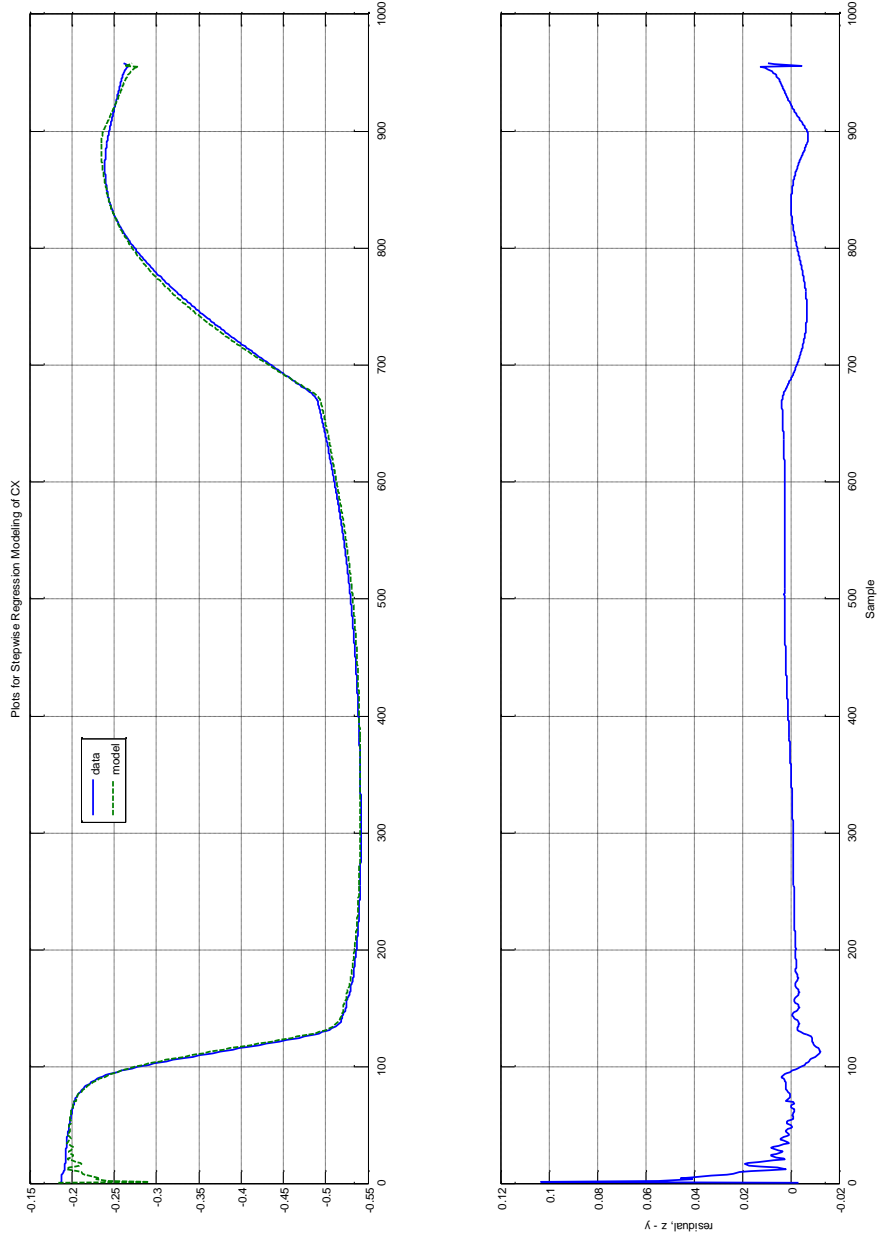


Figure 20. Estimated response vs data - Cx

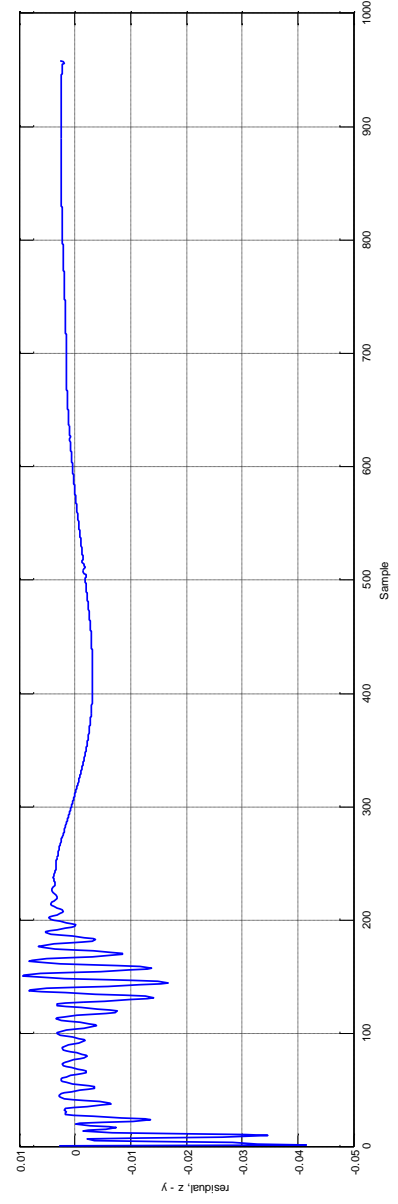
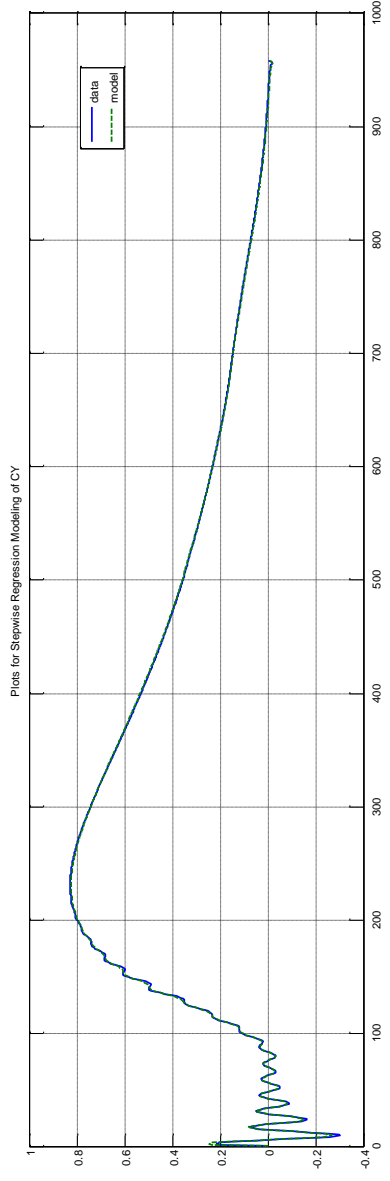


Figure 21. Estimated response vs data – C_y

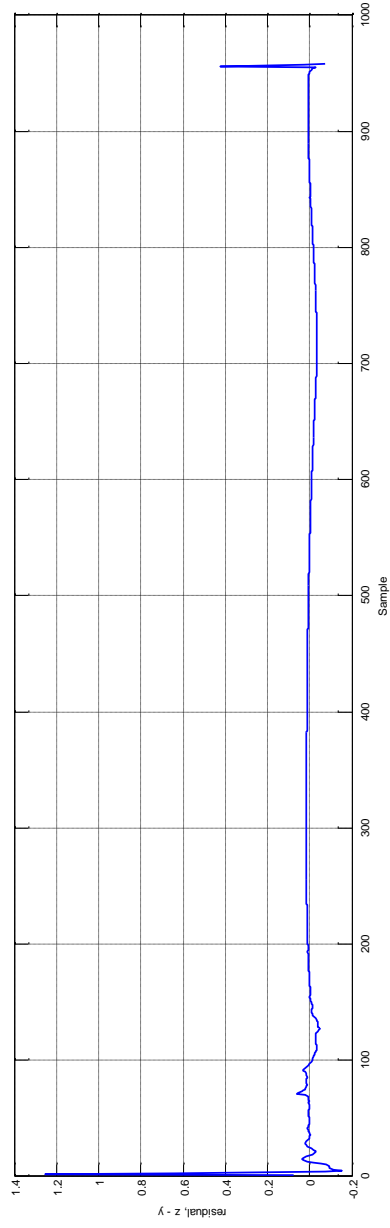
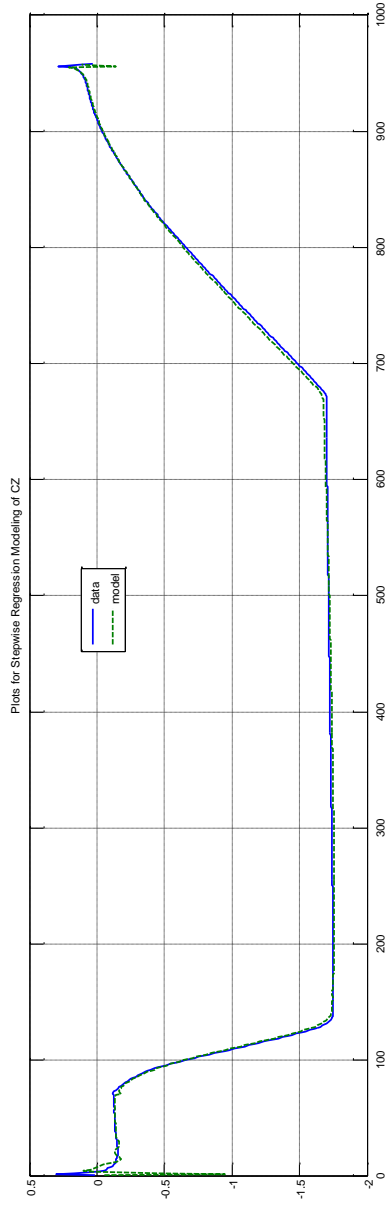


Figure 22. Estimated response vs data - Cz

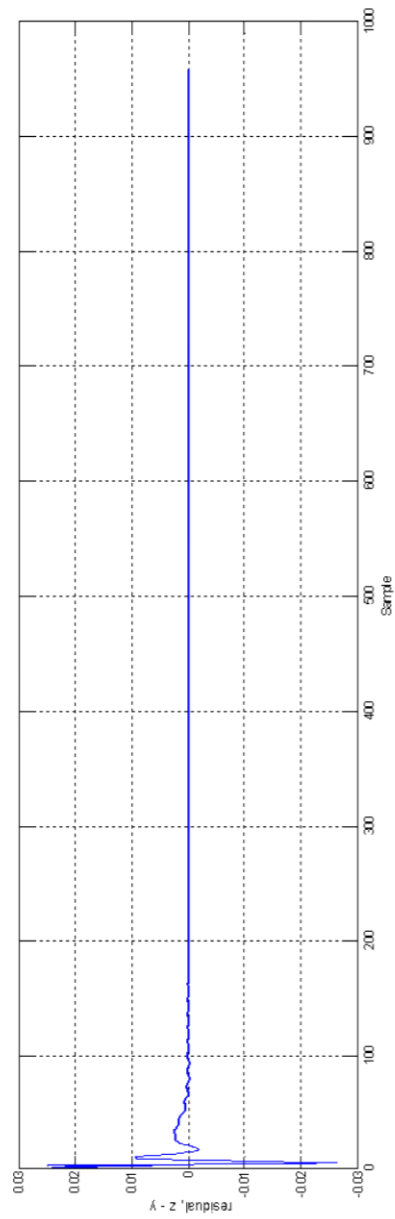
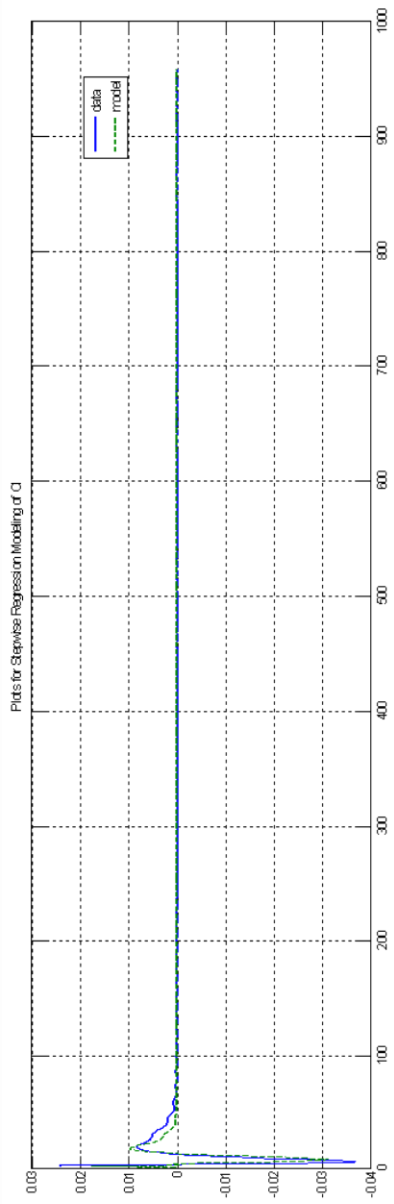


Figure 23. Estimated response vs data - C_i

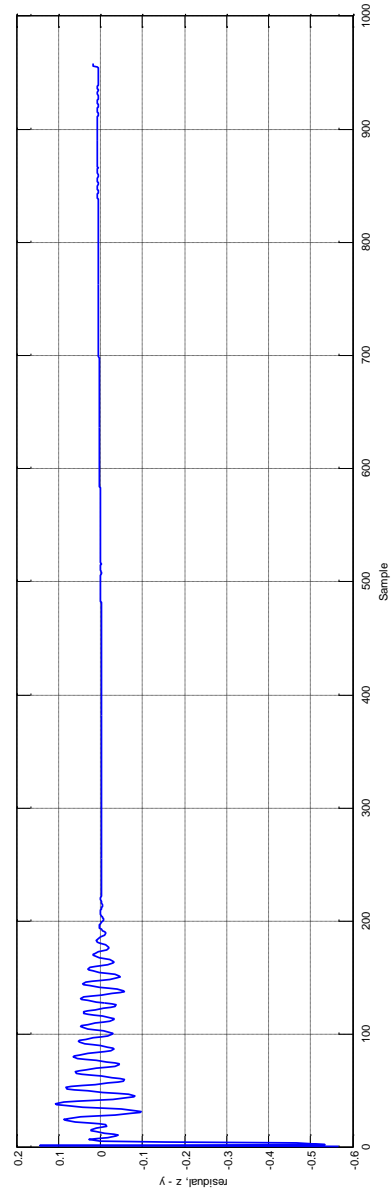
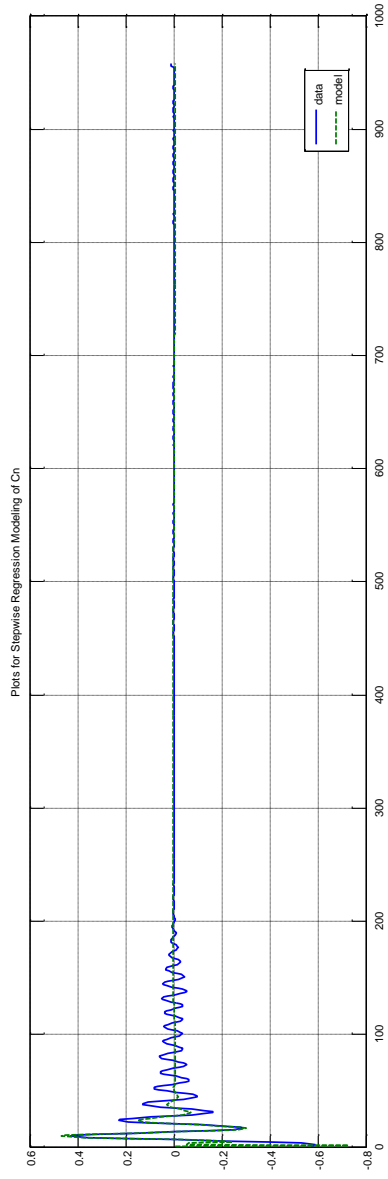


Figure 24. Estimated response vs data – C_n

5.1.2 Simulated Flight Test Data for Guided FV with Maneuvers

Although the simulated flight test data of test case 1 is free of any measurement errors and biases, which almost never is the case for an actual flight test data, the model structure algorithms failed to identify adequate and acceptable models. To test the famous saying "*If it is not in the data, it cannot be estimated*", two additional flight simulations are carried out, each with different set of maneuvers. The optimal flight test maneuver design is a broad subject, and not included in the scope of these thesis. Yet, a very basic approach is taken in maneuver design: The maneuvers are selected to excite the modes of the flight vehicle by disturbing the autopilot commands to fin actuation system. These maneuvers are constant frequency sine inputs (frequencies of inputs for aileron, elevator and rudder inputs are selected based on longitudinal and lateral mode frequencies of the vehicle) and square waves. Figure 25 and Figure 26 show the time history of simulated flight test data for test case 2.

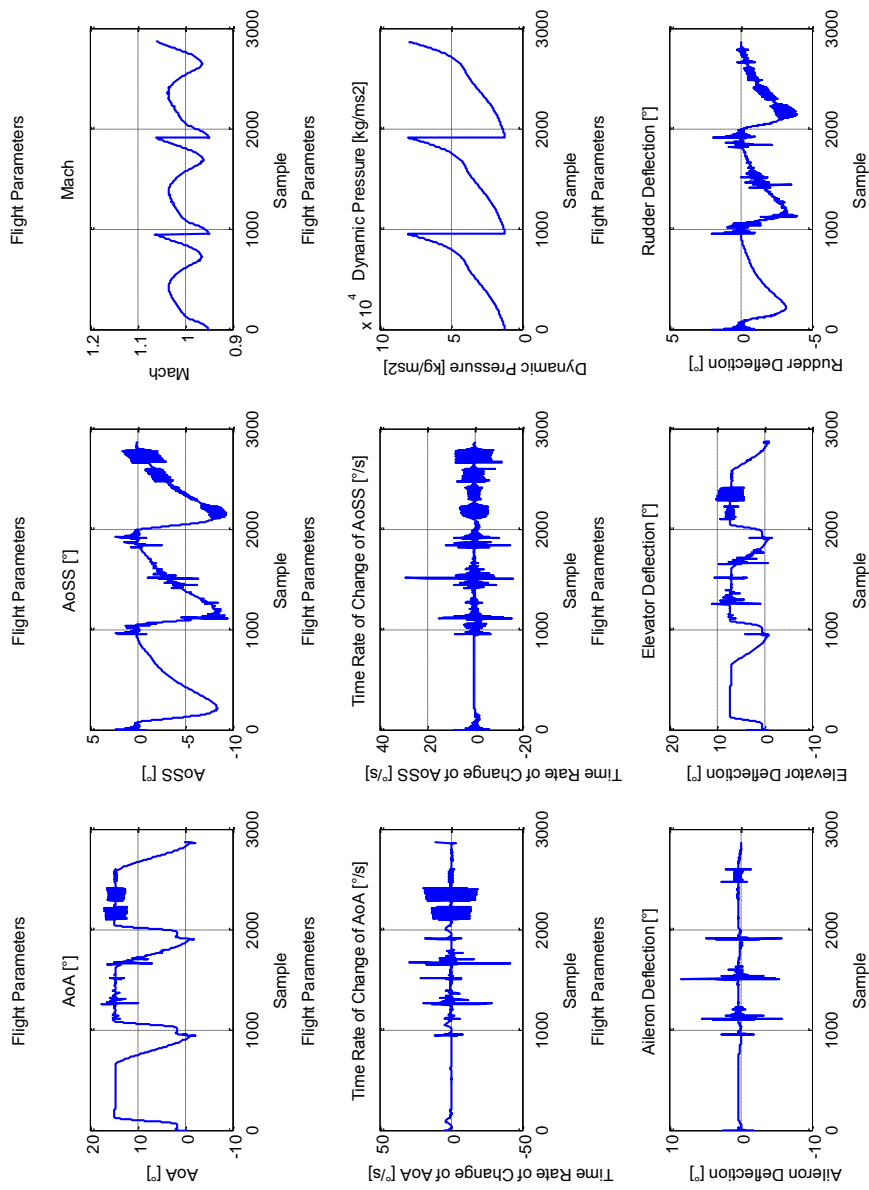


Figure 25. Simulated flight test data 2 flight parameters

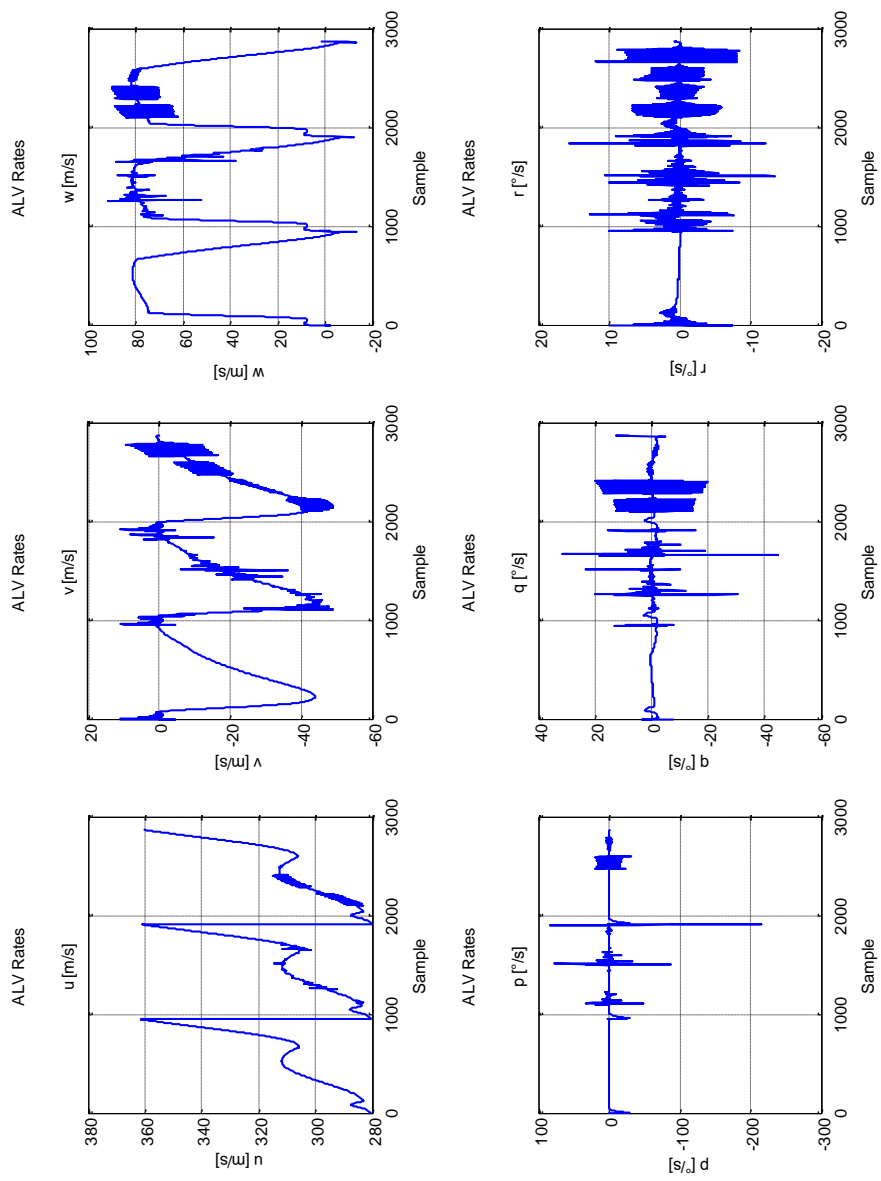


Figure 26. Simulated flight test data 2 rates

Once again, aerodynamic model structure identification followed by parameter estimation is performed using stepwise regression and equation error methods on the simulated flight test data. Table 9 - Table 14 show the identified models and parameter estimates (with predicted errors) and Figure 27 through Figure 32 show the response of the estimated model and residuals for each aerodynamic coefficient. The identified model responses seem to agree well with the simulated flight test data. A comparison of parameters between the original aerodynamic models and the identified ones reveals that the obtained models (especially for forces) are adequate and they capture the dominant parameters (and their values) acceptably. Yet, there are some unrelated terms in the identified models for moments. Also, some high residual values can be seen in the responses. Nevertheless, the test case 2 proves that, given an adequate flight test data, i.e., a flight test data that is rich enough in frequency content, the model structure determination and equation error based parameter estimation algorithms have the potential to identify adequate aerodynamic models. Yet, the phrase "*if it is not in the data, it cannot be estimated*" is validated, i.e., the success of the identification and estimation algorithms depend on the flight test maneuver design.

Table 9. Identified model and parameter estimates for C_X

CX	Parameter Estimates	Standard Error	Percent Error	95% Confidence LB	95% Confidence UB
Mach	-0.6902	0.0110	1.5945	-0.7122	-0.6682
alpha2	-4.3041	0.0131	0.3034	-4.3302	-4.2780
beta2	-1.1689	0.0515	4.4028	-1.2718	-1.0660
static term	0.4676	0.0110	2.3488	0.4456	0.4896

Table 10. Identified model and parameter estimates for C_Y

CY	Parameter Estimates	Standard Error	Percent Error	95% Confidence LB	95% Confidence UB
beta	-6.0821	0.0078	0.1285	-6.0977	-6.0664
dr	3.4046	0.0078	0.2302	3.3889	3.4203
beta3	-39.9475	0.4078	1.0209	-40.7631	-39.1318
static term	-0.0003	0.0002	80.8718	-0.0008	0.0002

Table 11. Identified model and parameter estimates for C_Z

CZ	Parameter Estimates	Standard Error	Percent Error	95% Confidence LB	95% Confidence UB
alpha	-5.9290	0.1305	2.2015	-6.1901	-5.6680
de	3.1745	0.1327	4.1806	2.9091	3.4399
alpha3	-37.1918	1.1341	3.0493	-39.4600	-34.9236
static term	0.0251	0.0096	38.1037	0.0060	0.0442

Table 12. Identified model and parameter estimates for C_I

CI	Parameter Estimates	Standard Error	Percent Error	95% Confidence LB	95% Confidence UB
da	1.2249	0.0589	4.8055	1.1072	1.3427
static term	-0.0043	0.0003	7.6287	-0.0050	-0.0037

Table 13. Identified model and parameter estimates for C_m

Cm	Parameter Estimates	Standard Error	Percent Error	95% Confidence LB	95% Confidence UB
alpha	-4.3669	0.1811	4.1468	-4.7290	-4.0047
de	12.6085	0.4306	3.4149	11.7473	13.4696
de2	17.1554	5.5337	32.2565	6.0879	28.2229
alpha3	-35.7358	1.5871	4.4411	-38.9100	-32.5617
de3	-79.3177	24.2586	30.5841	-127.8349	-30.8005
static term	0.0550	0.0124	22.4825	0.0302	0.0797

Table 14. Identified model and parameter estimates for C_n

Cn	Parameter Estimates	Standard Error	Percent Error	95% Confidence LB	95% Confidence UB
beta	4.2991	0.0389	0.9044	4.2213	4.3768
dr	-13.6642	0.0756	0.5535	-13.8154	-13.5129
beta2	-5.1522	0.2358	4.5763	-5.6238	-4.6807
static term	-0.0121	0.0008	6.4588	-0.0137	-0.0106

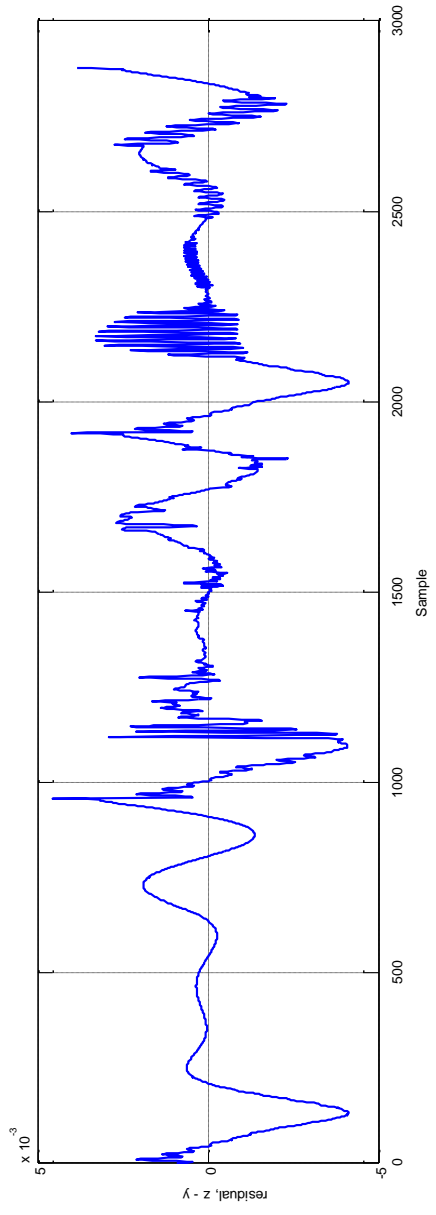
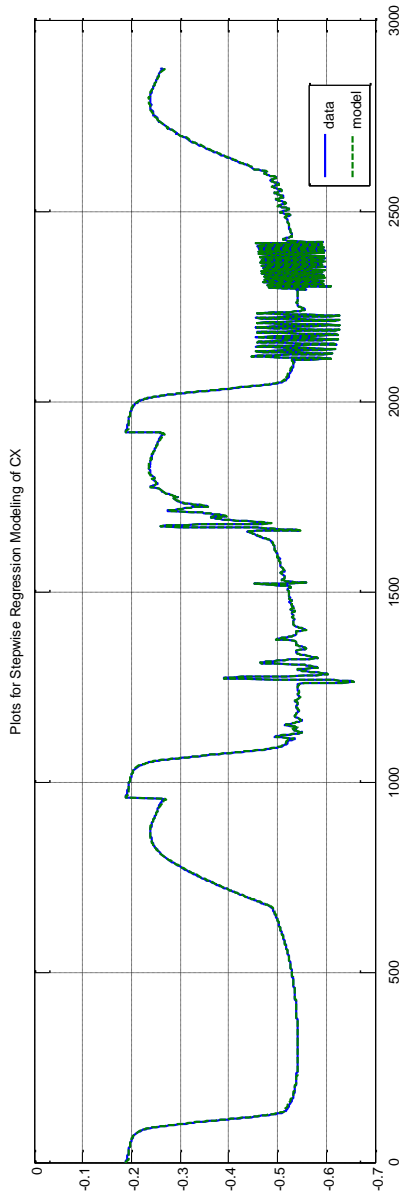


Figure 27. Estimated response vs data - Cx

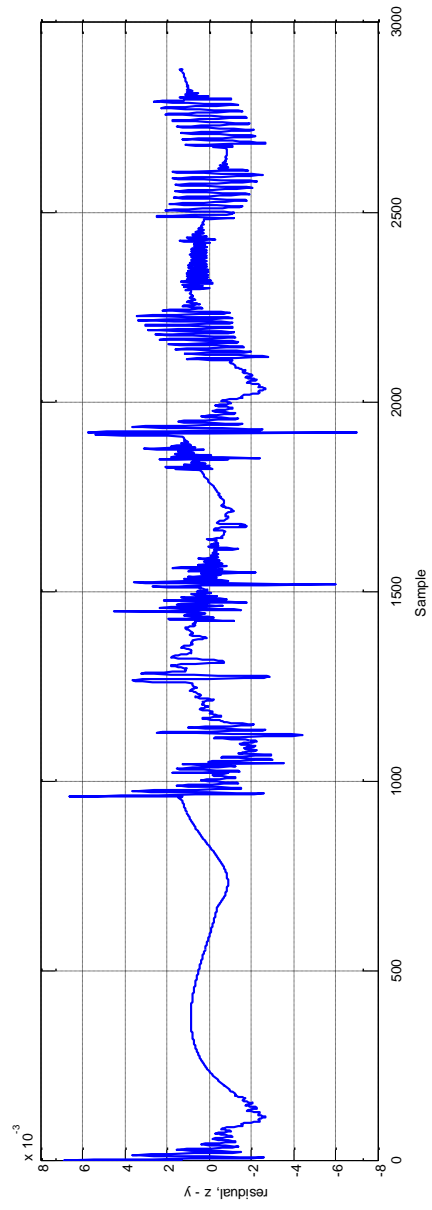
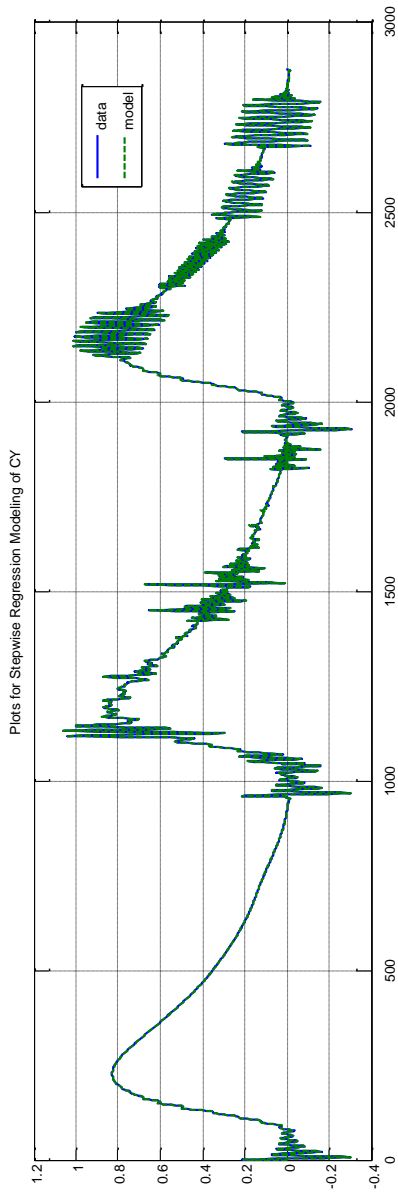


Figure 28. Estimated response vs data - C_y

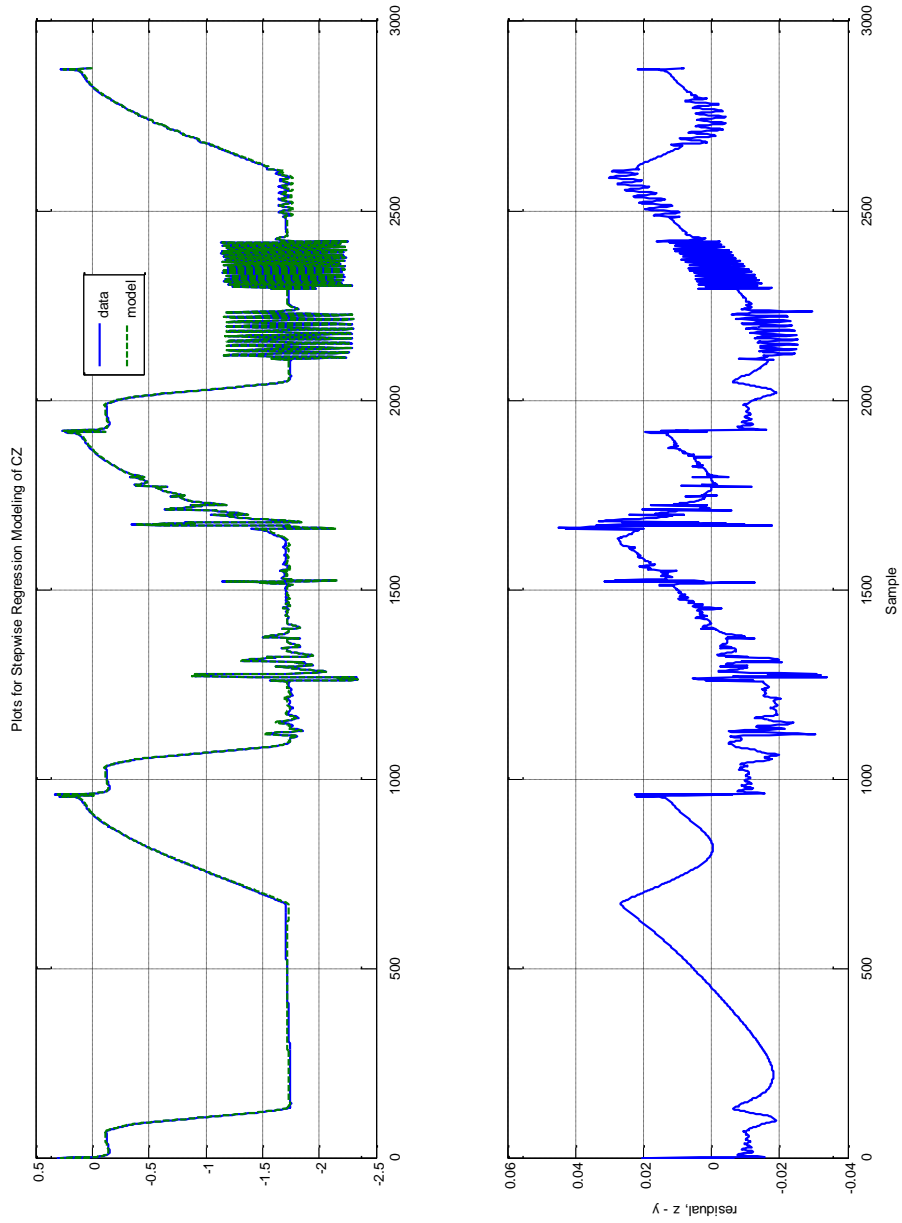


Figure 29. Estimated response vs data – Cz

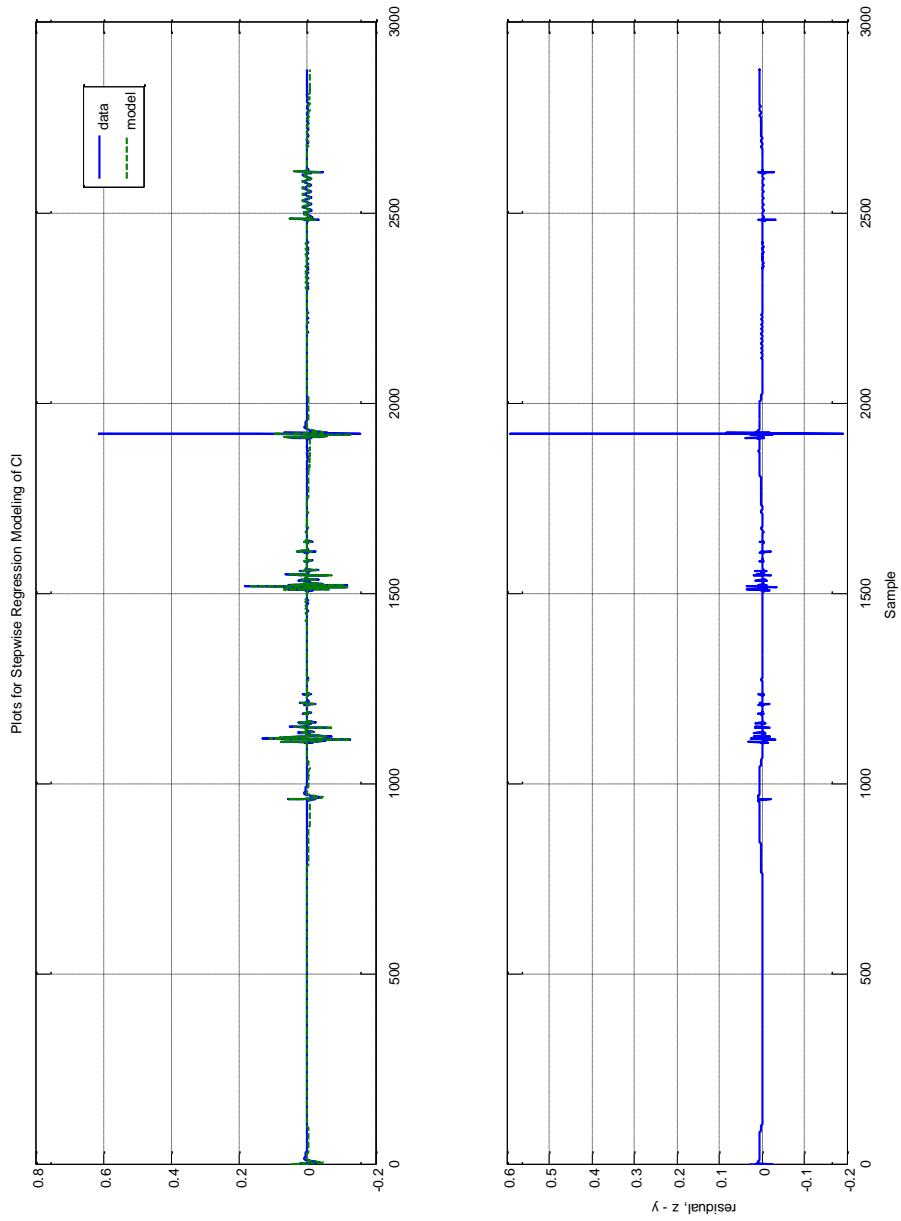


Figure 30. Estimated response vs data - C_j

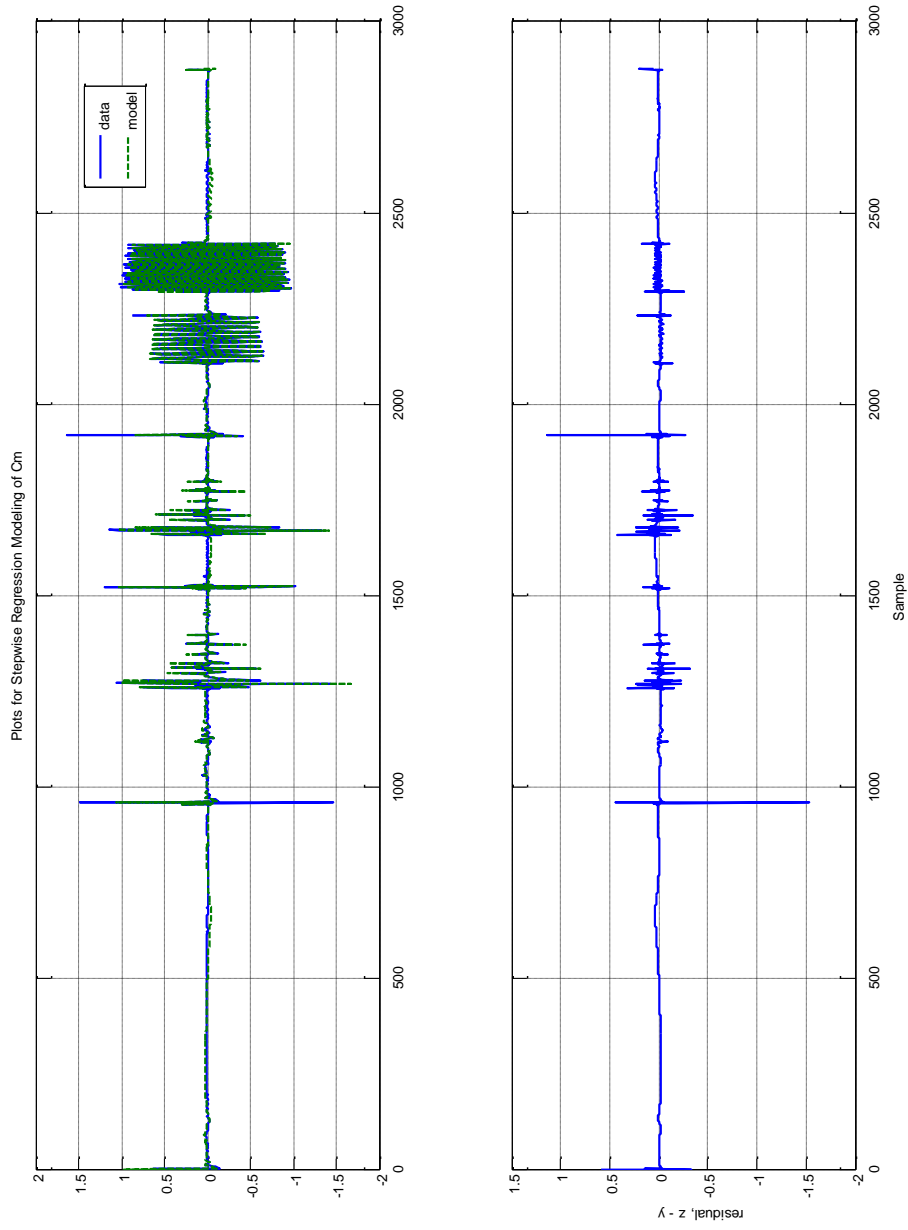


Figure 31. Estimated response vs data - C_m

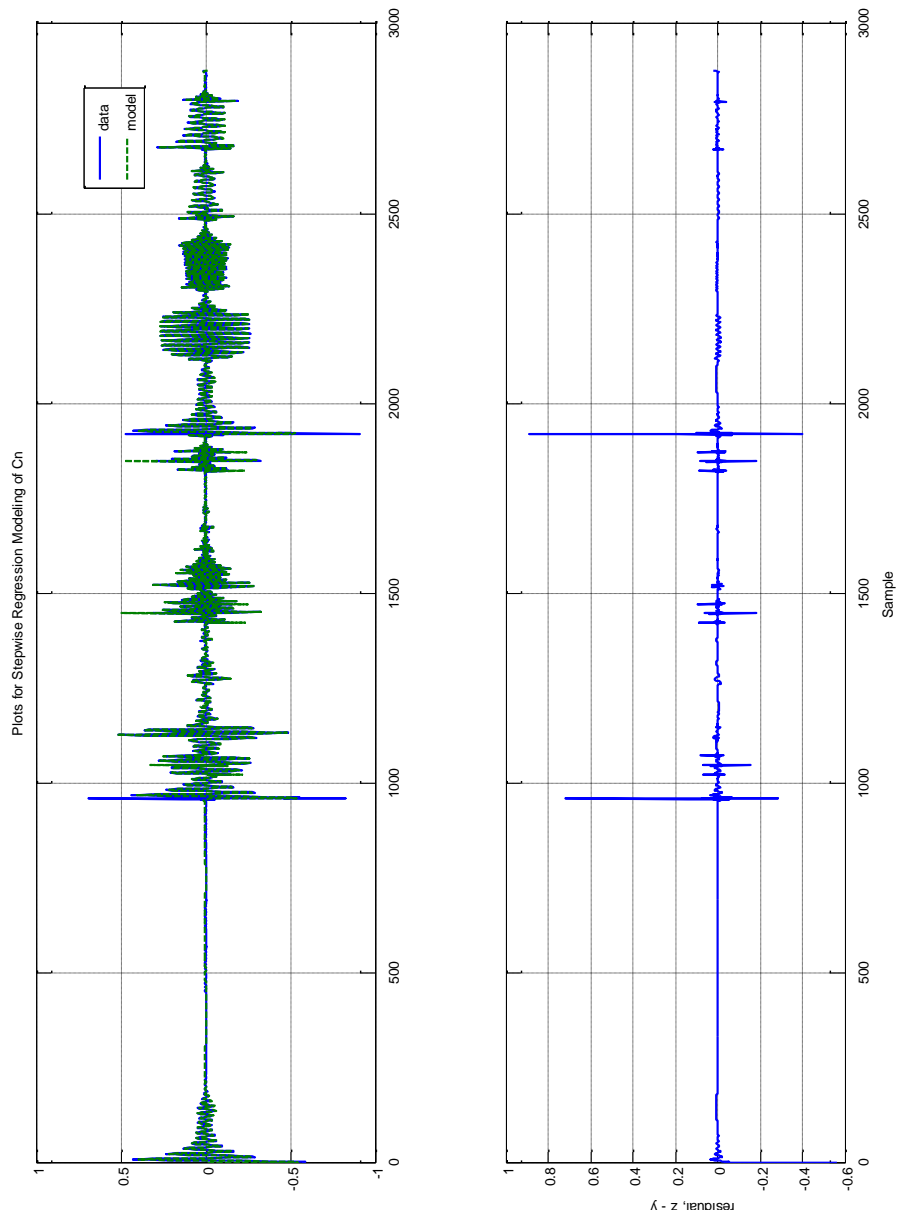


Figure 32. Estimated response vs data - C_n

5.1.3 Actual Flight Test Data for Guided FV

The third test case is the actual flight test data of an autonomous flight vehicle. The data is collected from four different test runs each with different initial conditions. Using the data processing methods explained in Section 3.4, the data is conditioned and trimmed yielding the result shown in Figure 33 and Figure 34.

The differences between the in-flight aerodynamics and the a priori aerodynamic model are shown in Figure 35 and Figure 36. Except for the axial force coefficient, the a priori aerodynamic model seems to catch the actual dynamics well for the small angle of attack and side slip cases. However, there are considerable differences between the in-flight and a priori aerodynamics in flight conditions for which the angle of attack and side slip are above 10° and below -10° .

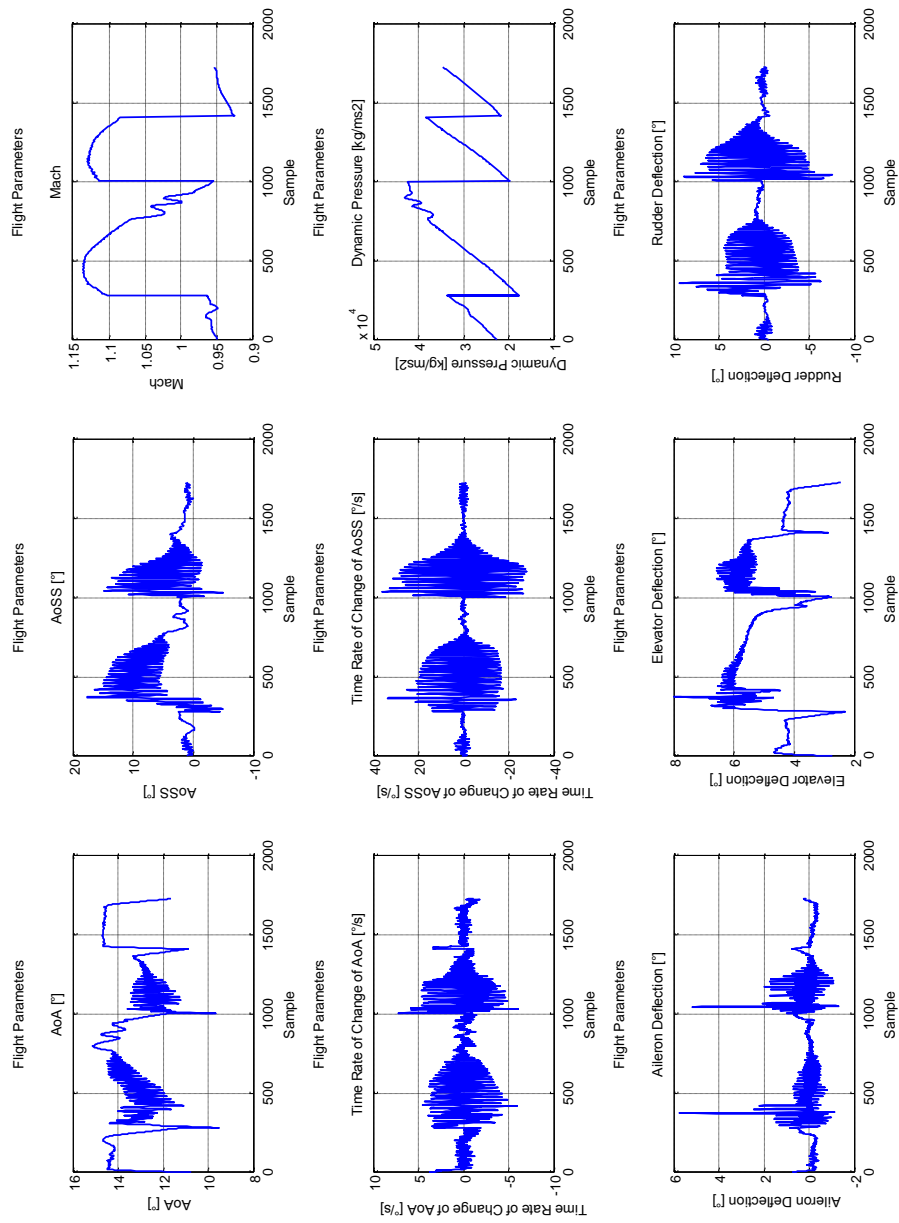


Figure 33. Actual flight test data 1 flight parameters

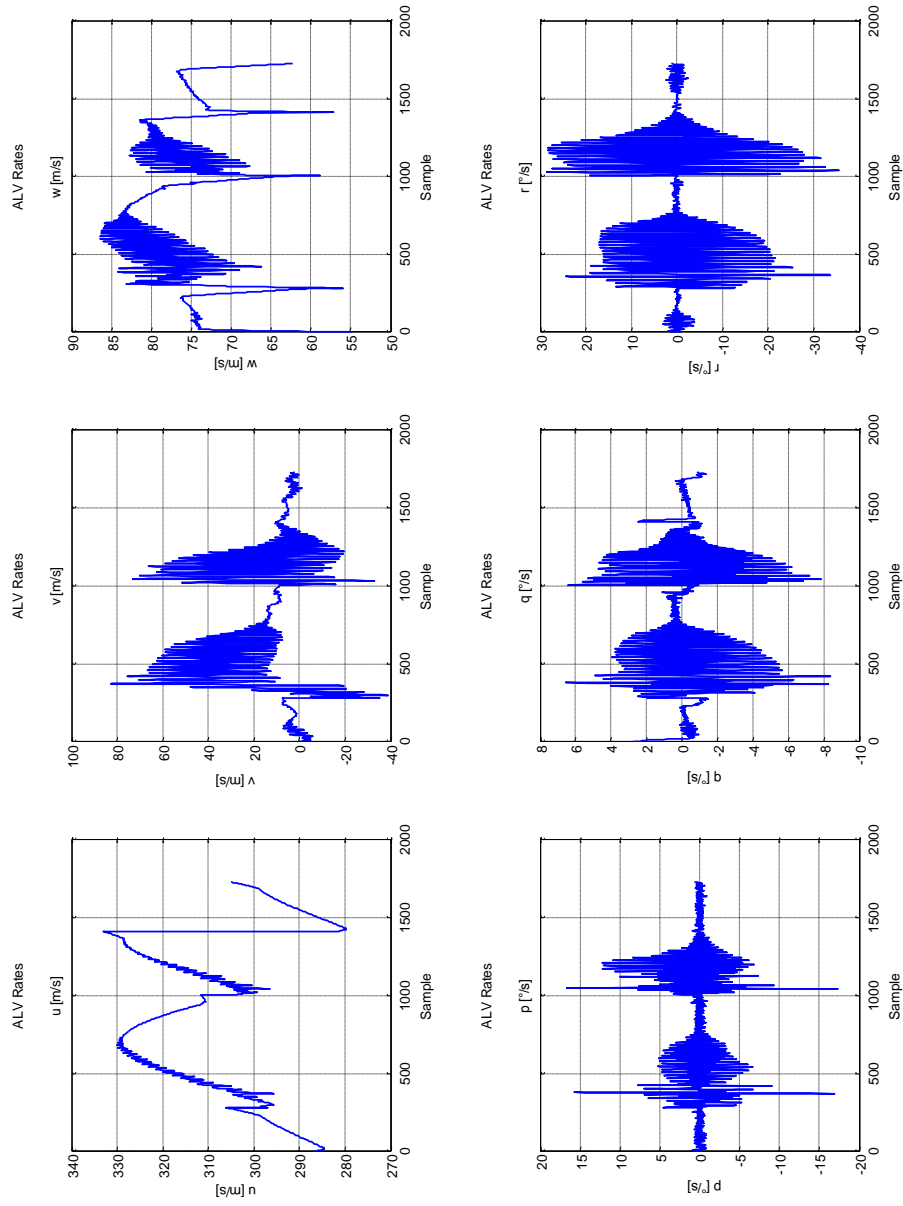


Figure 34. Actual flight test data 1 rates

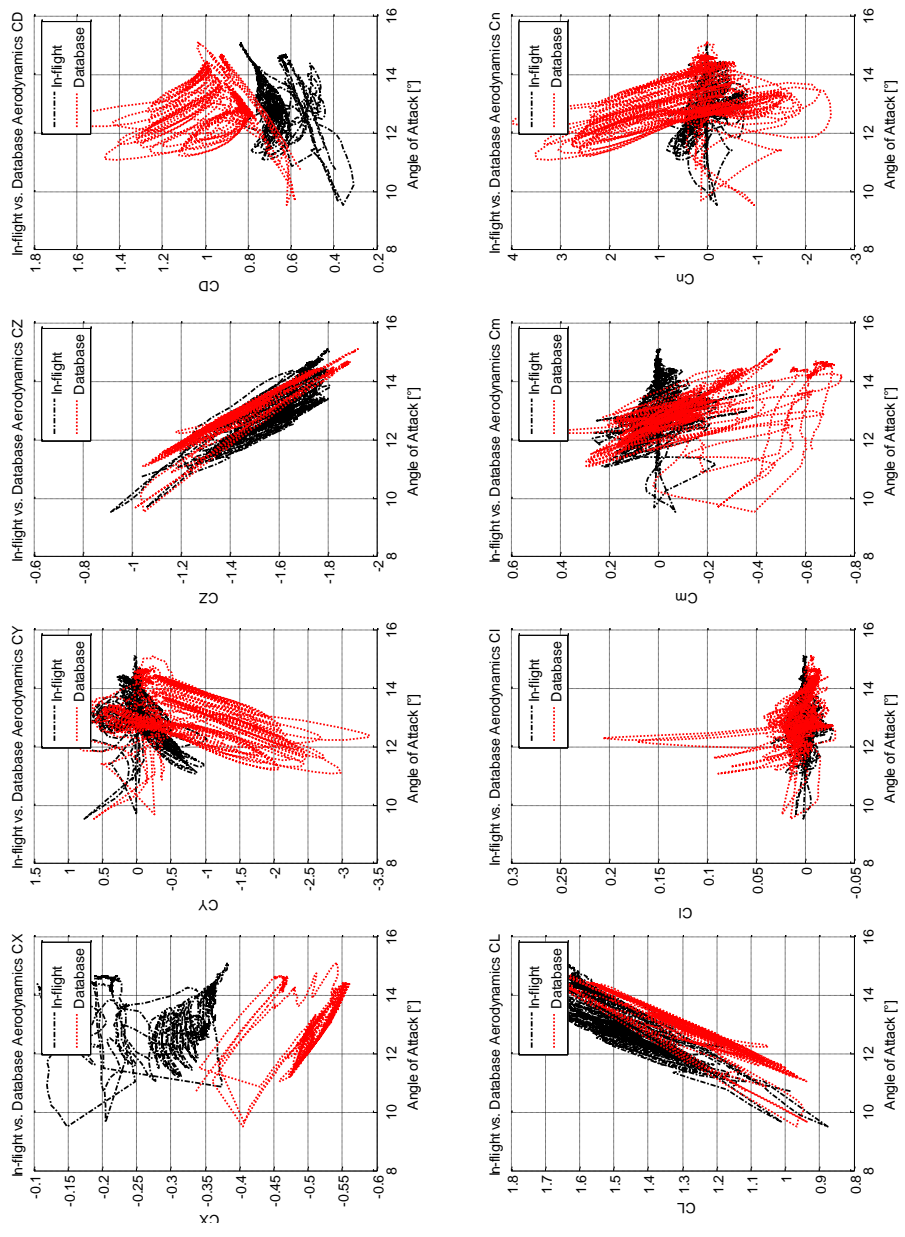


Figure 35. Difference of in-flight aerodynamics from the database (with respect to angle of attack)

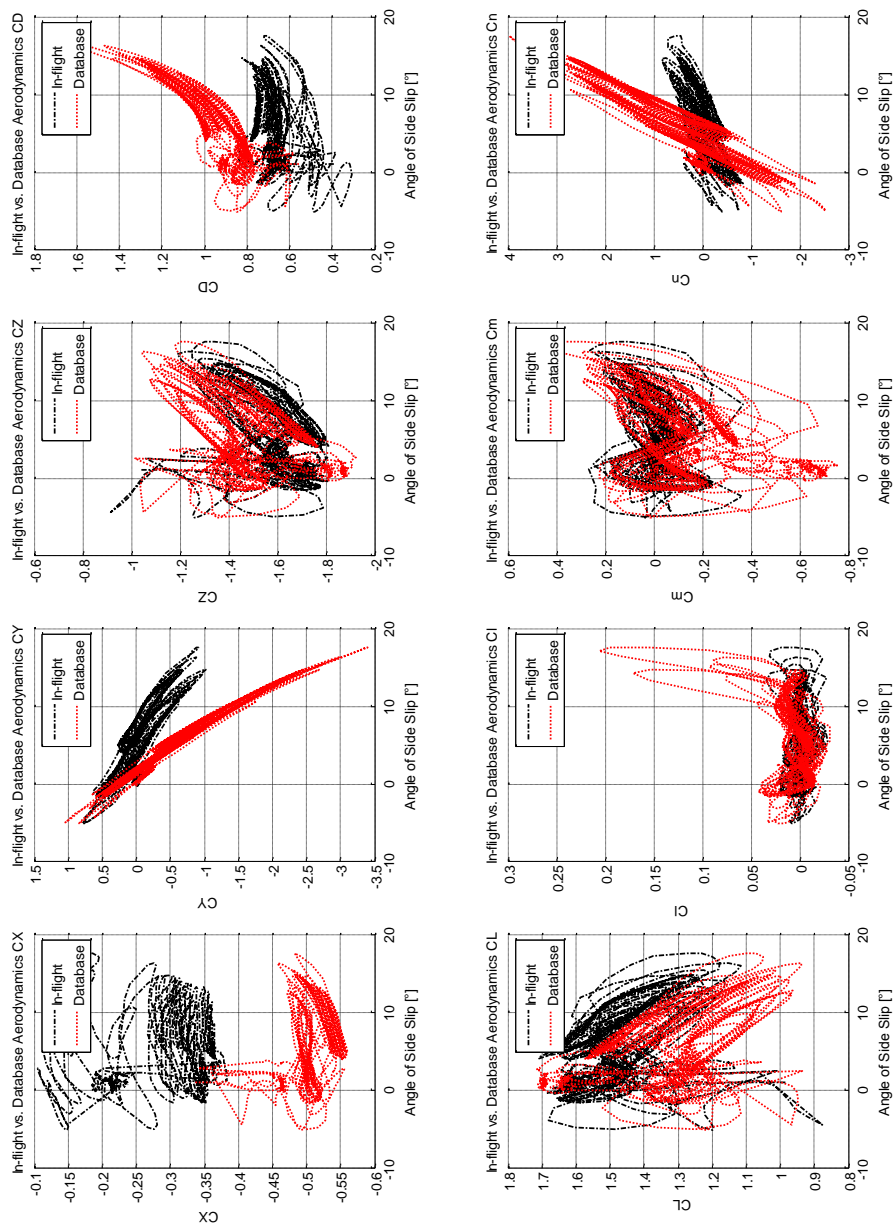


Figure 36. Difference of in-flight aerodynamics from the database (with respect to angle of sideslip)

The power spectral density estimates for the in-flight aerodynamics and the obtained delta aerodynamics are shown in Figure 37 and Figure 38.

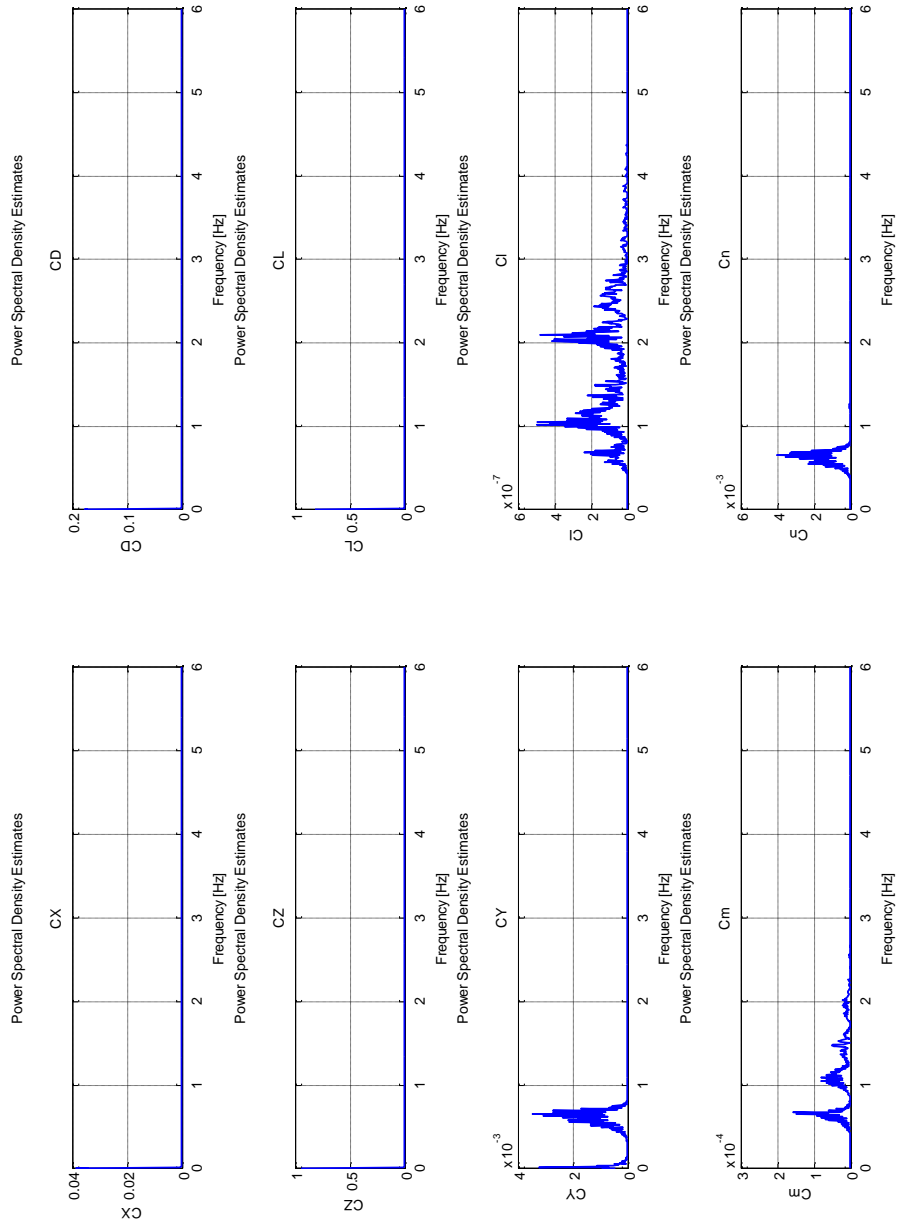


Figure 37. PSD Estimates for the in-flight aerodynamics

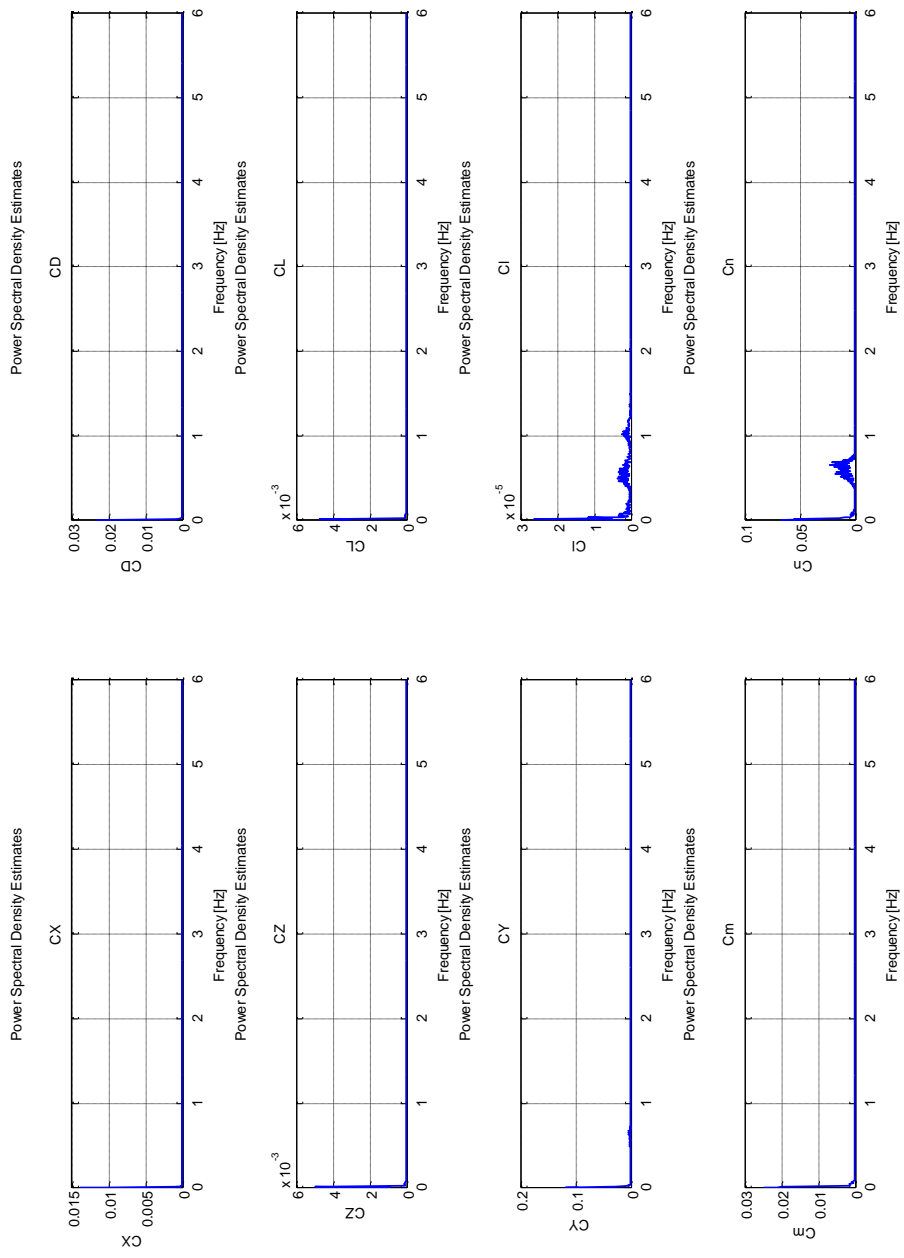


Figure 38. PSD Estimates for the delta aerodynamics

In contrast to what is expected, calculating a delta aerodynamics does not reduce the power of spectral density estimates, but amplify them for this flight vehicle. The reason behind this opposite behavior is the flight regime of the vehicle. As seen from Figure 33, the vehicle mostly flies in the high angle of attack and angle of side slip range. Since the database is quite erroneous for that flight regime, using the difference of the in-flight calculated and a-priori aerodynamics introduce additional power in the spectral estimates.

The aerodynamic model structure determination algorithm is run for 6 aerodynamic coefficients and as can be seen in Table 15 through Table 20. Some adequate models are obtained for all coefficients but the axial force coefficient. The model responses and the residuals are given in Figure 39 through Figure 44. The best agreements between the identified model and the actual data are obtained for lateral parameters. This is because of the content of the flight test data: During two of the runs, the flight vehicle encountered severe side wind, which caused a build-up in side slip angle. The autopilot responded, yet due the low fidelity of the aerodynamic database in the high angle of side slip flight condition, the control commands in lateral plane were miscalculated, causing the vehicle to start oscillating. Thus, the vehicle was excited in the lateral plane with the help of rudder input, which, unintentionally, allowed better model identification and parameter estimates in turn.

Table 15. Identified model and parameter estimates for C_x

CX	Parameter Estimates	Standard Error	Percent Error	95% Confidence LB	95% Confidence UB
alpha	0.8812	0.7548	85.6529	-0.6284	2.3908
static term	0.0057	0.1781	3119.4359	-0.3505	0.3620

Table 16. Identified model and parameter estimates for C_y

CY	Parameter Estimates	Standard Error	Percent Error	95% Confidence LB	95% Confidence UB
beta	3.4721	0.1746	5.0276	3.1230	3.8213
Mach	0.6578	0.0790	12.0083	0.4998	0.8158
da	1.7743	0.3304	18.6203	1.1136	2.4351
r	-273.5335	22.0325	8.0548	-317.5985	-229.4684
dr2	-9.0039	1.3683	15.1966	-11.7404	-6.2673
alphabeta2	57.2829	3.5531	6.2028	50.1766	64.3892
static term	-0.6012	0.0789	13.1219	-0.7590	-0.4434

Table 17. Identified model and parameter estimates for C_z

CZ	Parameter Estimates	Standard Error	Percent Error	95% Confidence LB	95% Confidence UB
alpha	-5.1026	1.8611	36.4730	-8.8247	-1.3805
Mach	-1.1907	0.1633	13.7173	-1.5174	-0.8640
q	803.0082	88.1220	10.9740	626.7642	979.2522
alpha5	469.6795	148.7196	31.6641	172.2403	767.1186
static term	2.0763	0.3264	15.7217	1.4235	2.7292

Table 18. Identified model and parameter estimates for C_i

CI	Parameter Estimates	Standard Error	Percent Error	95% Confidence LB	95% Confidence UB
da	-1.1995	0.0294	2.4485	-1.2583	-1.1408
beta2	-0.4627	0.0225	4.8602	-0.5077	-0.4177
static term	0.0056	0.0003	5.2972	0.0050	0.0062

Table 19. Identified model and parameter estimates for C_m

Cm	Parameter Estimates	Standard Error	Percent Error	95% Confidence LB	95% Confidence UB
alpha	6.1754	0.3545	5.7407	5.4664	6.8844
beta	0.3372	0.0695	20.6154	0.1982	0.4763
Mach	-1.2404	0.1211	9.7596	-1.4826	-0.9983
de	-8.2683	0.4976	6.0187	-9.2636	-7.2730
static term	0.8754	0.1566	17.8939	0.5621	1.1887

Table 20. Identified model and parameter estimates for C_n

Cn	Parameter Estimates	Standard Error	Percent Error	95% Confidence LB	95% Confidence UB
beta	-5.5715	0.3893	6.9866	-6.3500	-4.7930
Mach	0.9859	0.2122	21.5252	0.5615	1.4103
da	-2.6391	0.6494	24.6085	-3.9379	-1.3402
dr	7.1326	0.3591	5.0341	6.4145	7.8507
beta2	-9.5507	1.1260	11.7897	-11.8027	-7.2987
static term	-0.8946	0.2042	22.8299	-1.3031	-0.4861

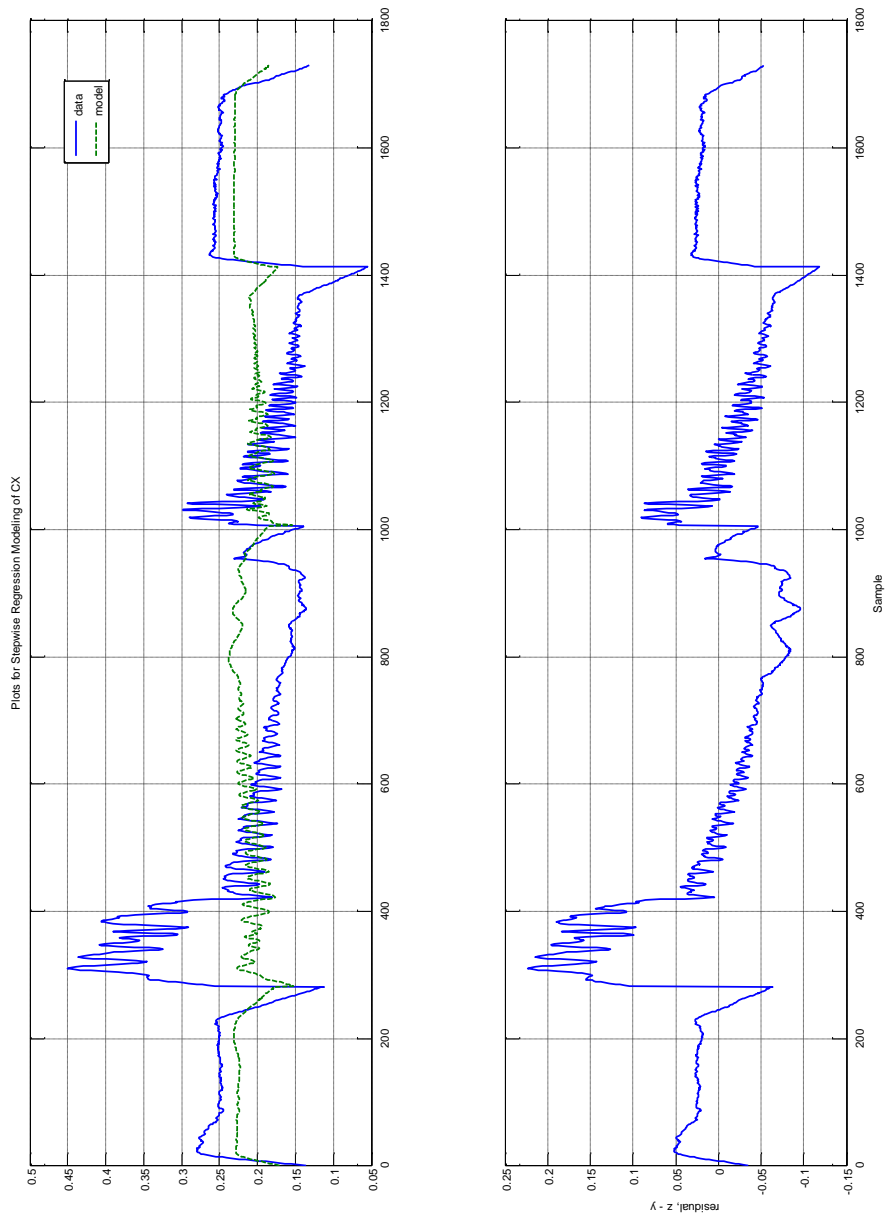


Figure 39. Estimated response vs data - Cx

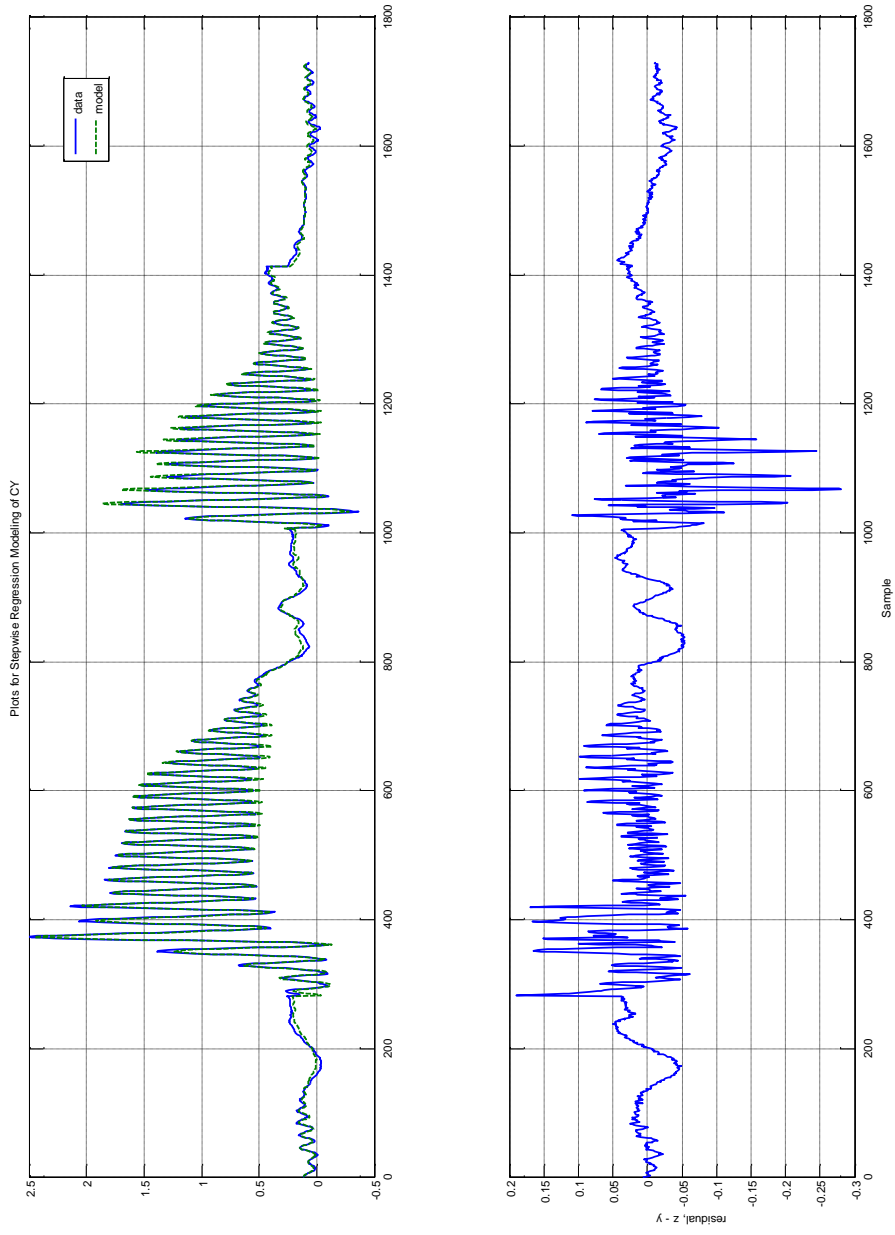


Figure 40. Estimated response vs data – C_y

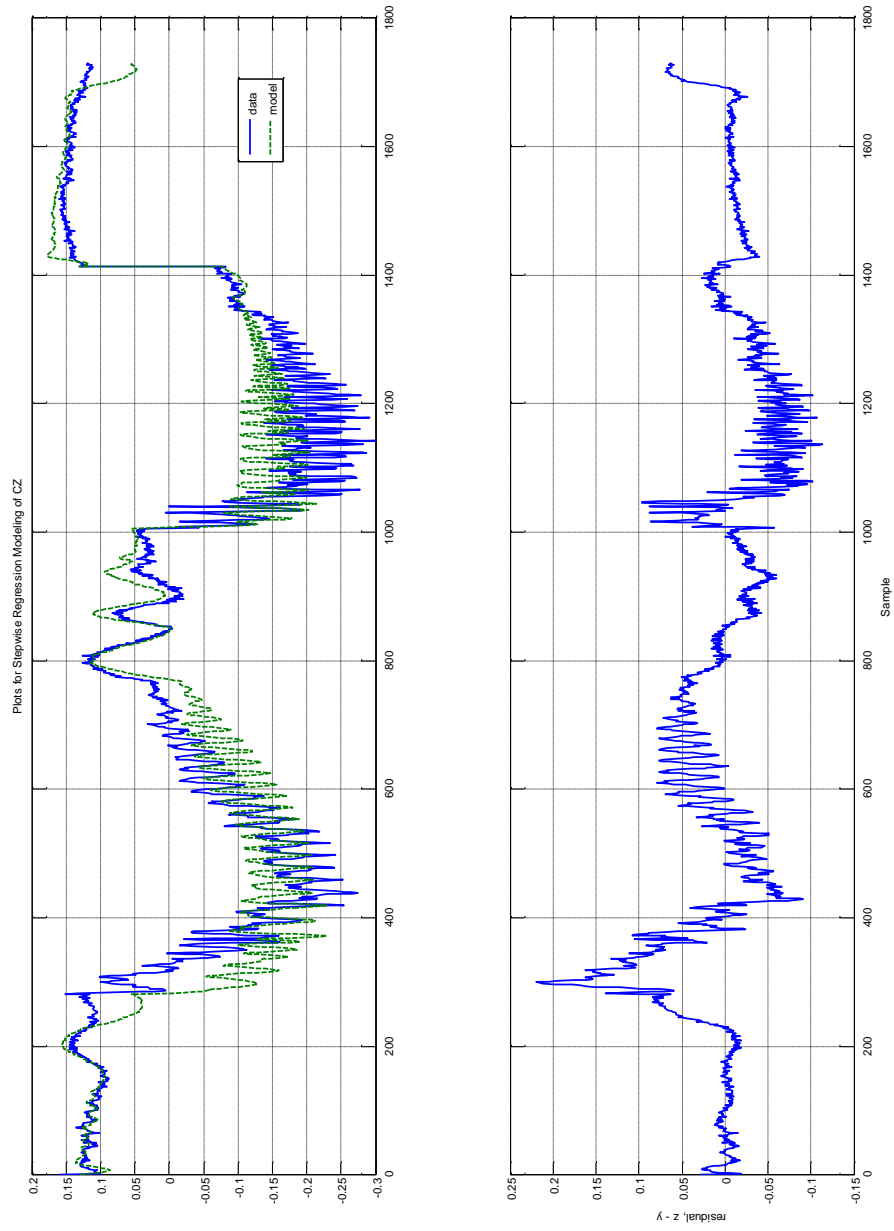


Figure 41. Estimated response vs data - Cz

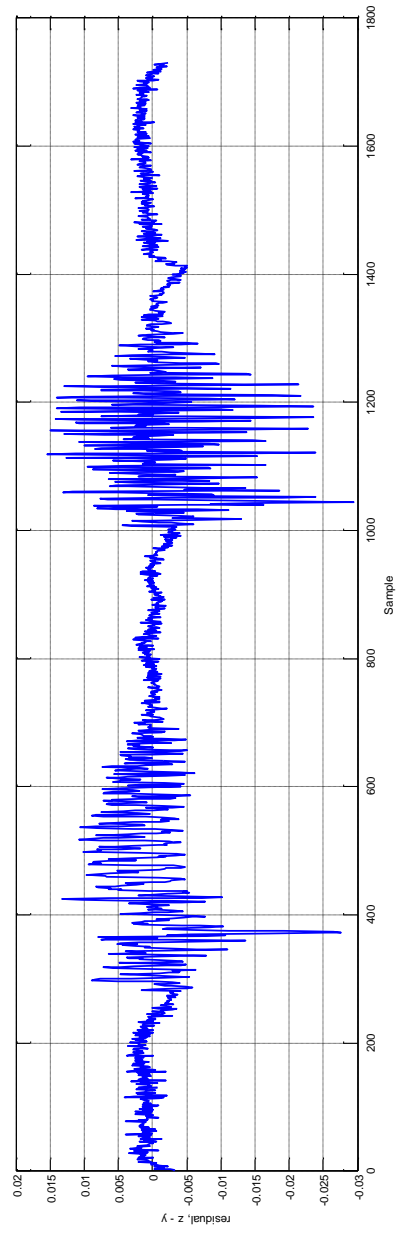
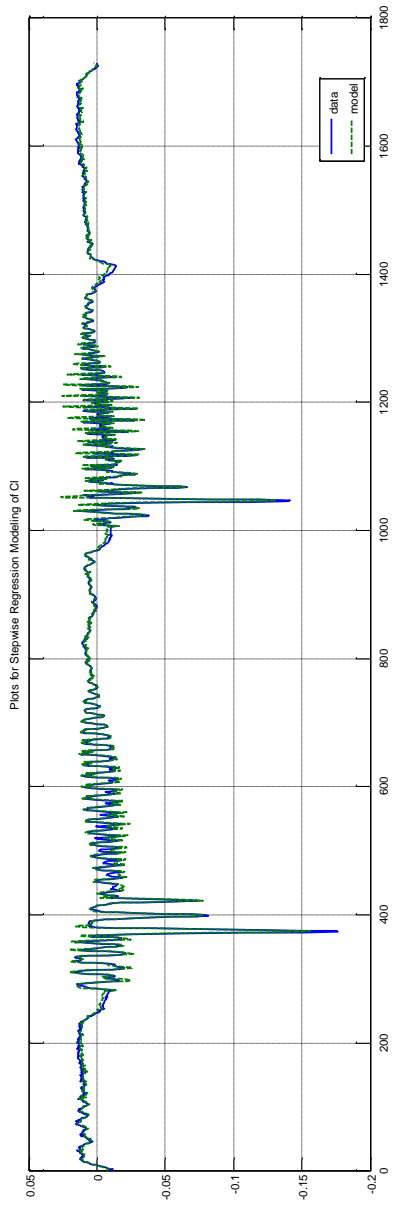


Figure 42. Estimated response vs data - C_j

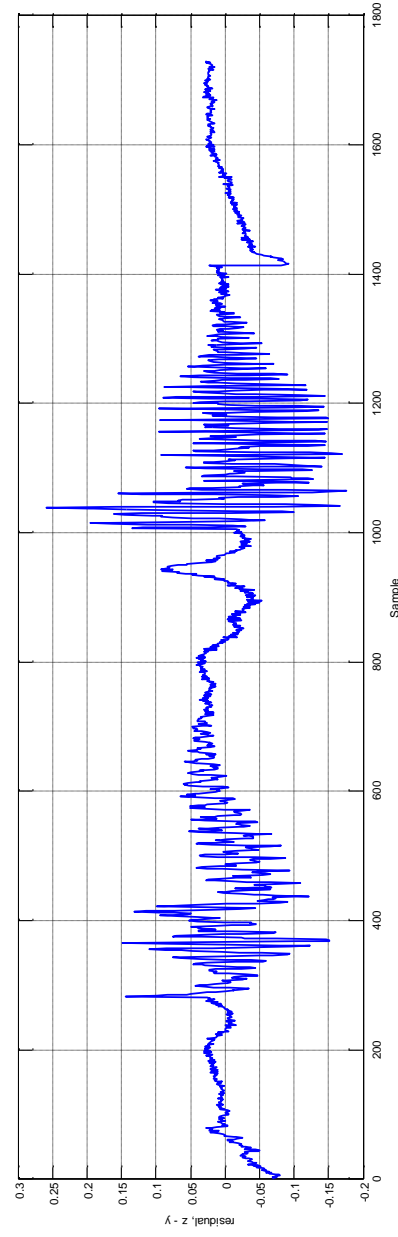
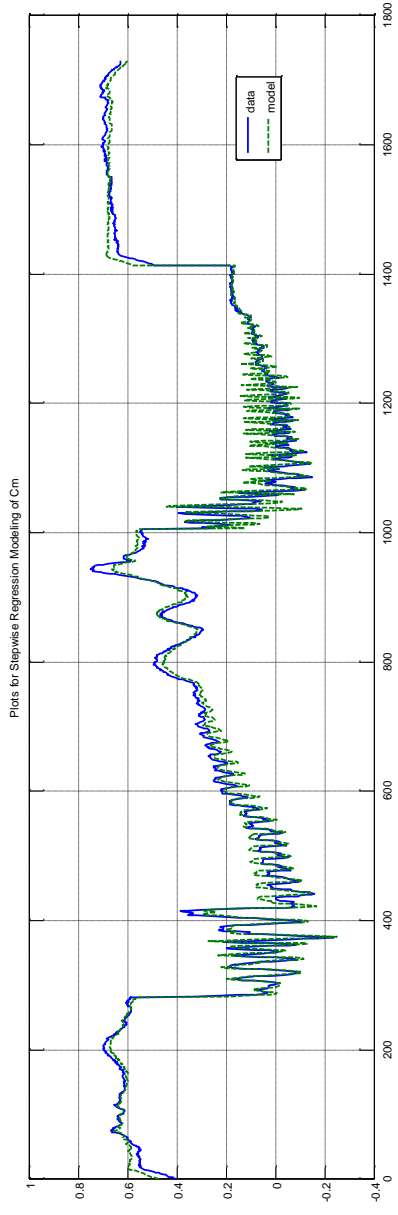


Figure 43. Estimated response vs data – C_m

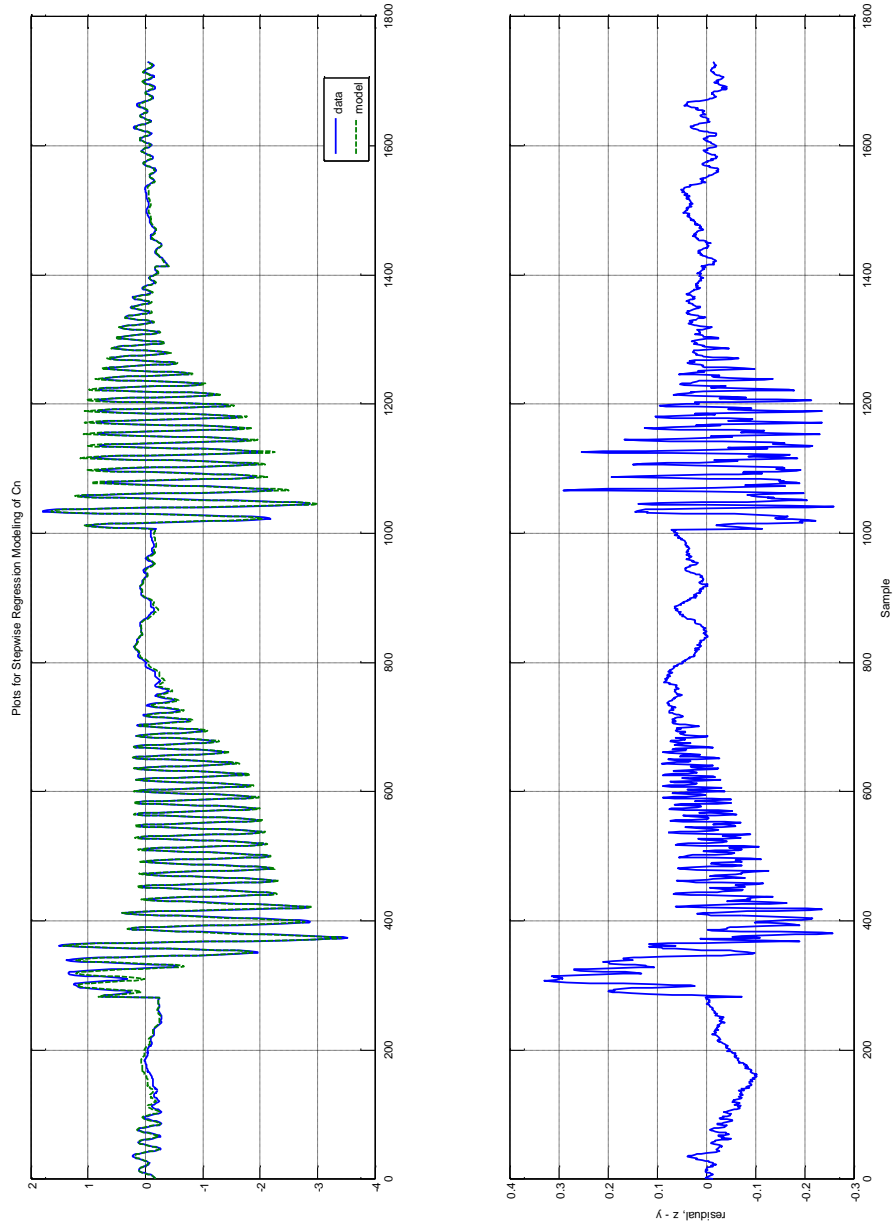


Figure 44. Estimated response vs data - C_n

5.1.4 Actual Flight Test Data for Freefall Separation Model

To further test the model structure determination and equation error based parameter estimation algorithms, a fourth test case is selected as the low fidelity flight test data of an free fall separation model. A complete 6dof trajectory information is not available in the flight test data since only limited measurements (body linear accelerations and body angular rates) were taken with a relatively low accuracy IMU. The atmospheric conditions were gathered by onboard data acquisition systems of the parent aircraft and a post test trajectory reconstruction was carried out to obtain the required variables. Figure 45 and Figure 46 show the time history of simulated flight test data for test case 4.

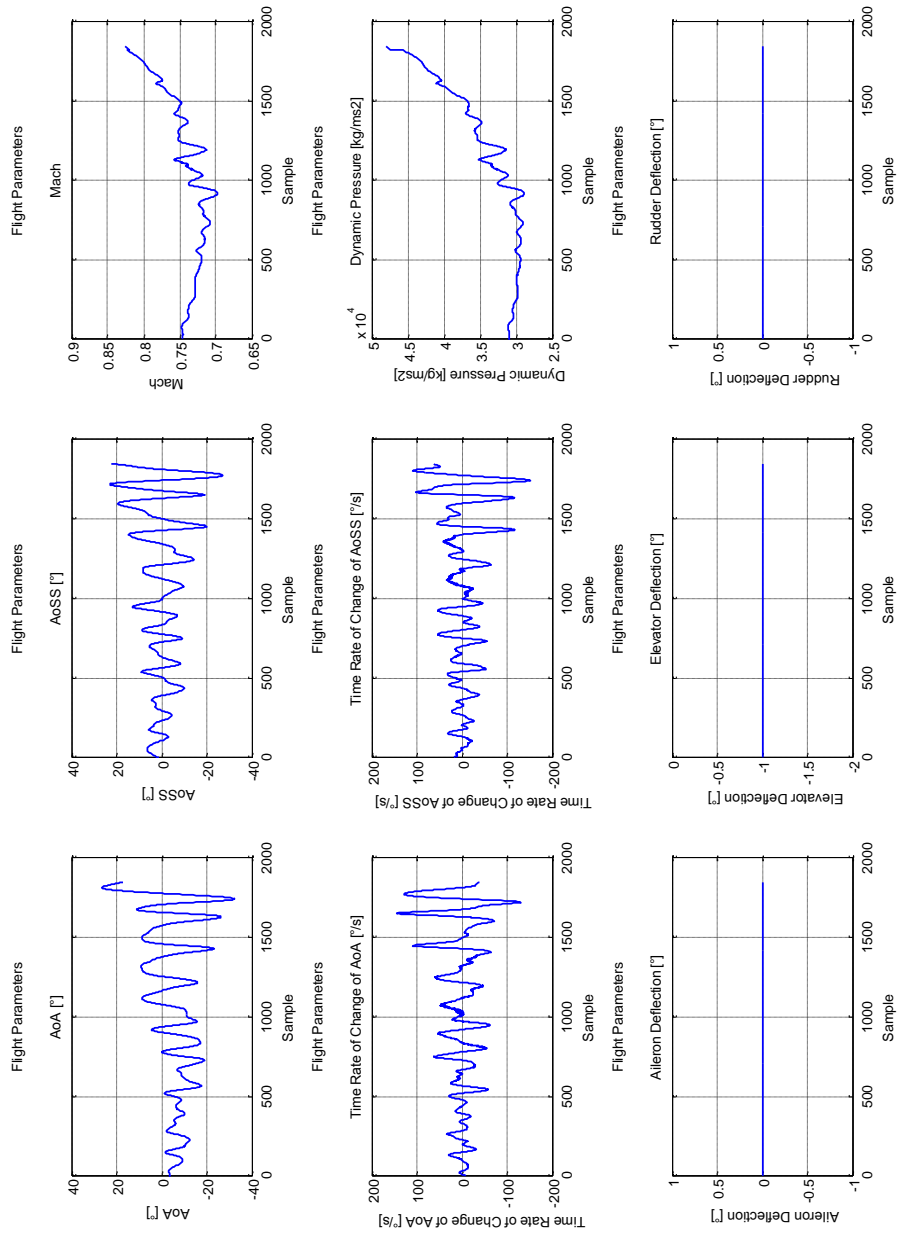


Figure 45. Actual flight test data 4 flight parameters

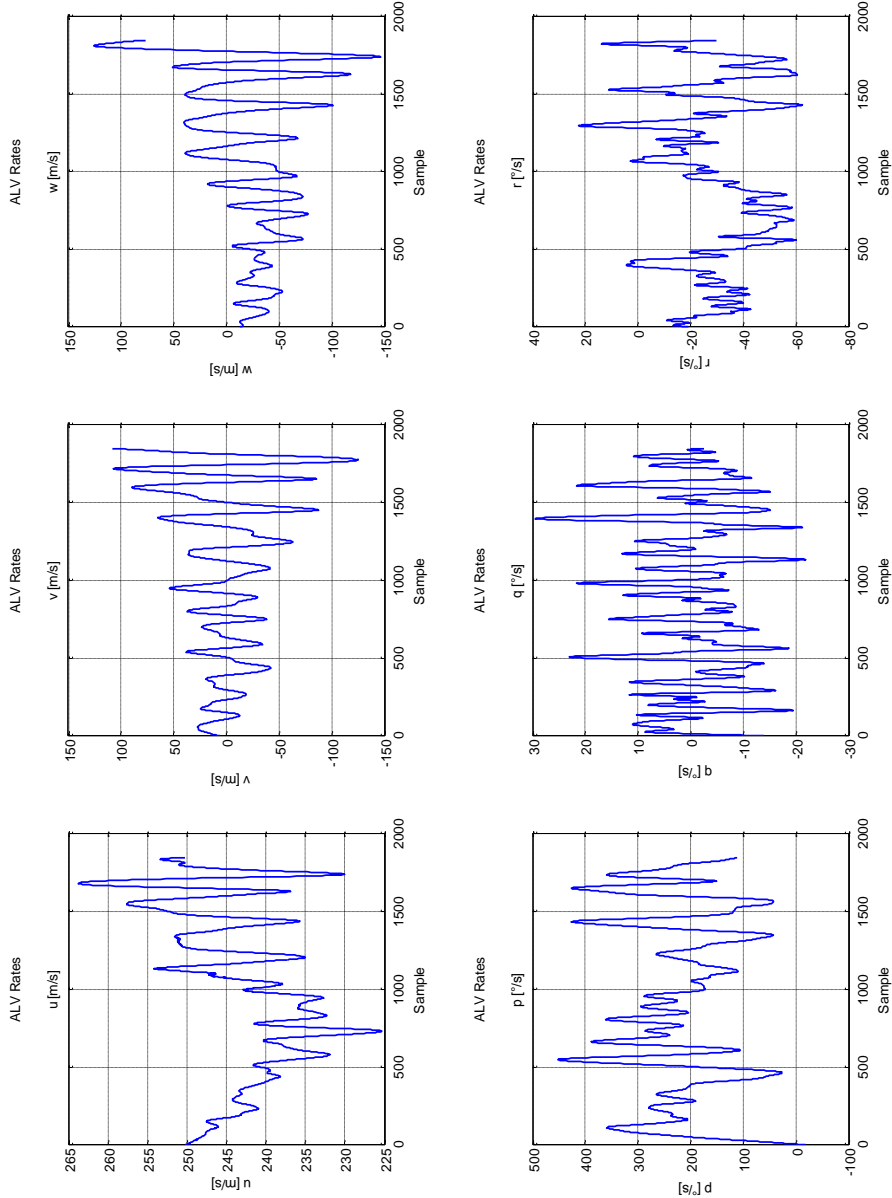


Figure 46. Actual flight test data 4 rates

The aerodynamic model structure determination algorithm is run for 6 aerodynamic coefficients. It can be seen from Table 21 through Table 26 that, some reasonable models are obtained for all coefficients. Yet, for some of the parameters, the predicted errors are quite high, and for some parameters they are unacceptable. Model responses and the residuals are given in Figure 47 through Figure 52. As can be seen from the plots, identified models represent almost all dynamics of the vehicle, but there are considerably large residuals left over. That is, the model structures are adequate, but the parameter estimates need to be refined.

Table 21. Identified model and parameter estimates for C_x

CX	Parameter Estimates	Standard Error	Percent Error	95% Confidence LB	95% Confidence UB
alpha	0.2239	0.0419	18.6993	0.1401	0.3076
Mach	-0.4840	0.2195	45.3427	-0.9229	-0.0451
alpha3	-0.8905	0.2726	30.6072	-1.4357	-0.3454
static term	0.3066	0.1634	53.3047	-0.0203	0.6334

Table 22. Identified model and parameter estimates for C_Y

CY	Parameter Estimates	Standard Error	Percent Error	95% Confidence LB	95% Confidence UB
beta	5.6930	0.3976	6.9849	4.8977	6.4883
r	339.6378	132.0473	38.8789	75.5432	603.7325
betaalpha2	77.0894	3.8767	5.0288	69.3361	84.8427
static term	0.0789	0.0719	91.0980	-0.0648	0.2226

Table 23. Identified model and parameter estimates for C_Z

CZ	Parameter Estimates	Standard Error	Percent Error	95% Confidence LB	95% Confidence UB
alpha	-19.2292	8.4252	43.8145	-36.0796	-2.3788
alpha2	-3.1140	1.0966	35.2160	-5.3073	-0.9208
beta2	5.7542	1.5341	26.6600	2.6861	8.8224
alphaMach	39.6169	11.0064	27.7821	17.6041	61.6297
alphabeta2	34.1308	4.4333	12.9892	25.2641	42.9974
static term	0.8274	0.0902	10.8980	0.6471	1.0078

Table 24. Identified model and parameter estimates for C_i

CI	Parameter Estimates	Standard Error	Percent Error	95% Confidence LB	95% Confidence UB
alpha	-0.0366	0.0395	107.8804	-0.1156	0.0424
beta	0.5030	0.0924	18.3672	0.3182	0.6878
p	-8.6068	4.3013	49.9754	-17.2093	-0.0042
r	-40.9471	18.1190	44.2498	-77.1852	-4.7091
beta3	49.9358	15.8466	31.7338	18.2427	81.6289
alphabeta	5.9892	0.5268	8.7957	4.9356	7.0428
betar	-363.9586	138.1934	37.9695	-640.3455	-87.5718
betaalpha2	6.5807	0.7707	11.7121	5.0392	8.1222
Machbeta3	-63.6458	19.5885	30.7773	-102.8227	-24.4688
alphabetap	412.0724	137.9240	33.4708	136.2244	687.9204
static term	0.0056	0.0126	223.7977	-0.0196	0.0309

Table 25. Identified model and parameter estimates for C_m

Cm	Parameter Estimates	Standard Error	Percent Error	95% Confidence LB	95% Confidence UB
alpha	5.8877	0.4540	7.7119	4.9796	6.7958
alpha3	-24.8083	2.4082	9.7071	-29.6247	-19.9920
alphabeta2	-28.8968	4.1181	14.2510	-37.1330	-20.6606
static term	0.3856	0.0342	8.8562	0.3173	0.4540

Table 26. Identified model and parameter estimates for C_n

Cn	Parameter Estimates	Standard Error	Percent Error	95% Confidence LB	95% Confidence UB
beta	-4.5061	0.2904	6.4449	-5.0870	-3.9253
beta3	42.3738	2.7912	6.5872	36.7913	47.9563
alphabeta	-3.5593	0.7908	22.2185	-5.1410	-1.9777
static term	0.0108	0.0130	120.8272	-0.0153	0.0368

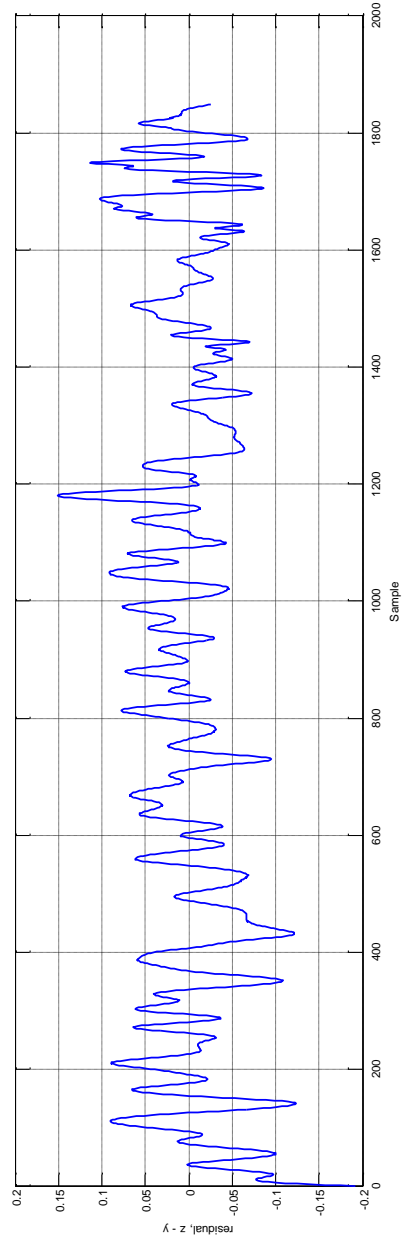
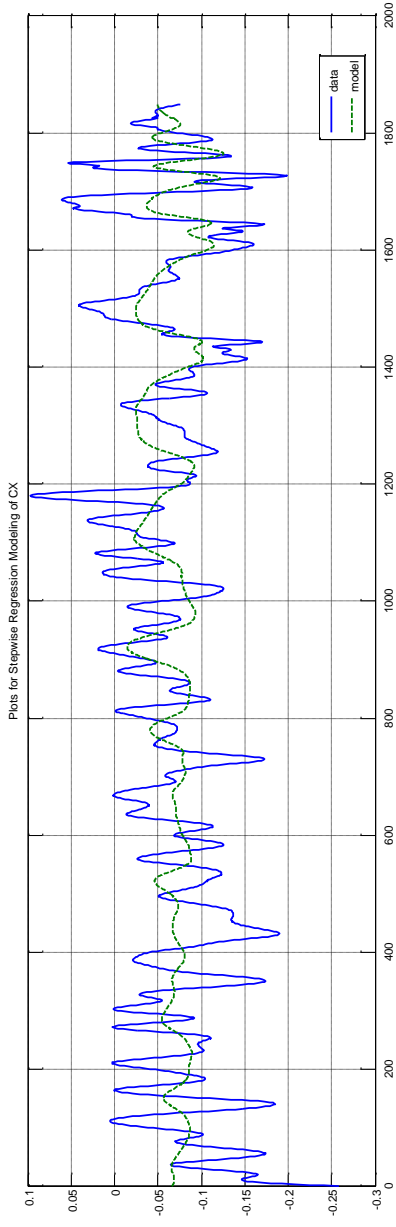


Figure 47. Estimated response vs data - Cx

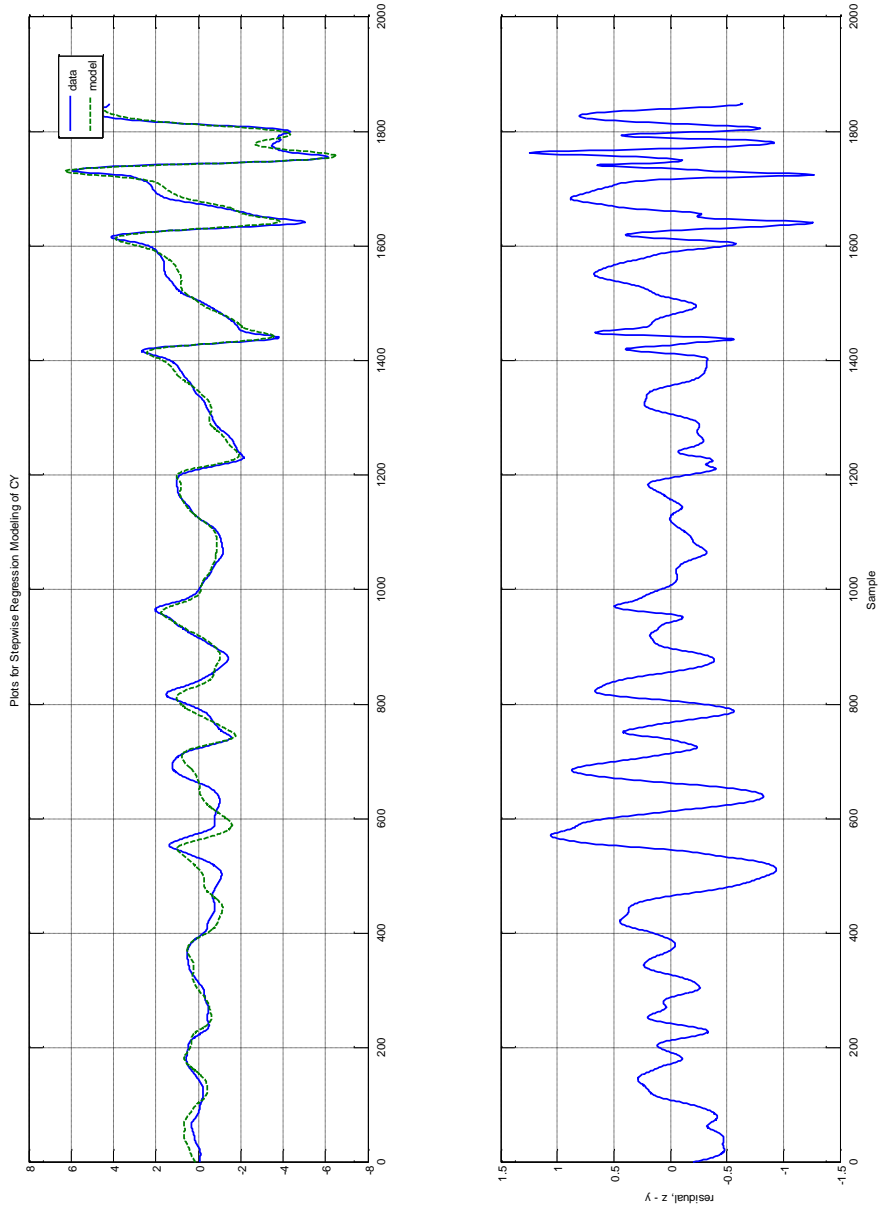


Figure 48. Estimated response vs data – C_y

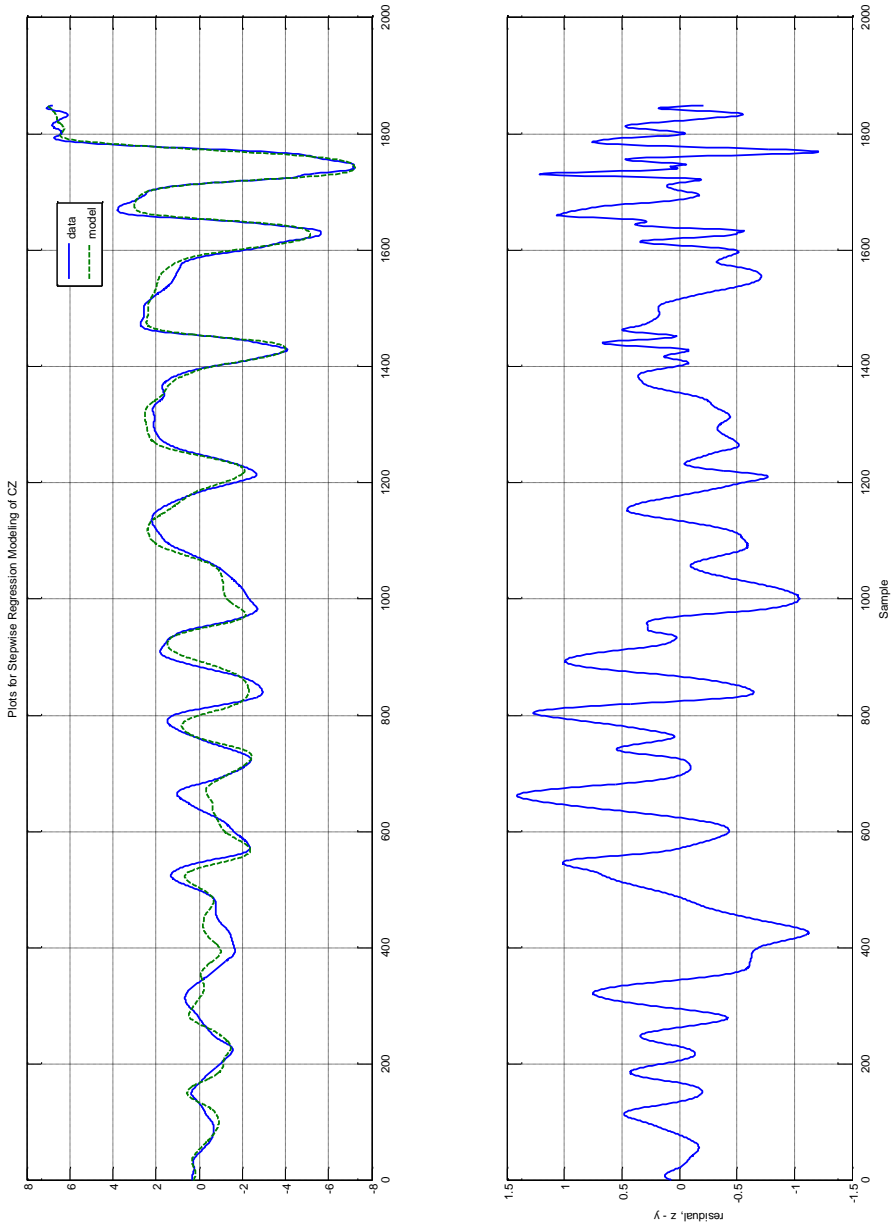


Figure 49. Estimated response vs data – Cz

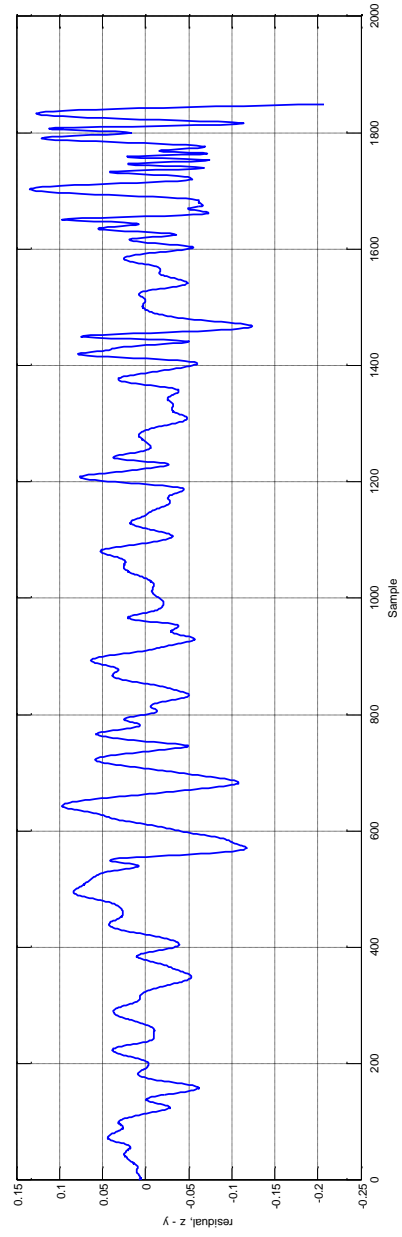
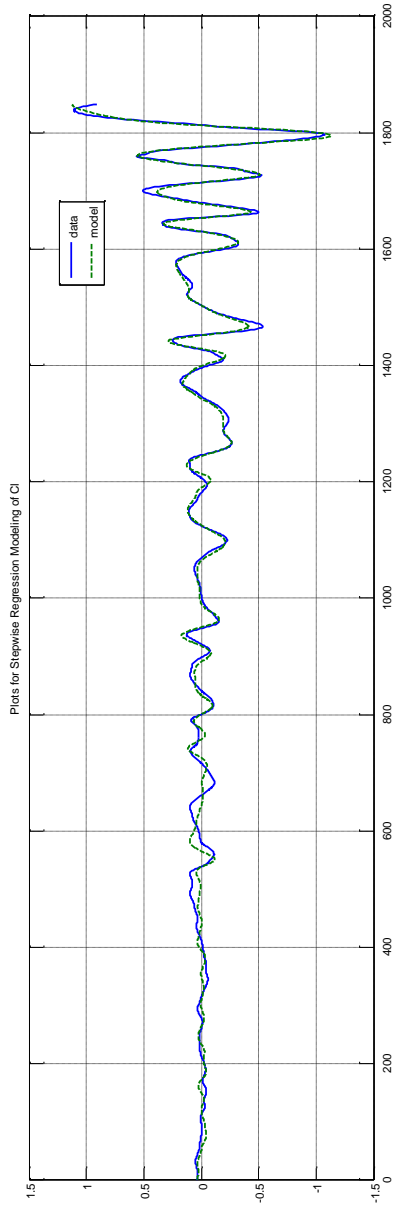


Figure 50. Estimated response vs data – C_i

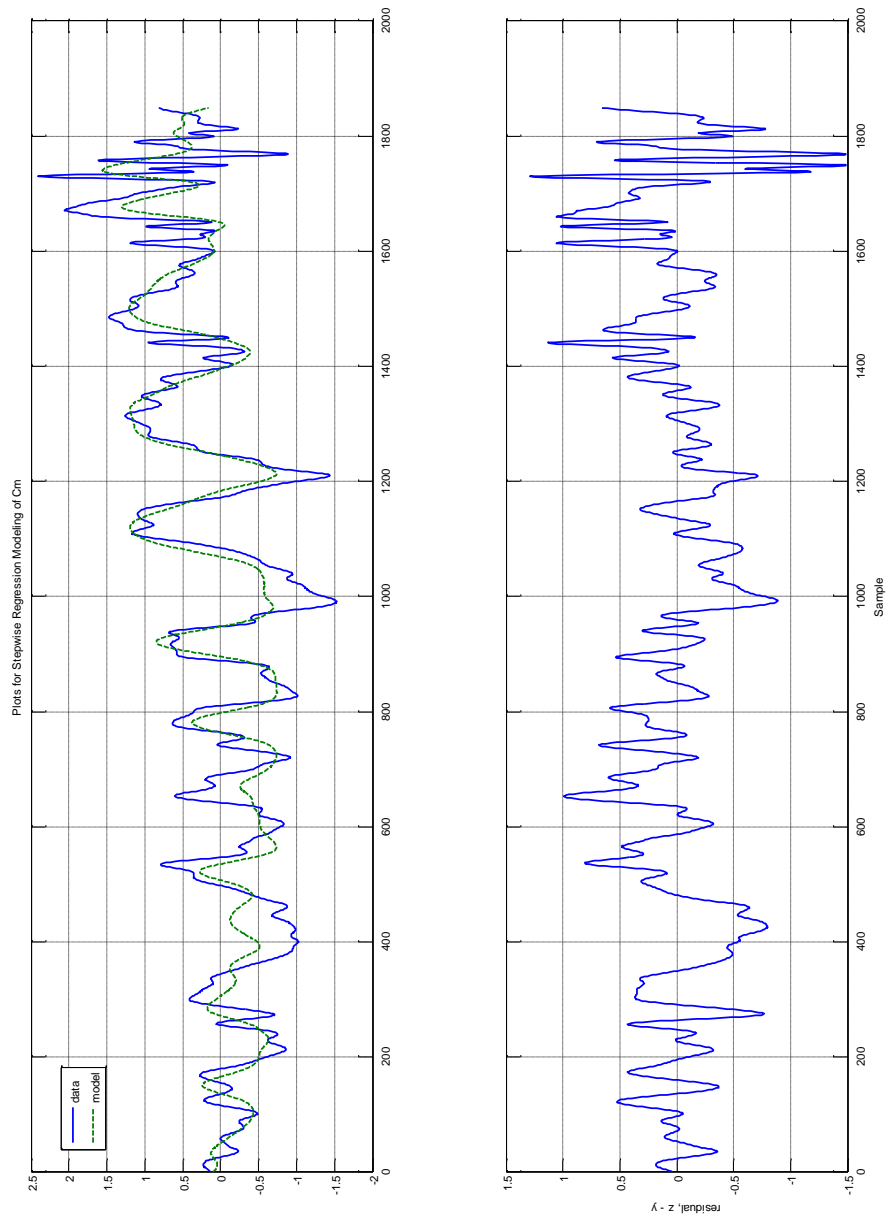


Figure 51. Estimated response vs data – C_m

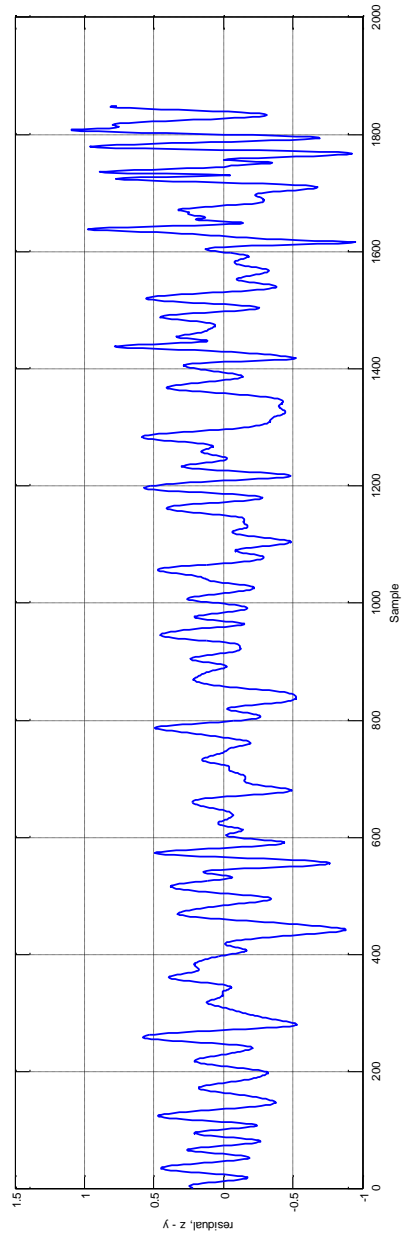
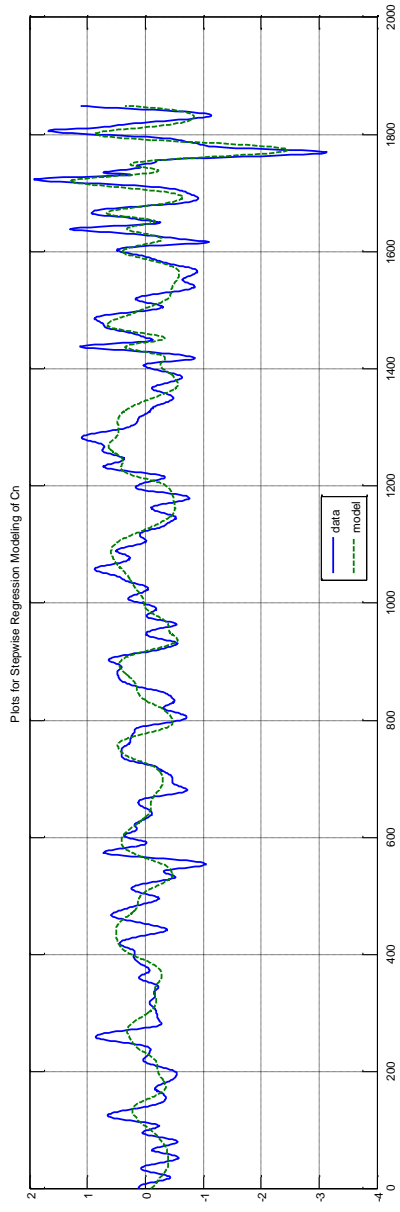


Figure 52. Estimated response vs data - C_n

5.2 Test Cases for Closed Loop Parameter Estimation

The closed loop parameter estimation method is tested with two different set of flight test data. The first set is the simulated flight test data of the guided FV, and the second set is the actual flight test data of the guided FV. Once again, the actual flight test data was gathered during performance demonstration flight tests of the FV and is not specifically designed for system identification/parameter estimation purposes.

5.2.1 Simulated Flight Test Data for Guided FV

The first test case has the identical flight test data of Section 5.1.1: a standard trajectory for the autonomous flight vehicle (Figure 18 and Figure 19)

The closed loop aerodynamic parameter estimation converged in about two weeks of run time on a quad core AMD Opteron 280 workstation with 7.83 GB of RAM. The final value of the cost function was 3.718 at the end of the genetic algorithm run and this value was reduced to 0.595 after a hybrid run. The following plots show the response of the estimated model parameters with the actual data.

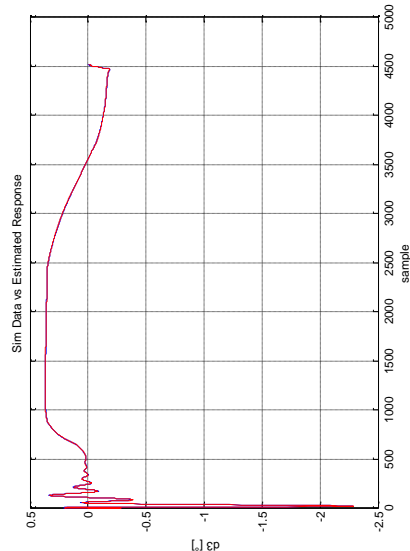
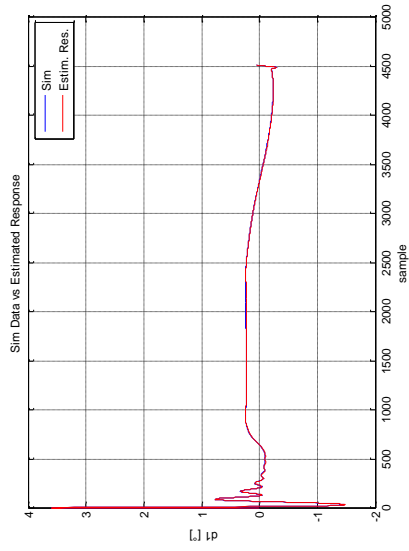
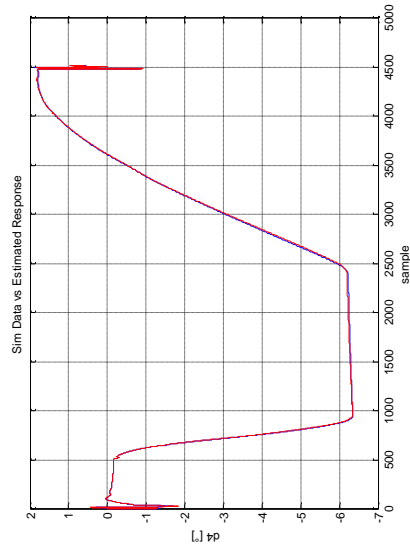
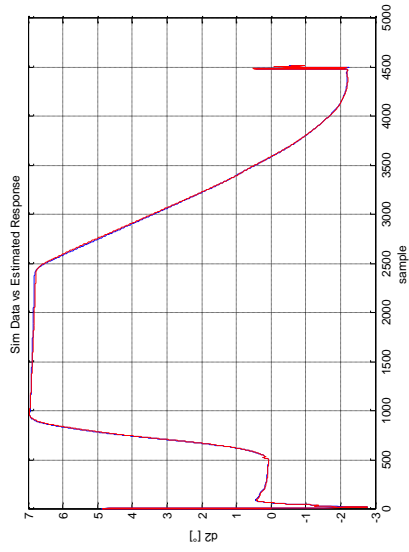


Figure 53. Deflections for test case 1

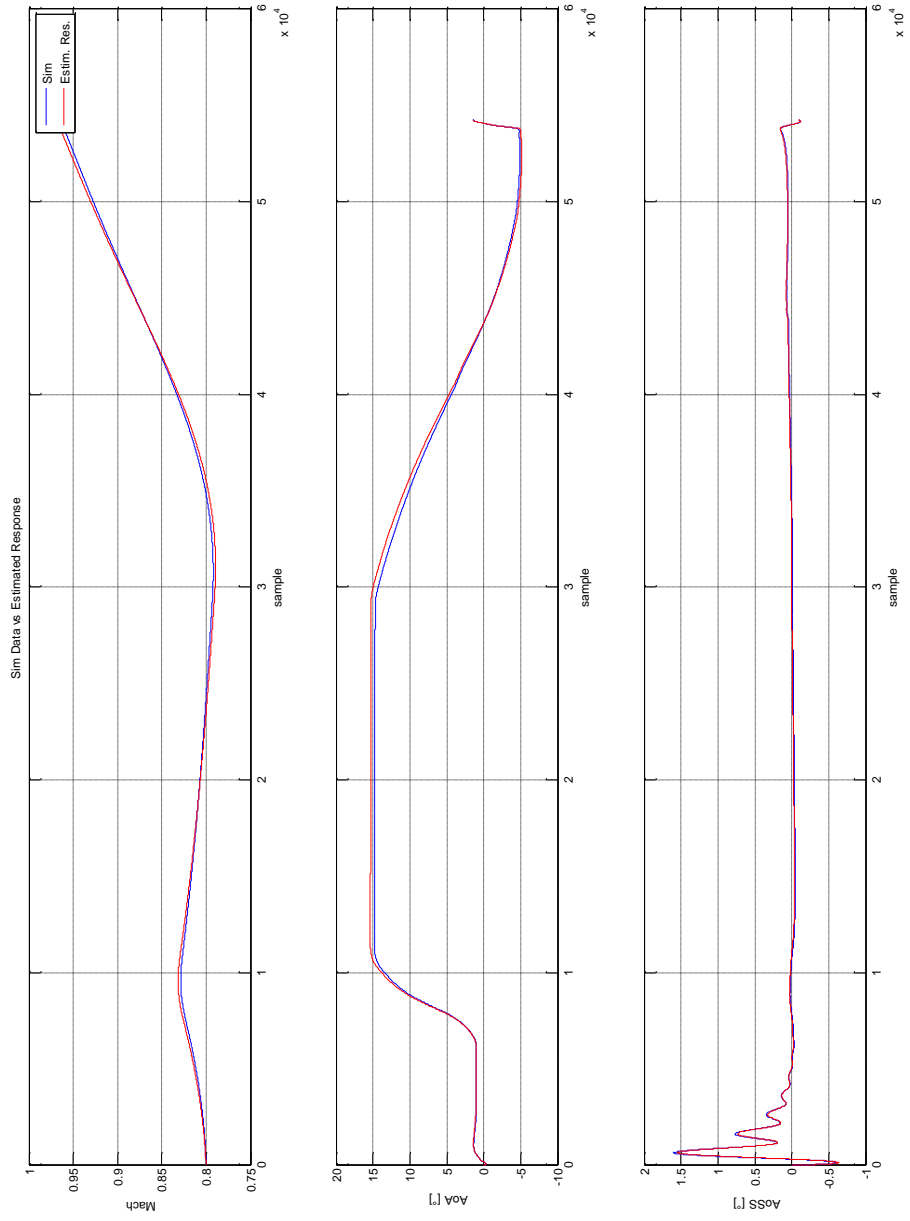


Figure 54. Flight parameters for test case 1

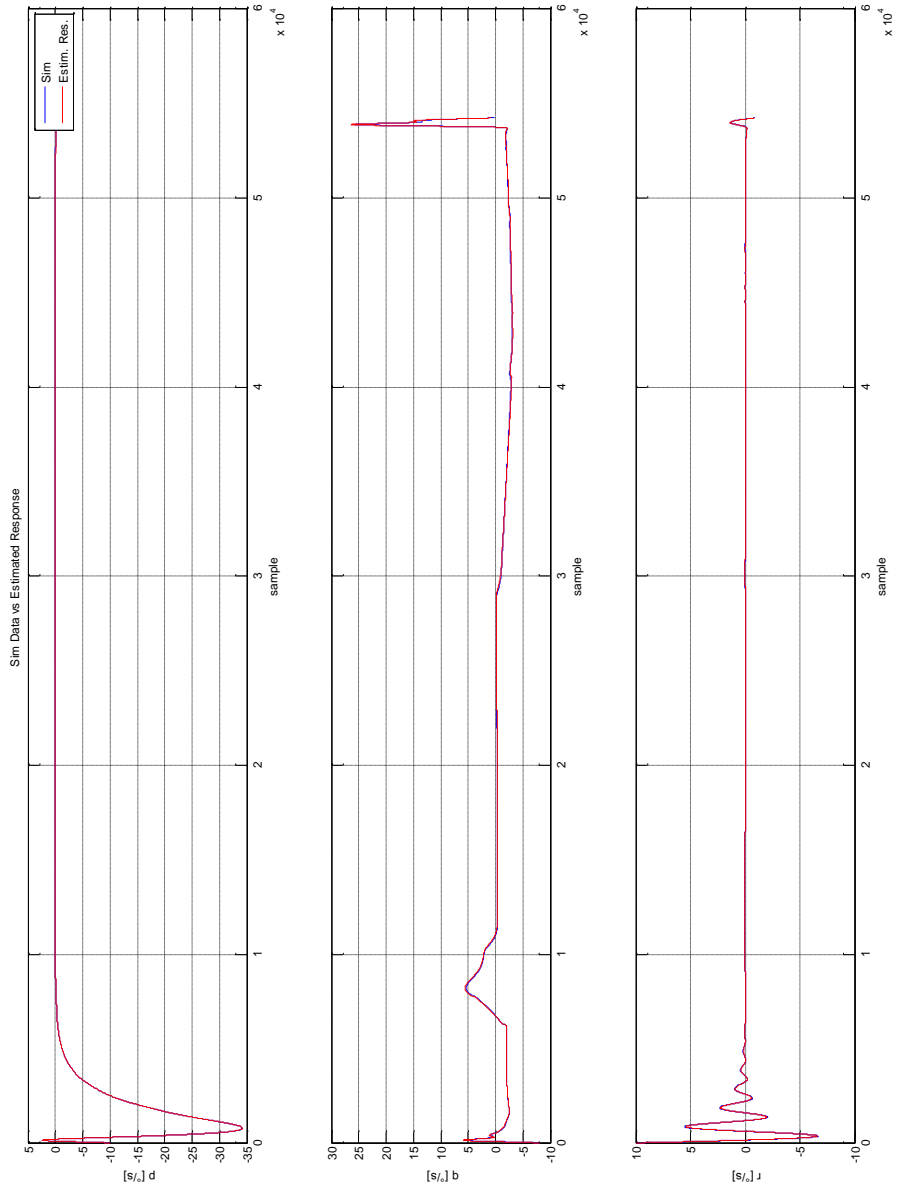


Figure 55. Rates for test case 1

The estimated parameter values are shown in Figure 56 through Figure 61. The estimation errors range between 0.1 – 20% for C_x , 0.2 – 24% for C_y , 0.5 – 22% for C_z , 2.2 – 46% for C_l , 0.2 – 35% for C_m , 0.8 – 38 % for C_n . It is worth noting that, the dominant terms for each coefficient (for example α^2 for C_x and β for C_n) are estimated with smaller errors than those with less importance (for example higher order parameters such as $\beta^2\delta_r$). Also, almost all parameters including rate terms have higher estimation errors when compared to others. This is due to the flight profile, since the vehicle is almost continuously in trimmed flight. As a consequence of this, the rates do not build up, and thus the estimation algorithm makes higher errors in converging for those terms.

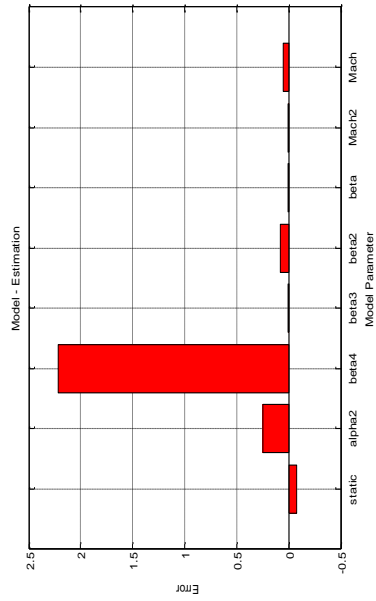
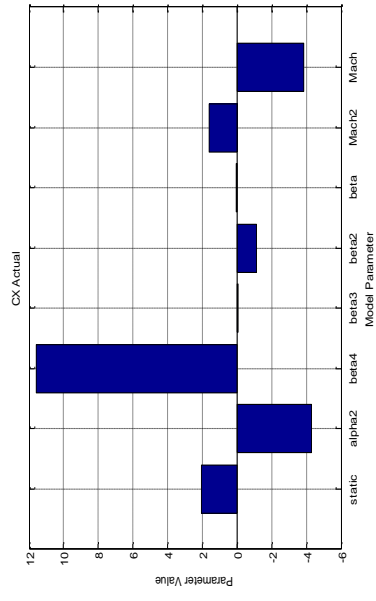
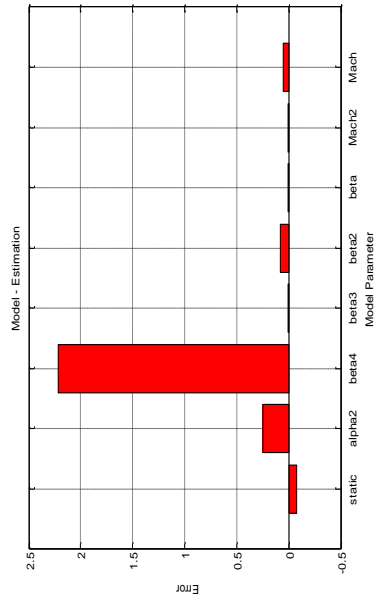
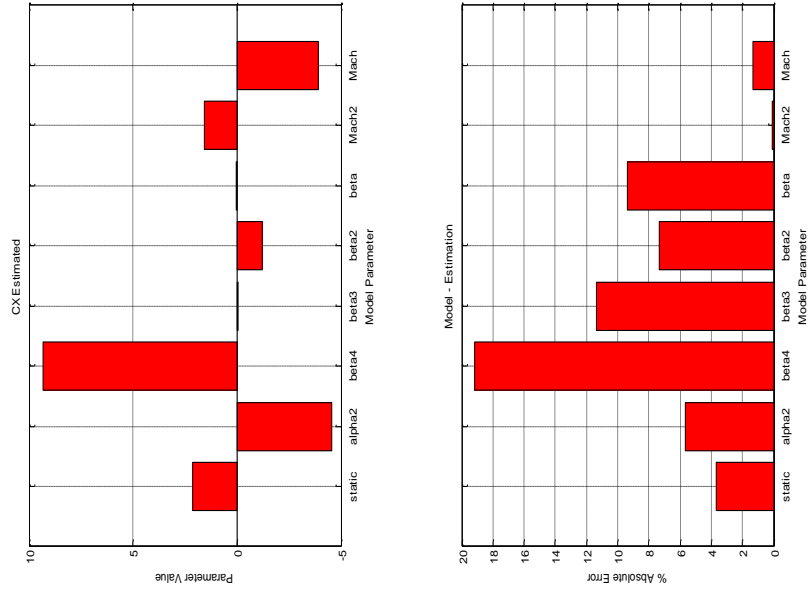


Figure 56. Estimation result for C_x – test case 1

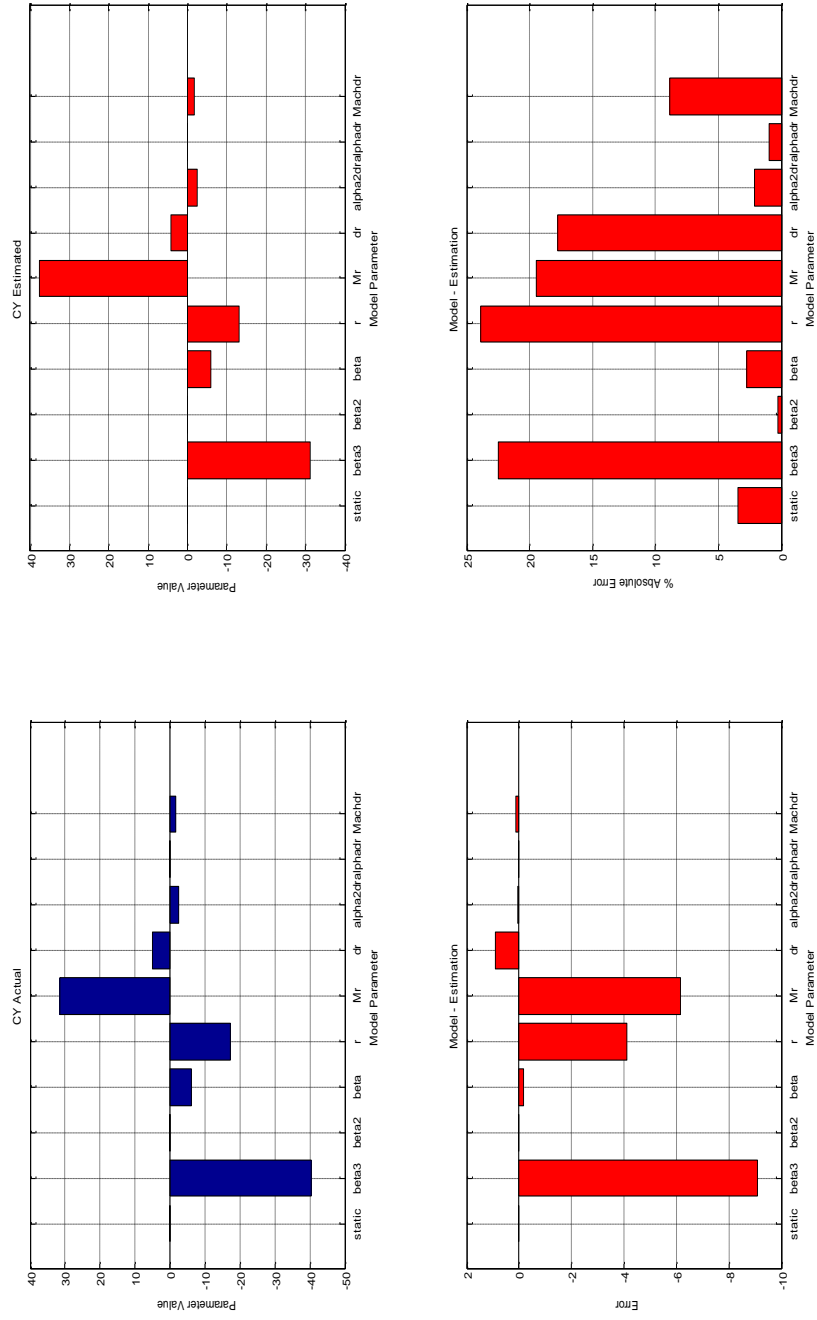


Figure 57. Estimation result for C_Y – test case 1

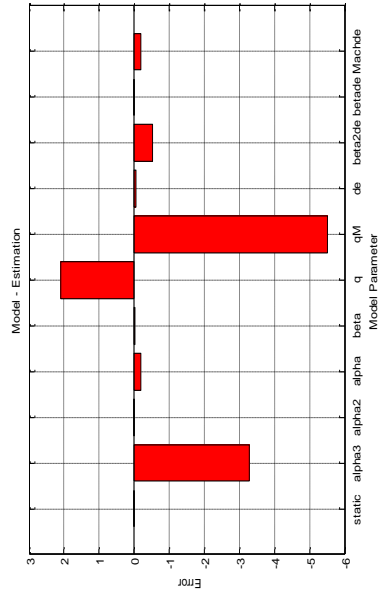
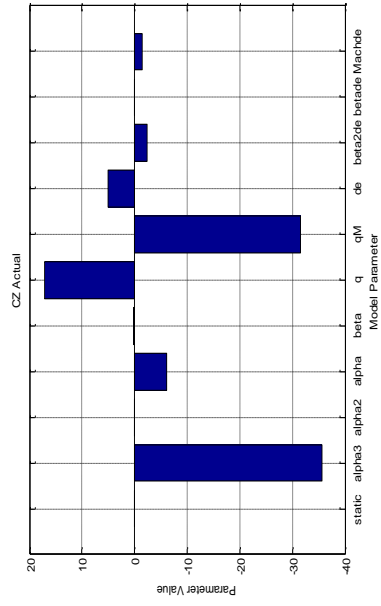
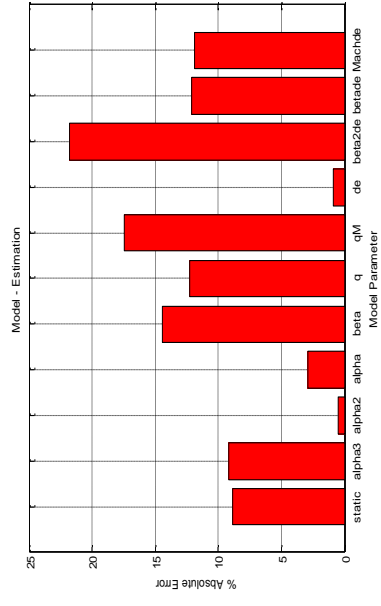
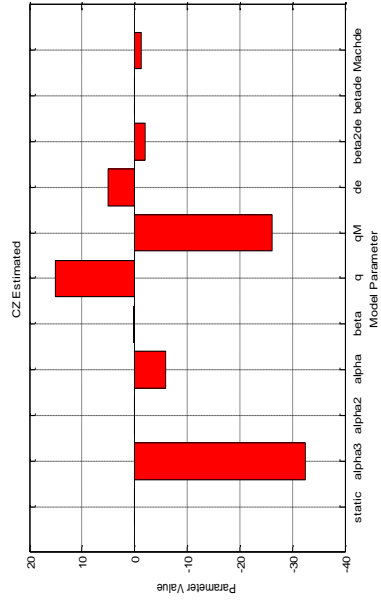


Figure 58. Estimation result for C_z – test case 1

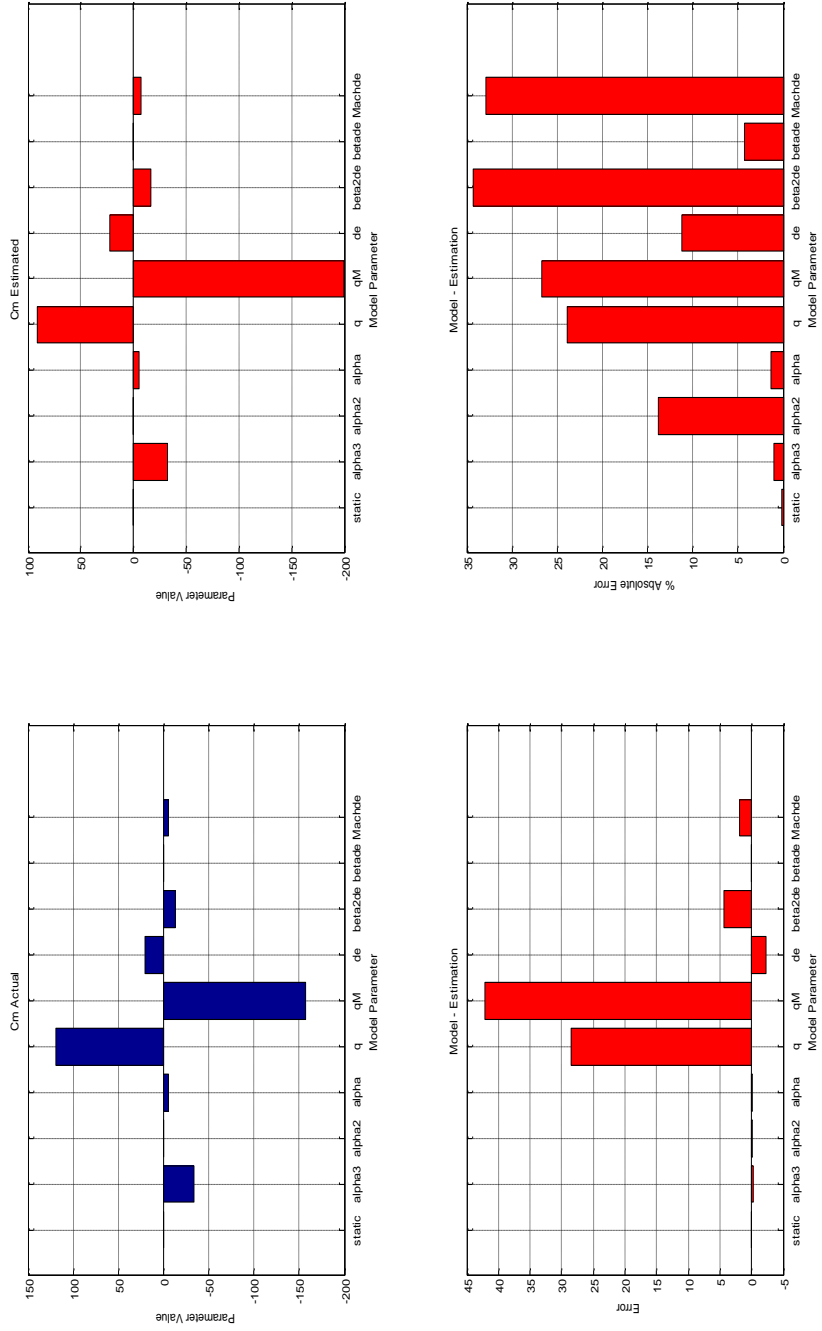


Figure 60. Estimation result for C_m – test case 1

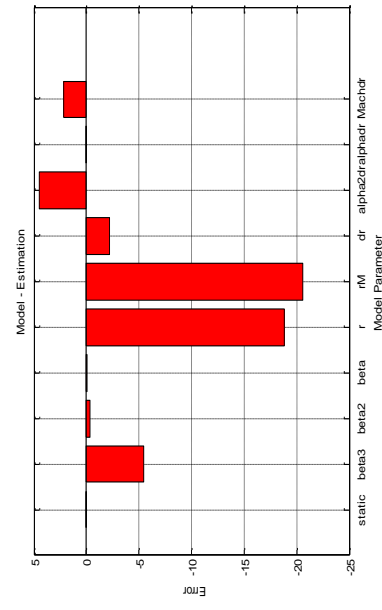
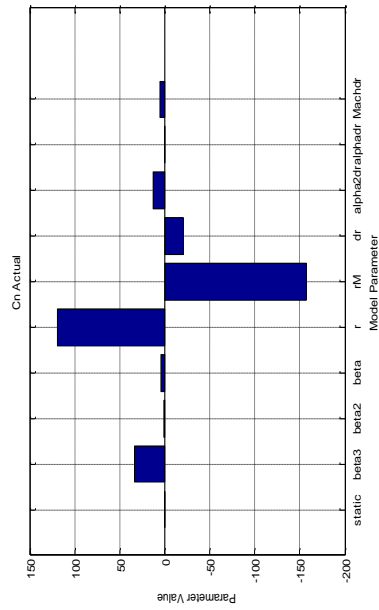
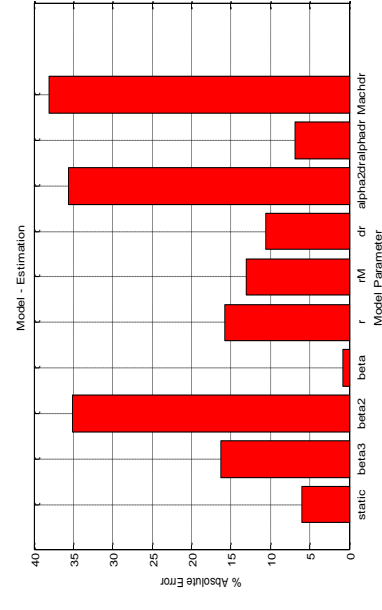
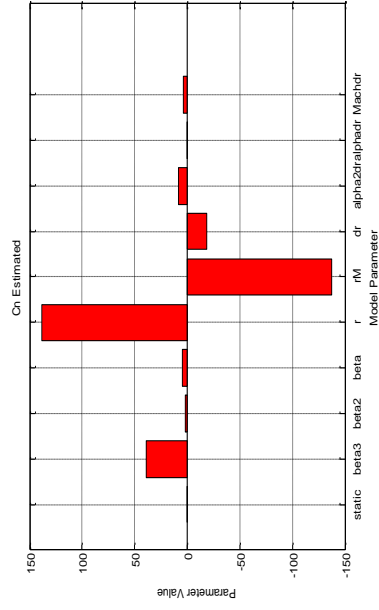


Figure 61. Estimation result for C_n – test case 1

5.2.2 Simulated Flight Test Data for Guided FV with Maneuvers

The simulated flight test data includes a basic set of system identification maneuvers: Constant frequency sine inputs on aileron, elevator, and rudder commands. Figure 62 through Figure 63 show the time history of simulated flight test data for test case 2.

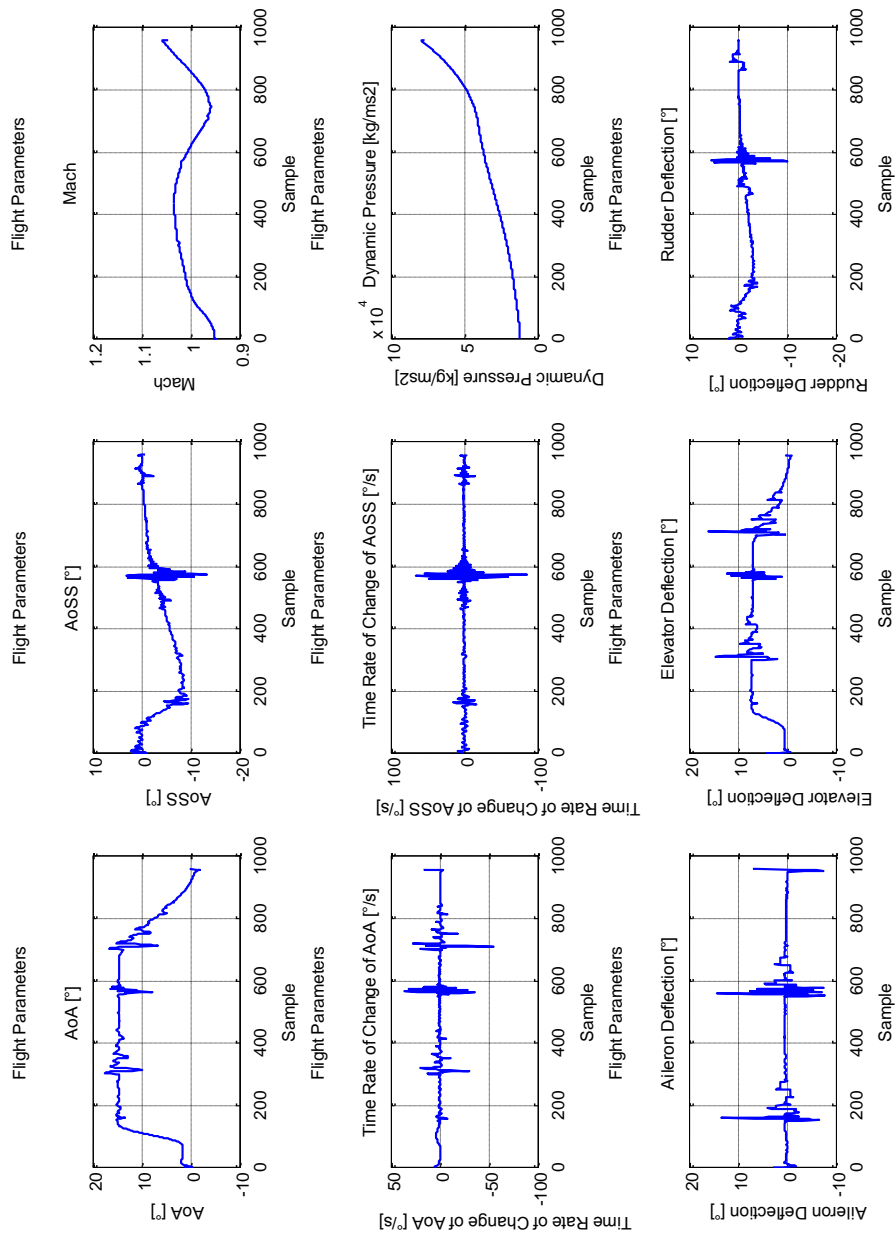


Figure 62. Simulated flight test data 1 flight parameters

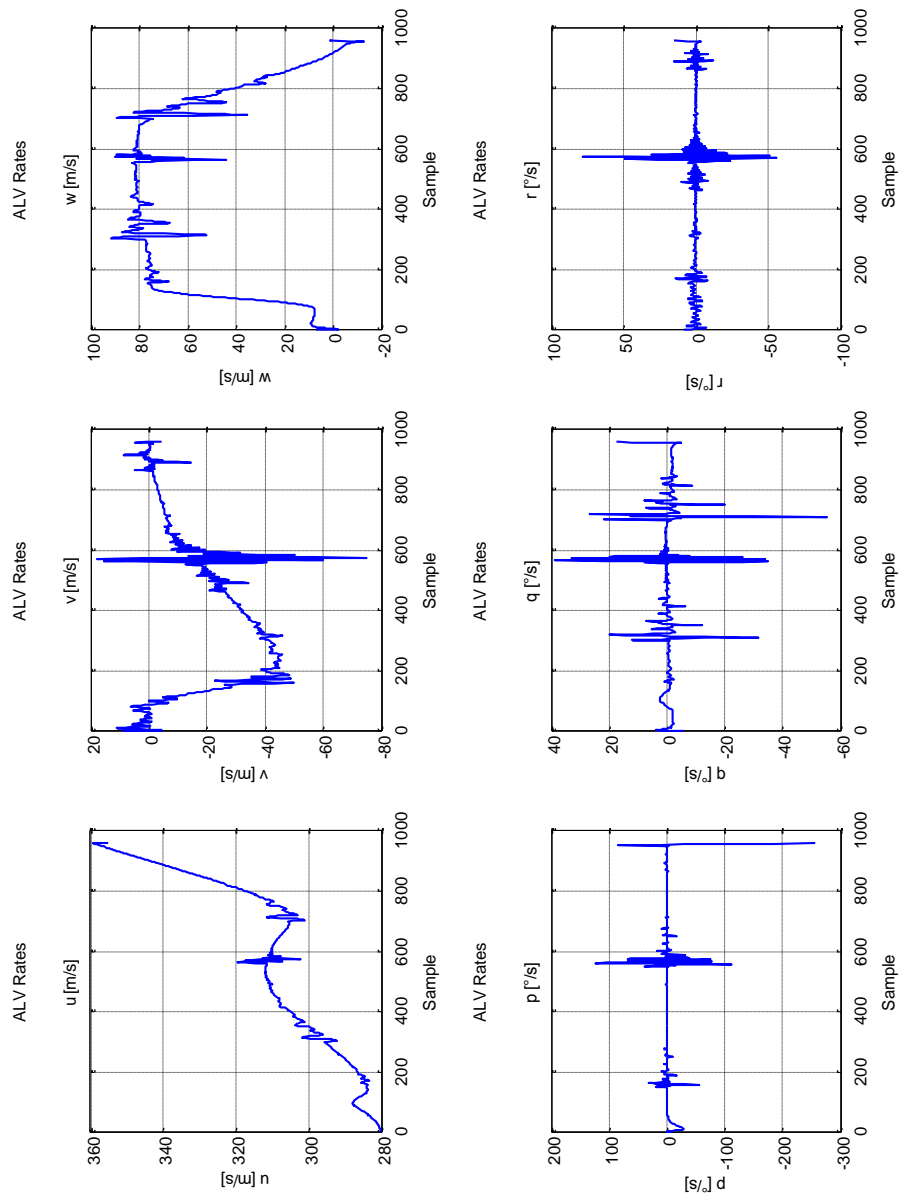


Figure 63. Simulated flight test data 1 rates

The closed loop aerodynamic parameter estimation converged in about four weeks of run time on a quad core AMD Opteron 280 workstation with 7.83 GB of RAM. The final value of the cost function was 6.725 at the end of the genetic algorithm run and this value was reduced to 0.494 after a hybrid run. The following plots show the response of the estimated model parameters together with the actual data.

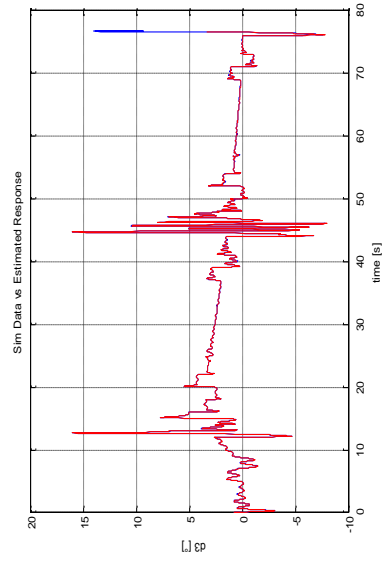
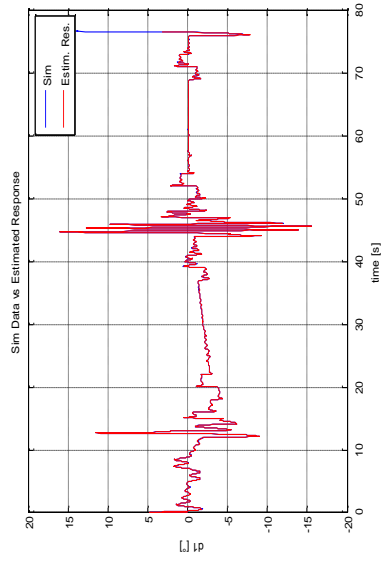
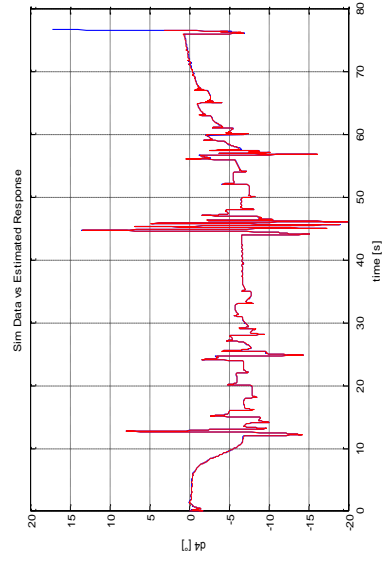
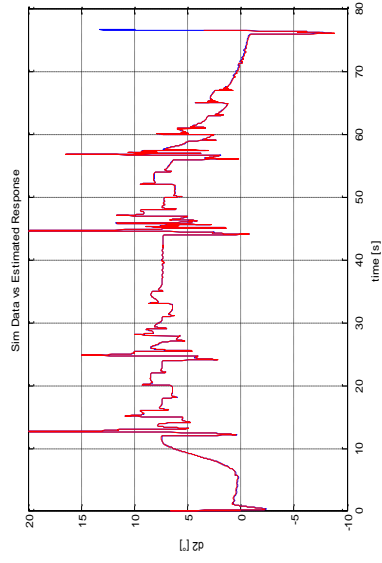


Figure 64. Deflections for test case 2

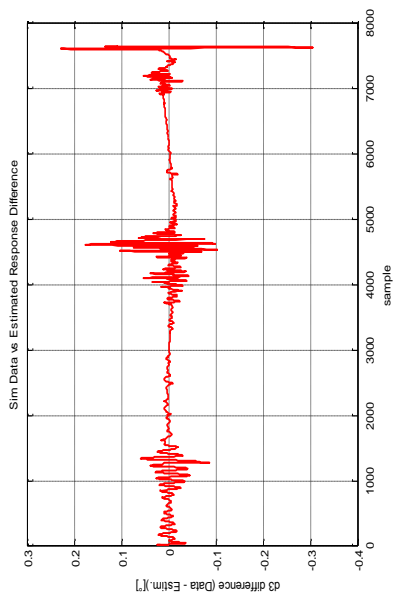
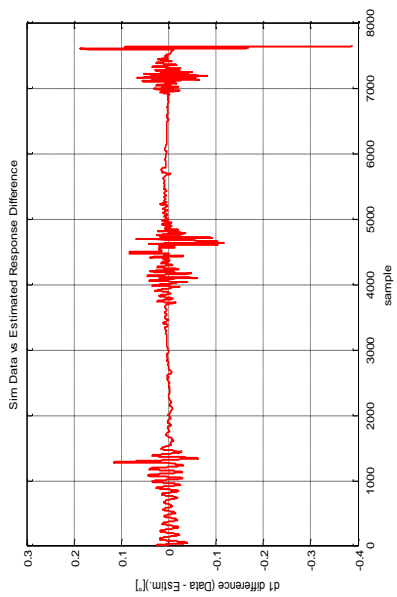
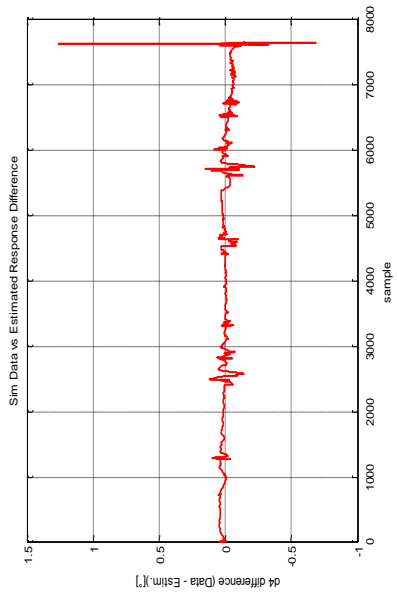
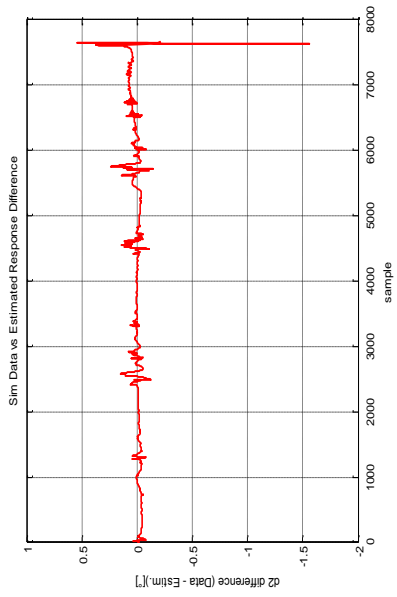


Figure 65. Error in deflections for test case 2

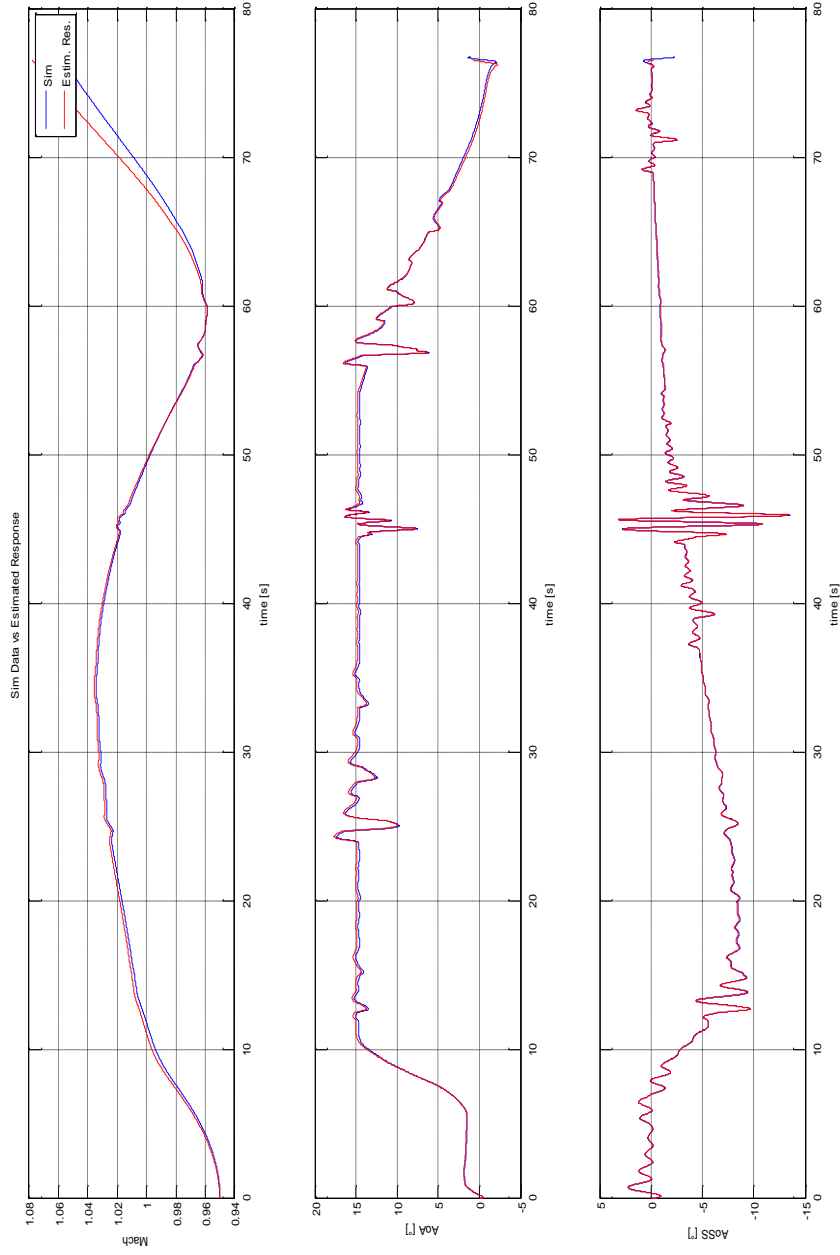


Figure 66. Flight parameters for test case 2

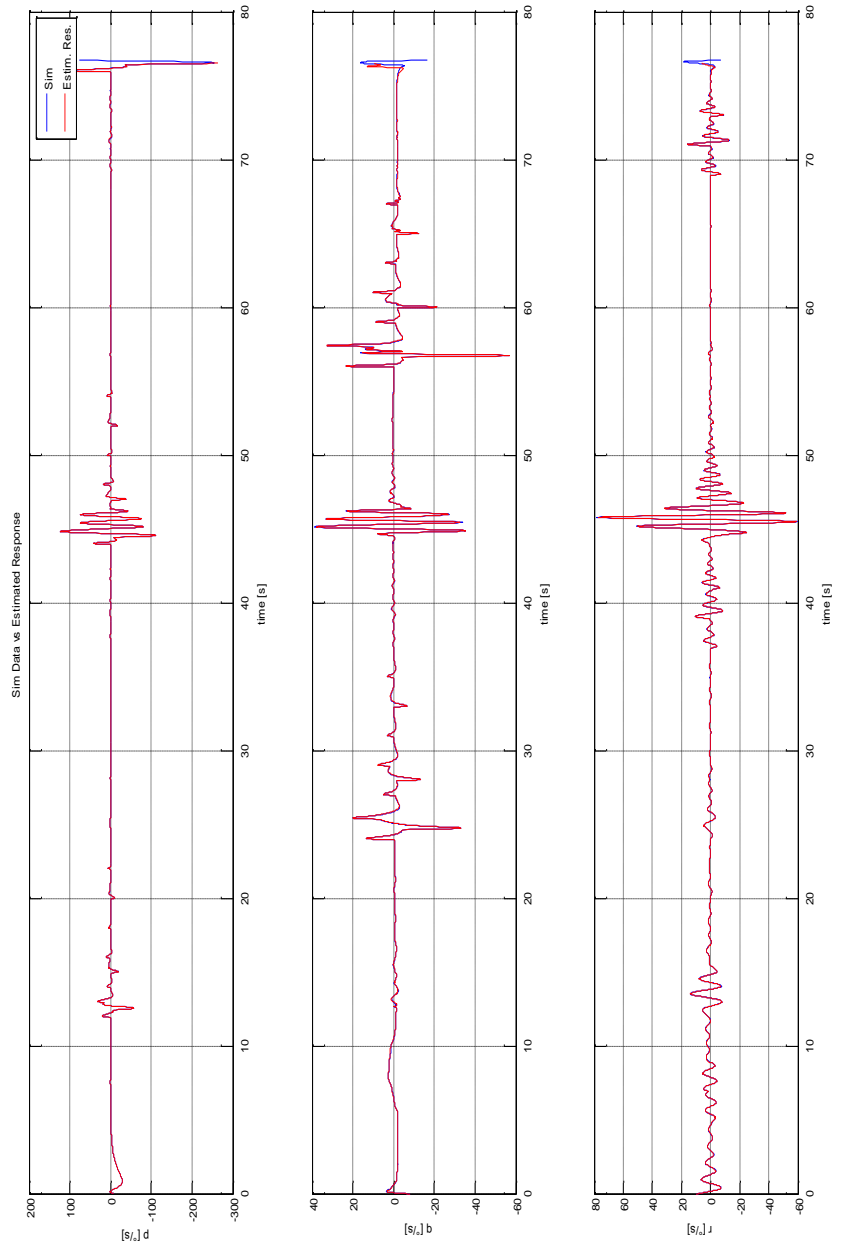


Figure 67. Rates for test case 2

The estimated parameter values are shown in Figure 68 through Figure 73. The estimation errors range between 6 – 24% for C_x , 0.2 – 21% for C_y , 5 – 25% for C_z , 2 – 50% for C_l , 0.5 – 46% for C_m , 2 – 46 % for C_n . The rate derivatives are much better estimated this time, when compared to the results of test case -1. Once again, the dominant terms for each coefficient are estimated with smaller errors than those with less importance.

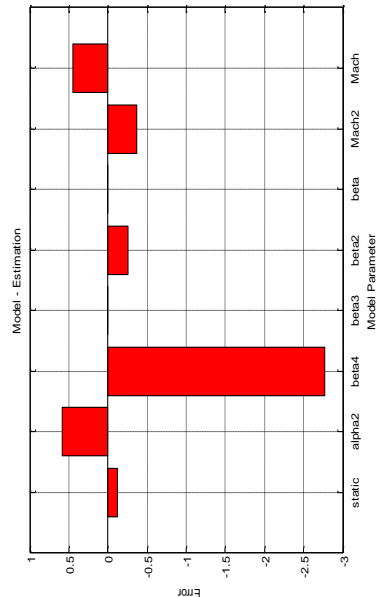
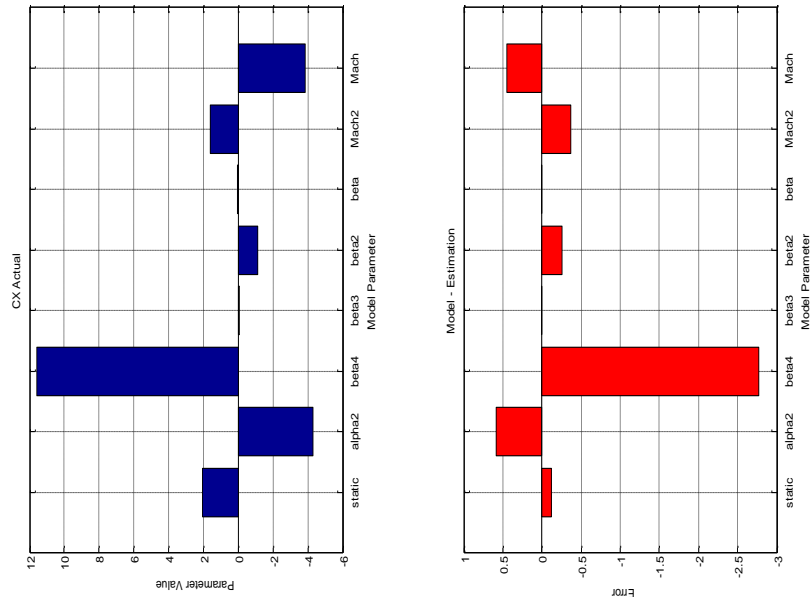
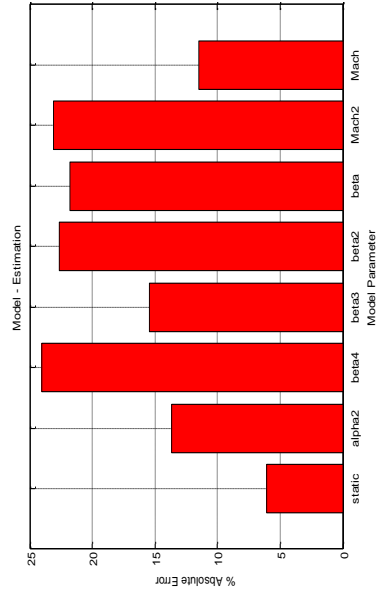
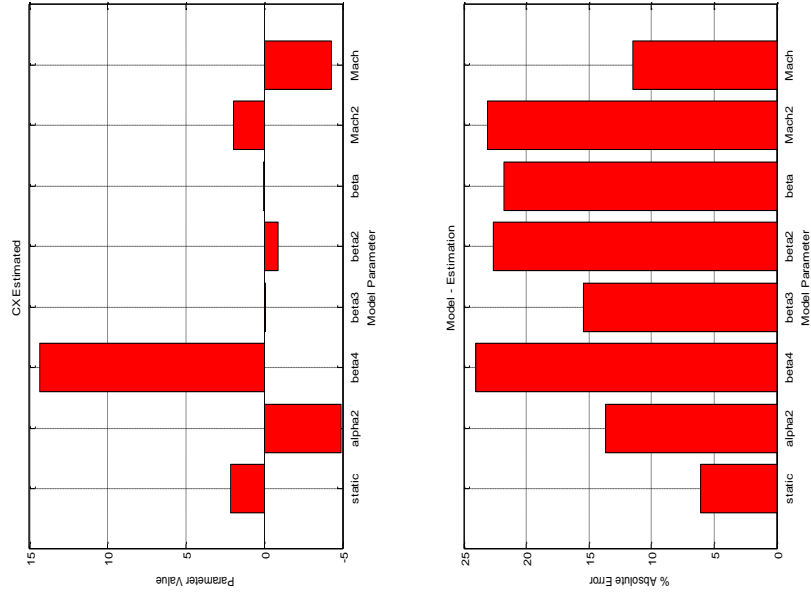


Figure 68. Estimation result for C_x – test case 2

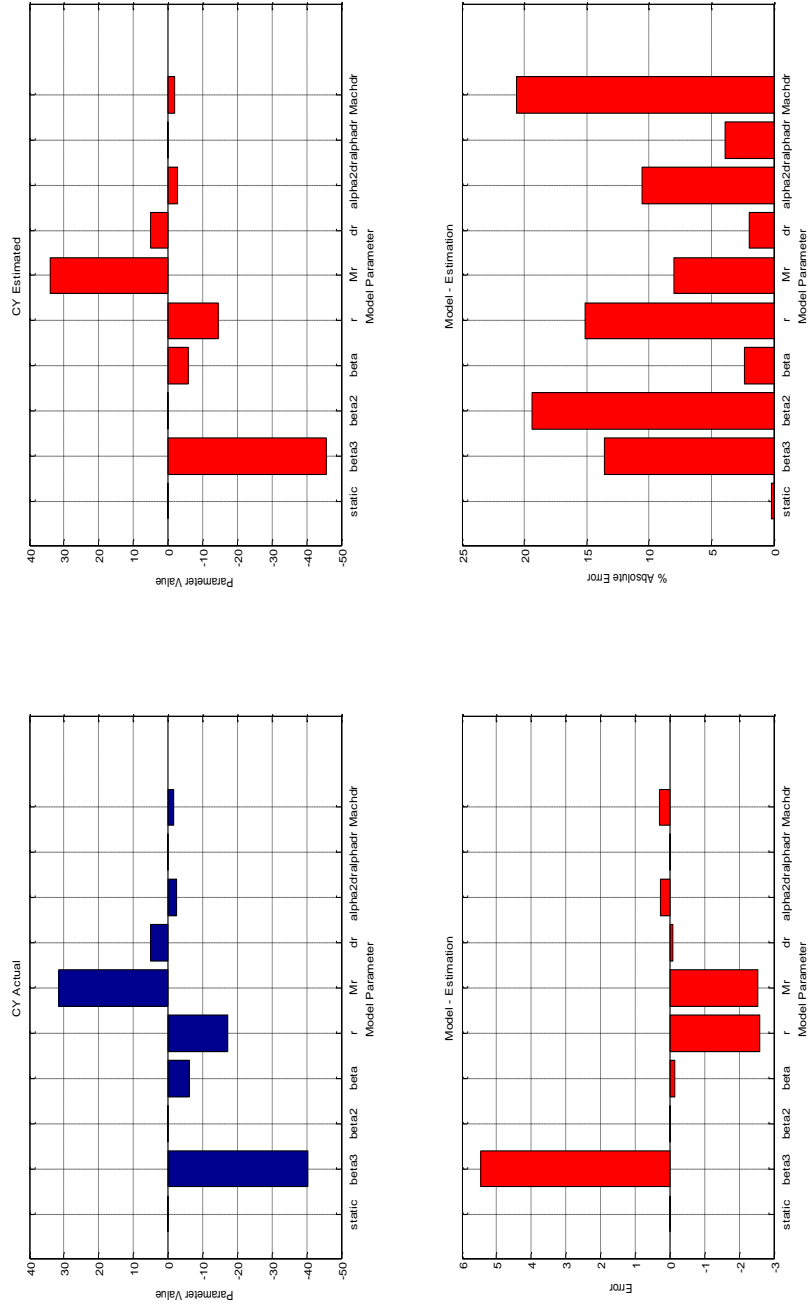


Figure 69. Estimation result for C_Y – test case 2

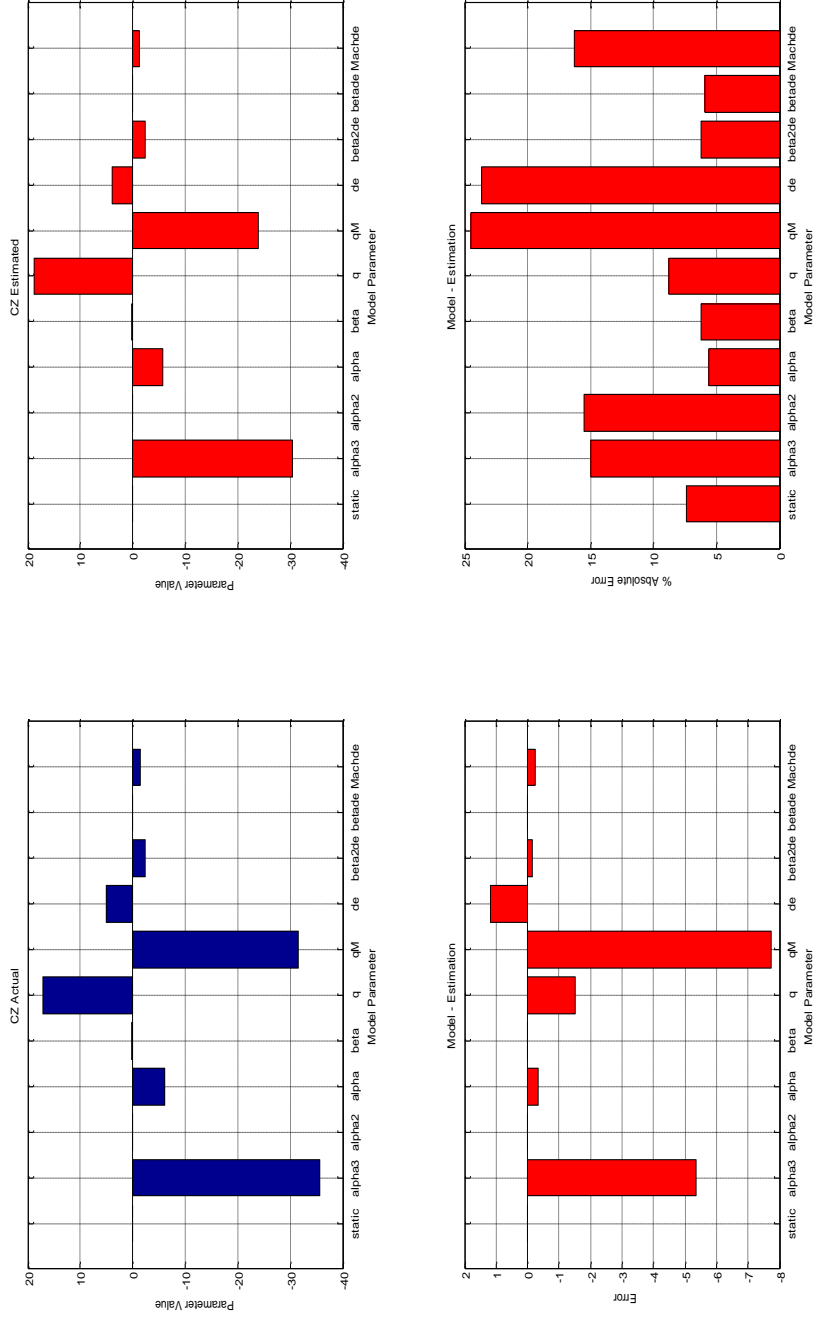


Figure 70. Estimation result for C_z – test case 2

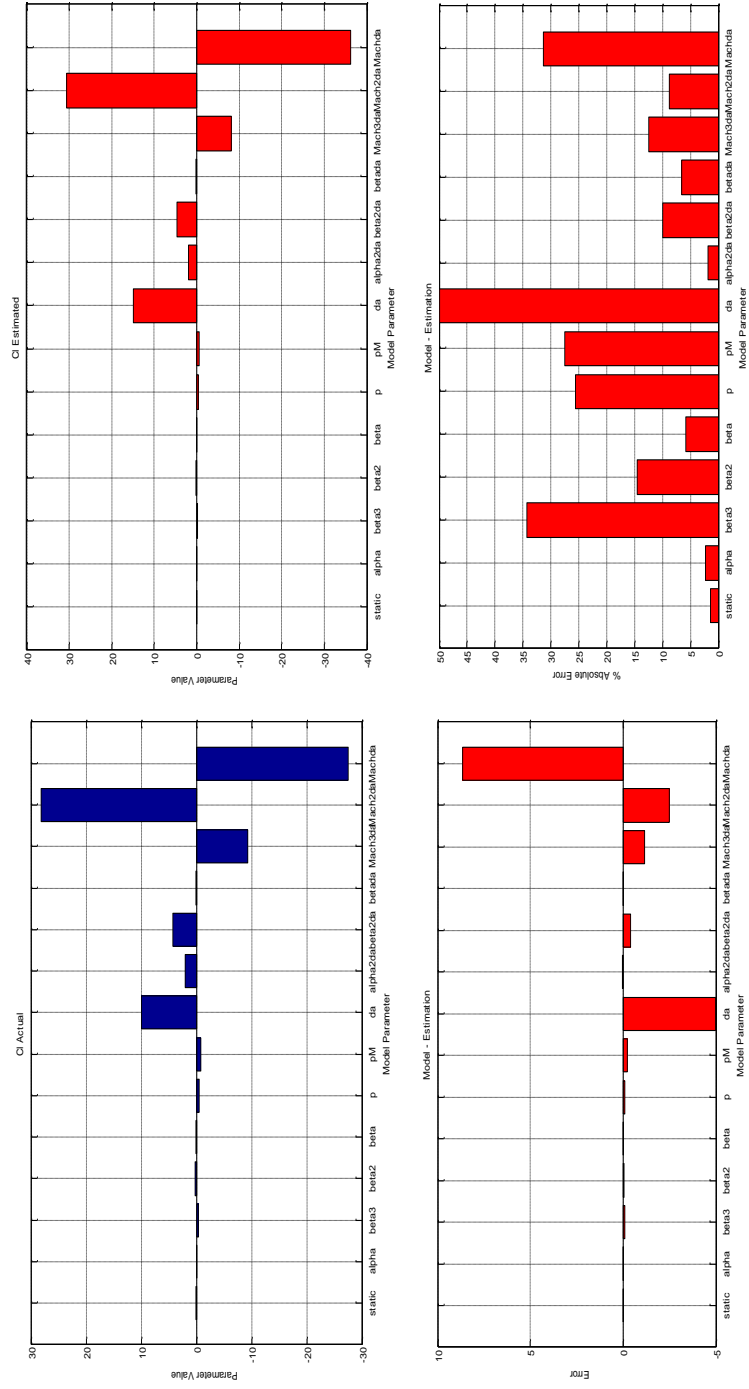


Figure 71. Estimation result for C_j – test case 2

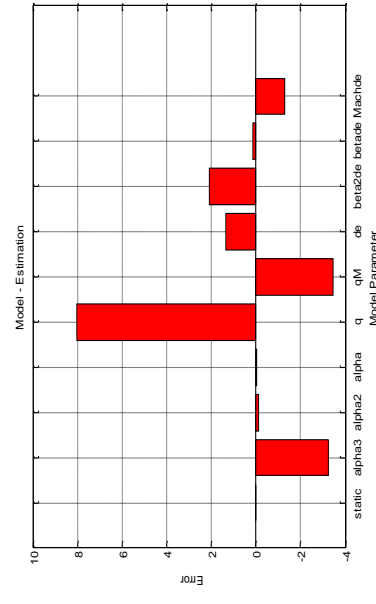
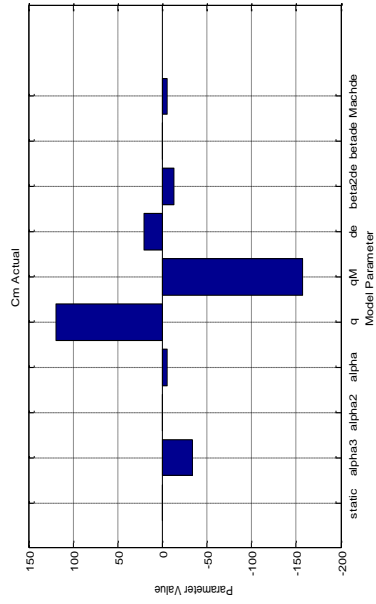
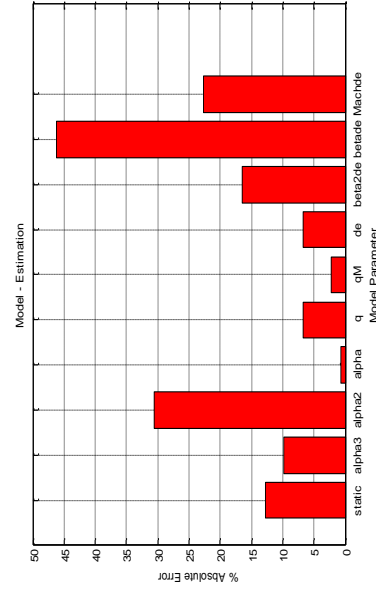
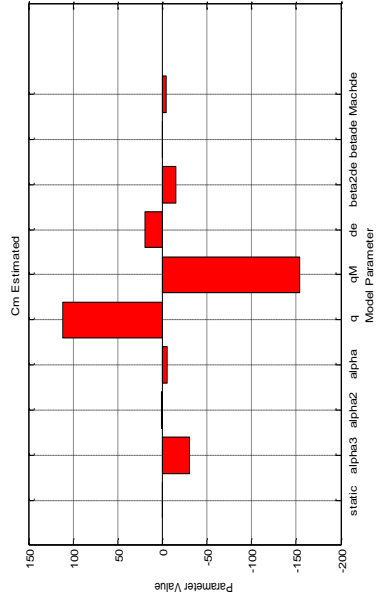


Figure 72. Estimation result for C_m – test case 2

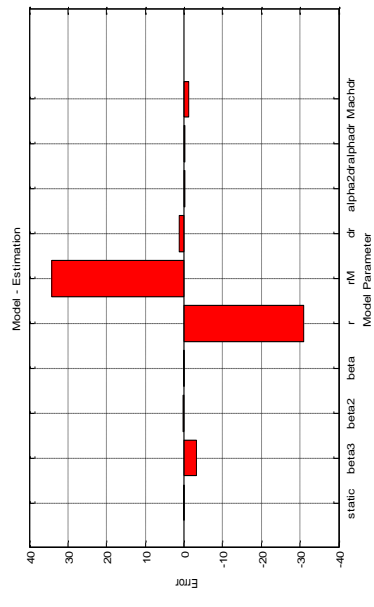
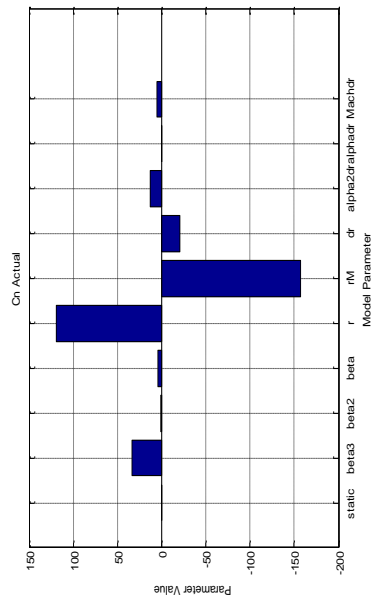
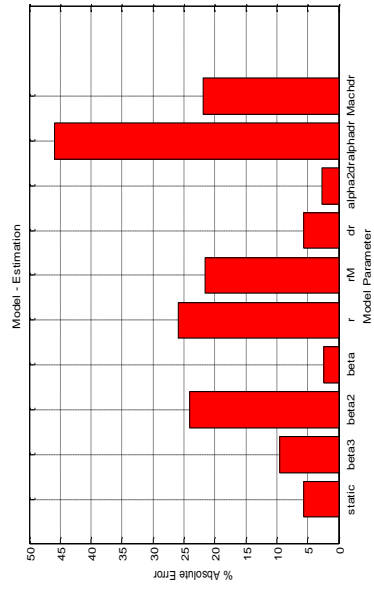
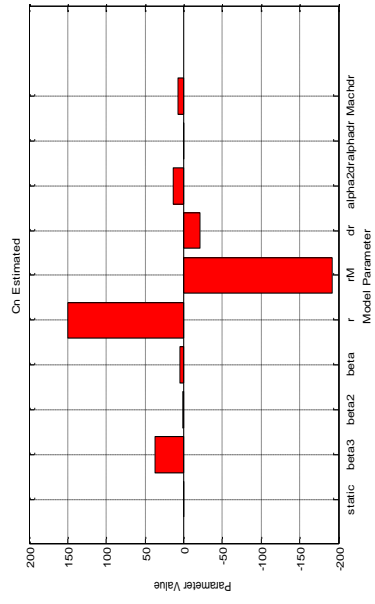


Figure 73. Estimation result for C_n – test case 2

5.2.3 Actual Flight Test Data for Guided FV

The third and final test case for the closed loop parameter estimation method is the actual flight test data of the guided flight vehicle.

In the first attempt to estimate aerodynamic model parameters, the closed loop estimation algorithm was run on a quad core AMD Opteron 128 workstation with 7.83 GB of RAM for about 13 days. The genetic algorithm was terminated with a final cost value of 17.150, which was later reduced to 16.696 by the hybrid run. Following figures show the response of the estimated model with the actual flight test data. The selected cost function included final position penalty and the selected mutation method was the adaptation feasible mutation.

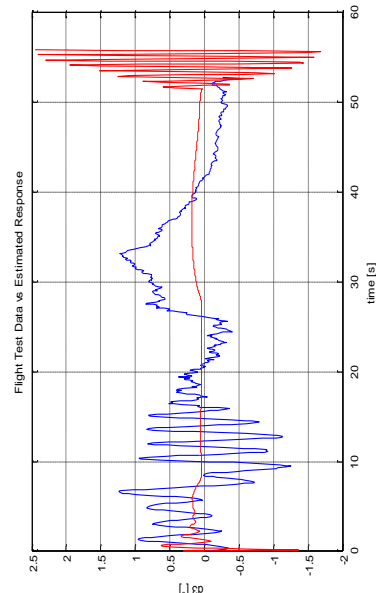
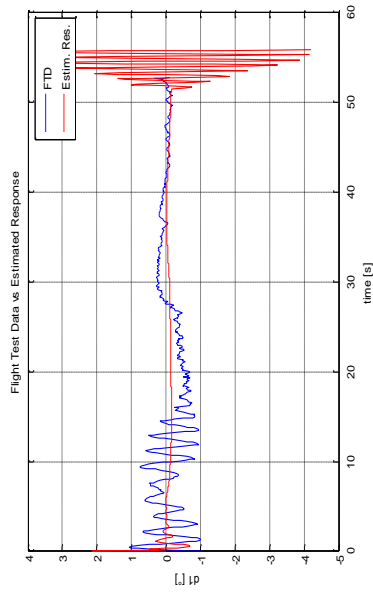
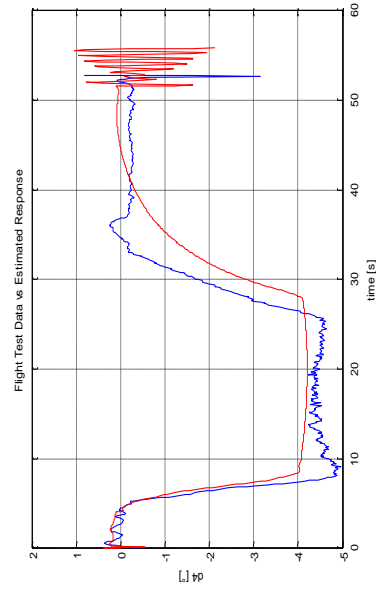
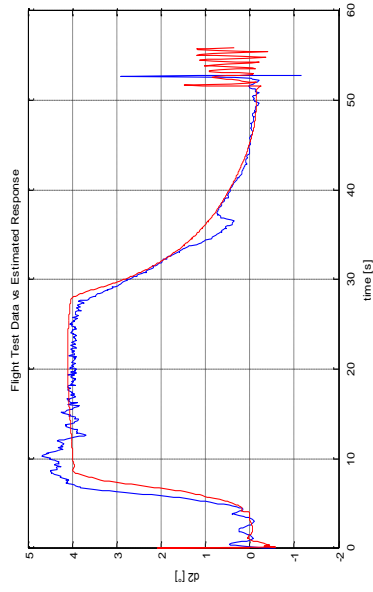


Figure 74. Deflections for test case 3 (attempt 1)

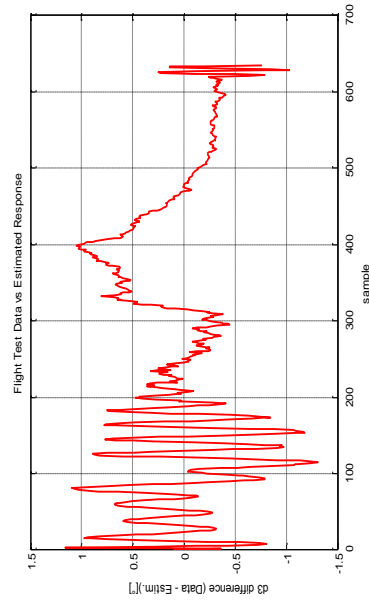
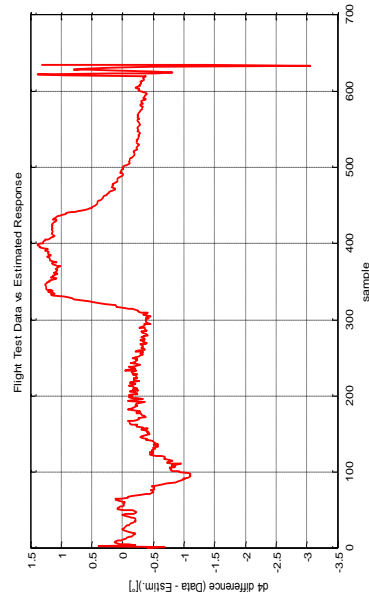
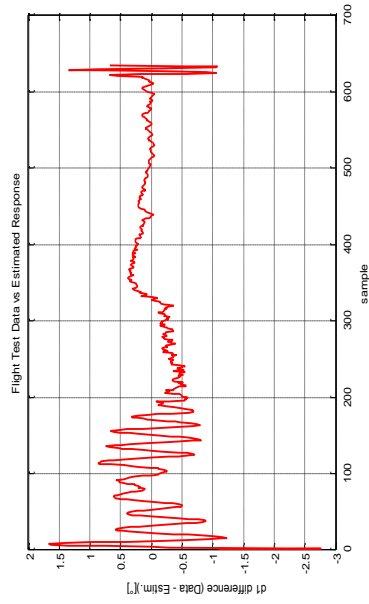
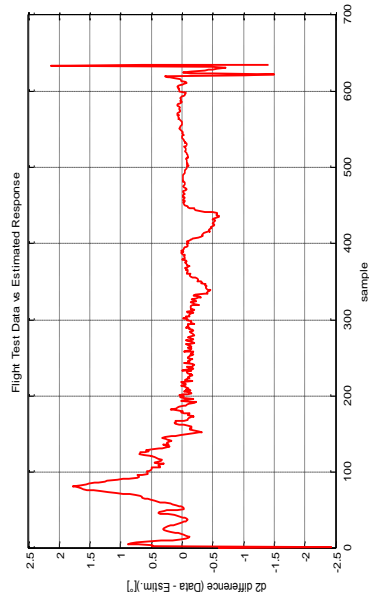


Figure 75. Error in deflections for test case 3 (attempt 1)

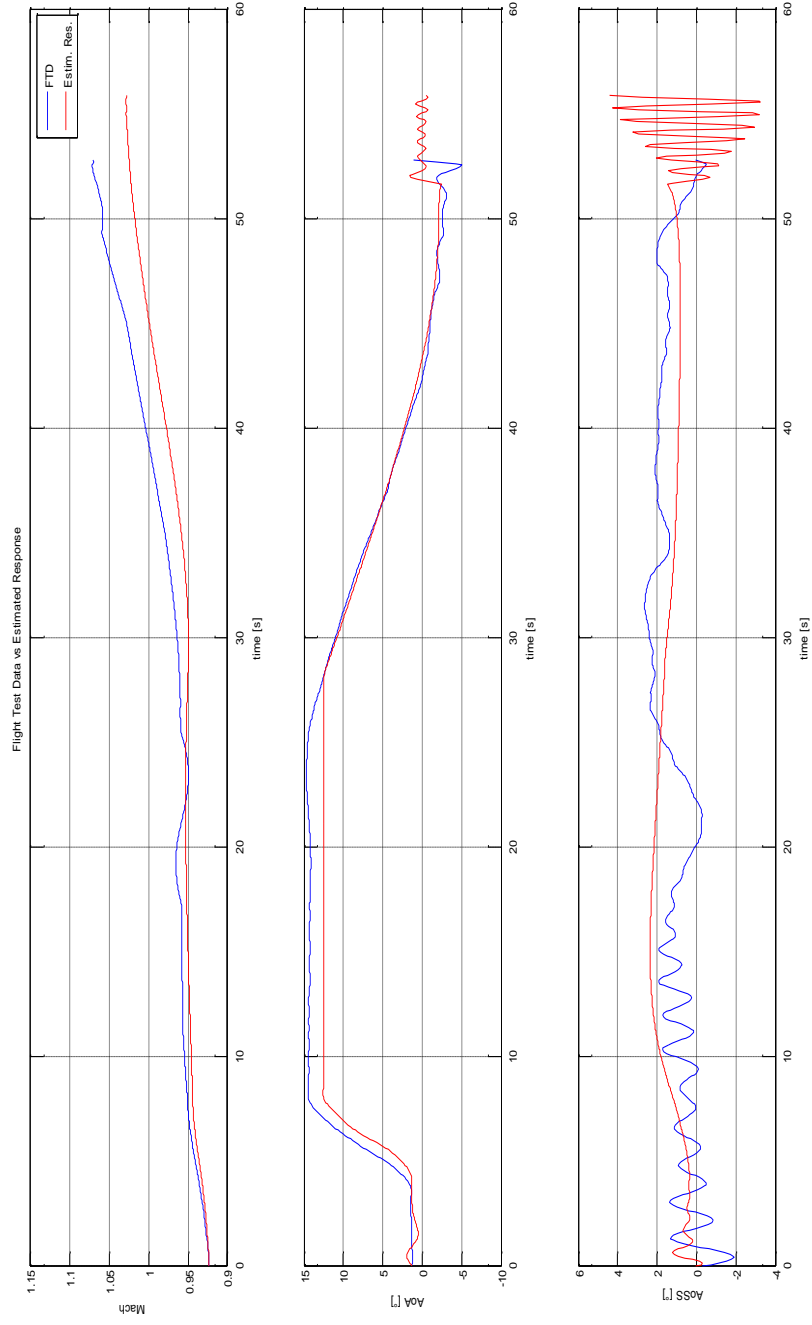


Figure 76. Flight parameters for test case 3 (attempt 1)

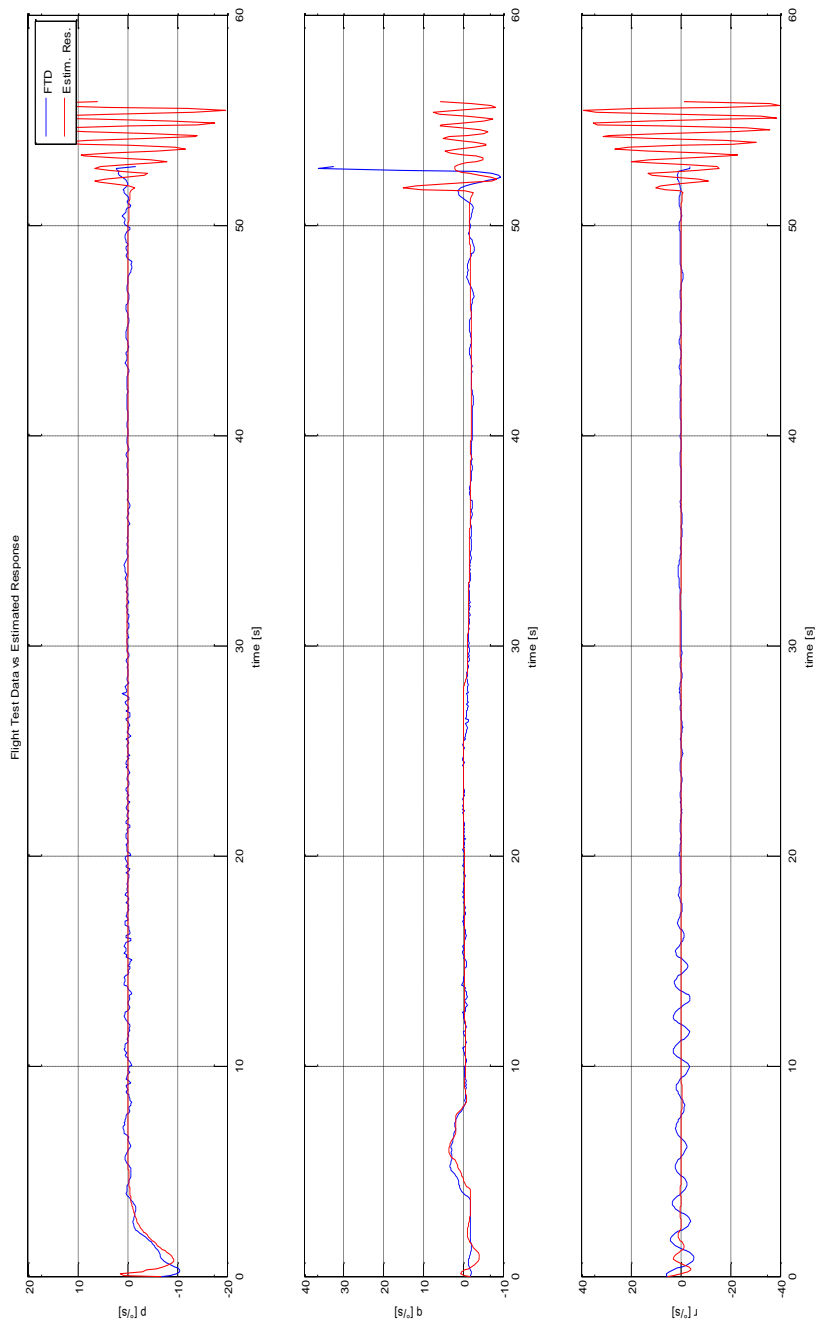


Figure 77. Rates for test case 3 (attempt 1)

The response of the estimated model starts oscillating towards the end of the trajectory. There, the guidance law tries to compensate for the final position error and match the final attitude constraints on the trajectory (such as final dive angle and angle of attack). Thus, the autopilot gives harsh commands to the fins. Since the model response deviates from the actual flight test data, there might be two different explanations for the cause of these oscillations in the model response. First, some oscillations occur for a small portion of the trajectory, that is, it takes the optimization algorithm too long to compensate for these oscillations. The genetic algorithm run was terminated at reaching the 200th generation and the hybrid run was also terminated before reaching the optimal value (at the maximum function evaluation limit). Then, allowing the runs to carry on longer might solve this oscillation problem. Yet, they might also be caused by the model error; if the model is short of representing the some dynamics of the vehicle, these oscillations can occur.

Nevertheless, Figure 78 through Figure 83 show the contribution of individual parameters to the coefficient value during the simulation with the final model parameters: Higher the relative value of the parameter, more dominant the parameter is. As can be seen, some parameters are obviously having less importance on the overall coefficient values (at least for the conditions of the flight test).

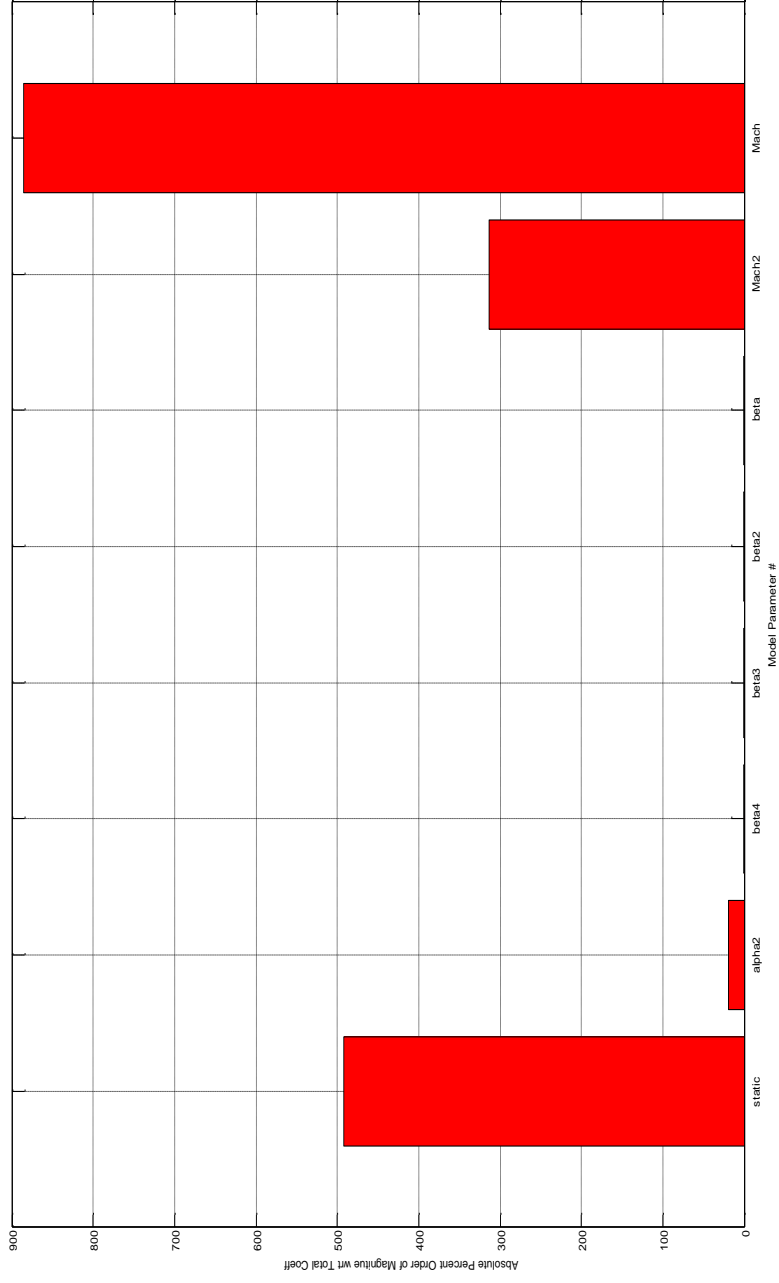


Figure 78. Dominant terms for C_x - test case 3

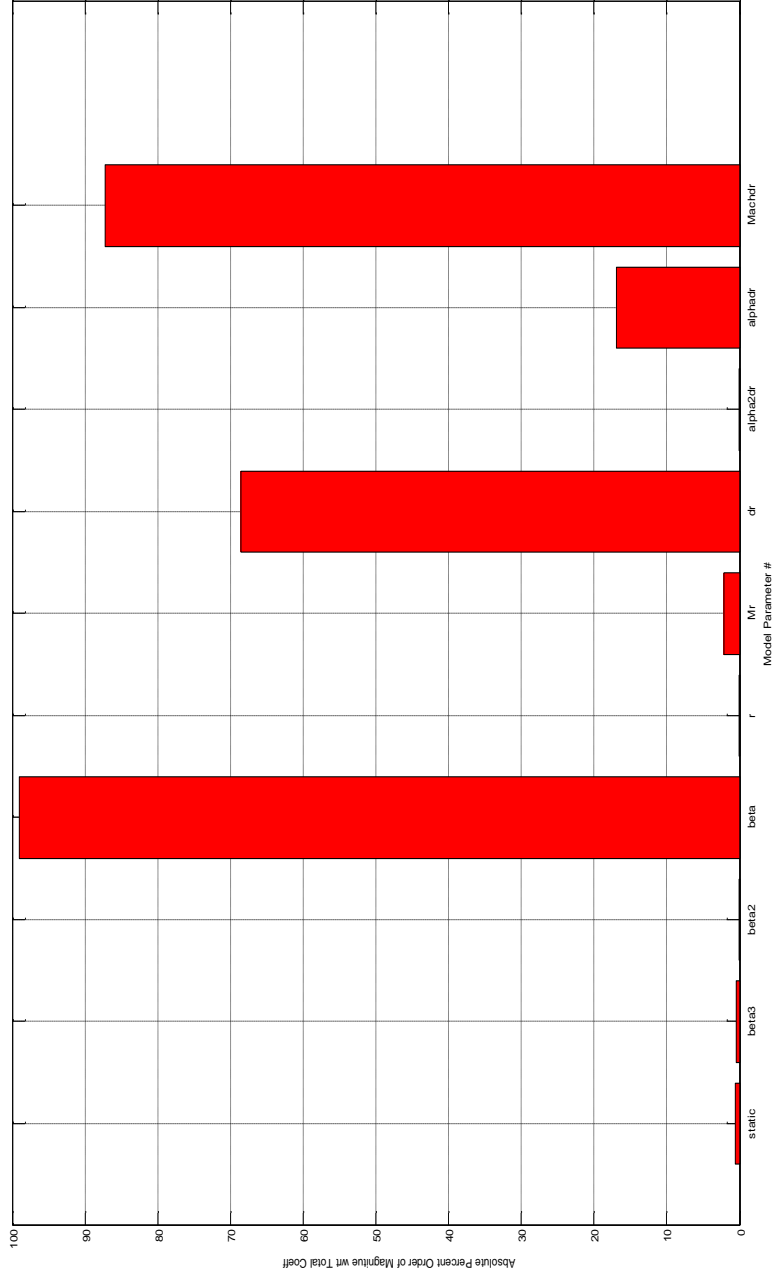


Figure 79. Dominant terms for C_y – test case 3

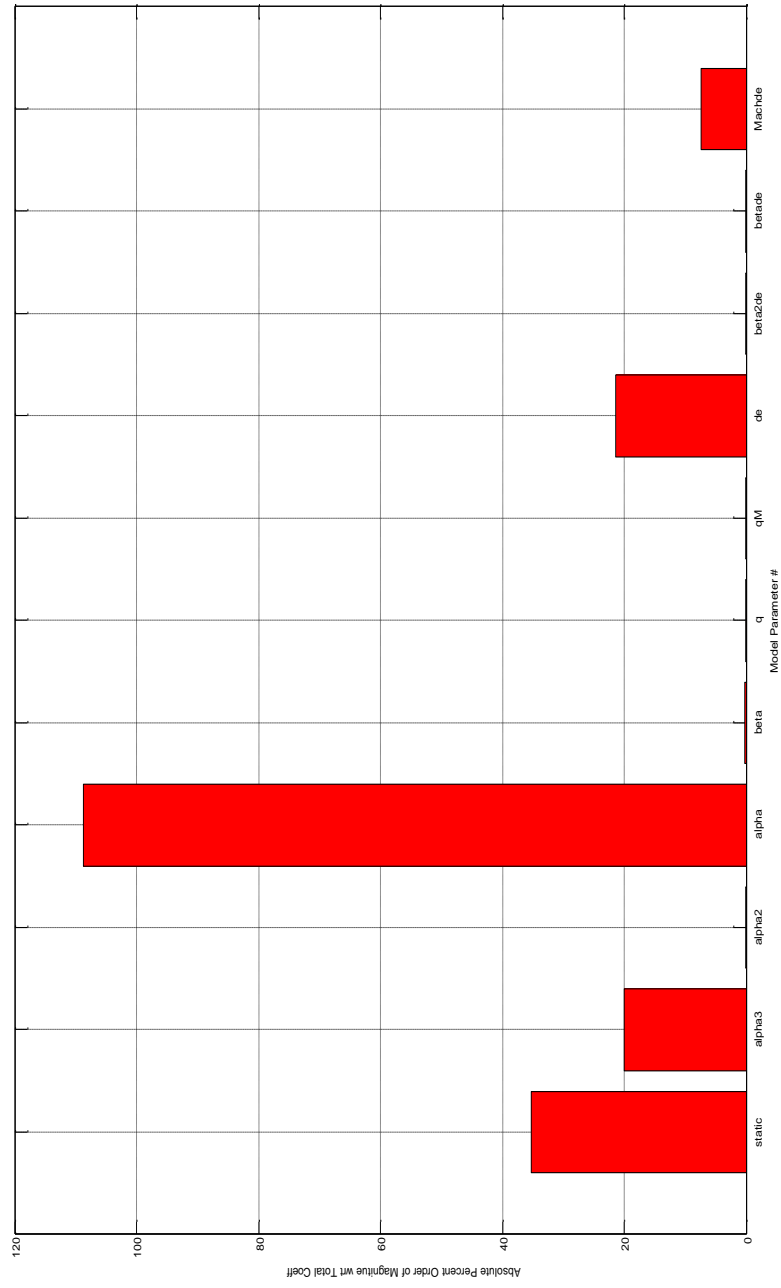


Figure 80. Dominant terms for C_z - test case 3

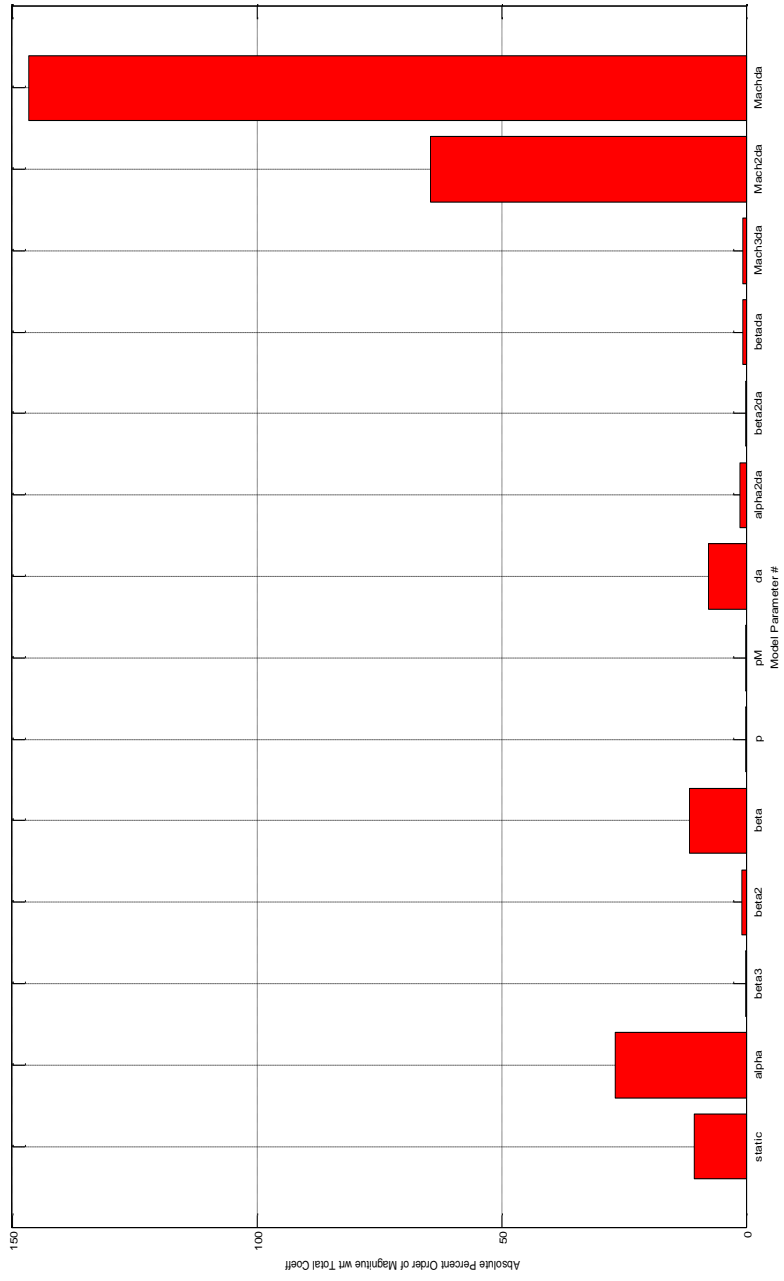


Figure 81. Dominant terms for C_j – test case 3

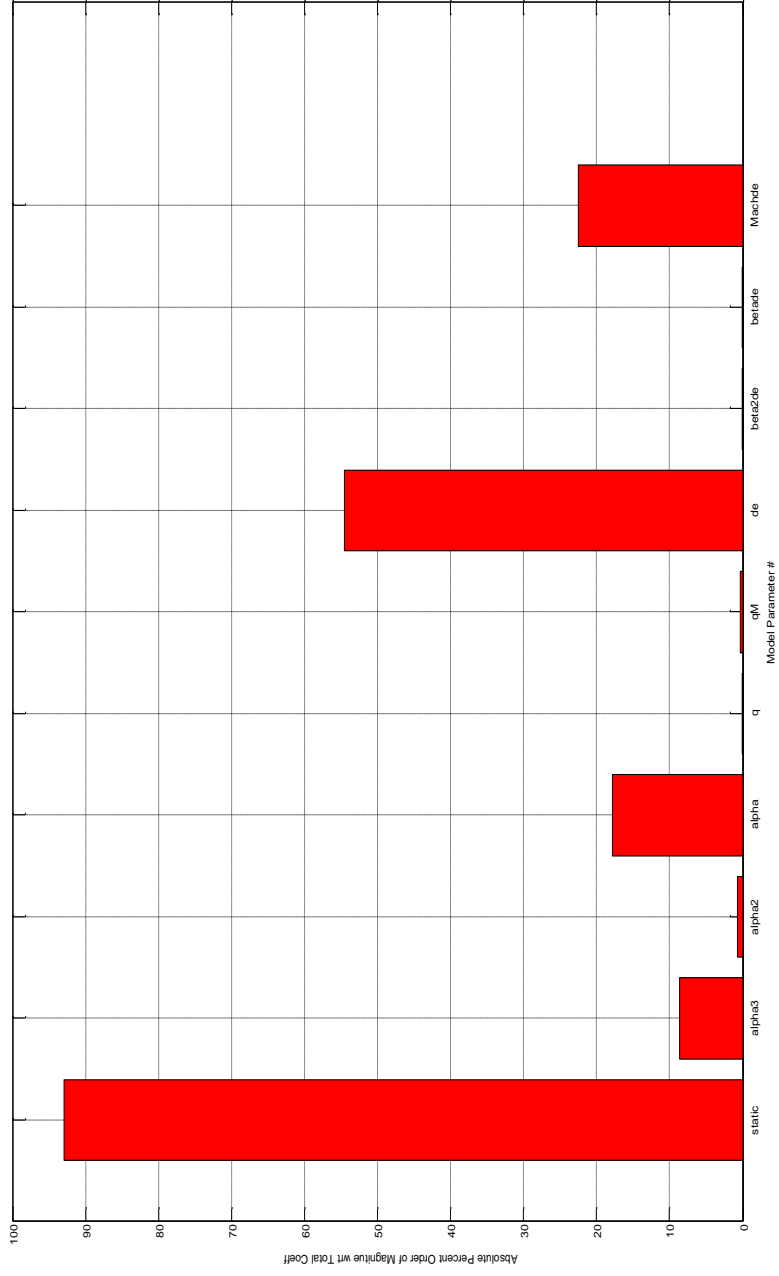


Figure 82. Dominant terms for C_m – test case 3



Figure 83. Dominant terms for C_n – test case 3

This situation suggests that, better parameter estimates can be obtained if the number of parameters to be estimated is reduced so that the parameter estimation algorithm focuses on dominant terms. This is realized by defining an aerodynamic model for which the only dominant parameters are estimated, while the less dominants are fixed at some a priori values. In contrast to 81 parameters of the previous model, this reduced model includes only 34 parameters to be estimated. Table 27 shows the selected parameters for estimation.

Table 27. Selected dominant parameters for attempt 2

Coefficients	C_x	C_y	C_z	C_l	C_m	C_n
Model Parameters	Static Term	Static Term	Static Term	Static Term	Static Term	Static Term
	alpha2	beta3	alpha3	alpha	alpha3	beta3
	Mach2	beta	alpha	da	alpha	beta2
	Mach	dr	beta	alpha2da	de	beta
		alpha2dr	de	Mach3da	beta2de	dr
		Machdr	beta2de	Mach2da	betade	alpha2dr
			Machde	Machda	Machde	Machdr

Once again, the closed loop estimation algorithm was run on a quad core AMD Opteron 128 workstation with 7.83 GB of RAM. This time the results obtain in about 5 days (almost 60% shorter than attempt 1). The genetic algorithm was terminated with a final cost value of 17.090, which later was reduced to 17.030 by the hybrid run. Following figures show the response of the estimated model with the actual flight test data. The selected cost function included final position penalty and the selected mutation

method was the adaptation feasible mutation, the same as attempt 1.

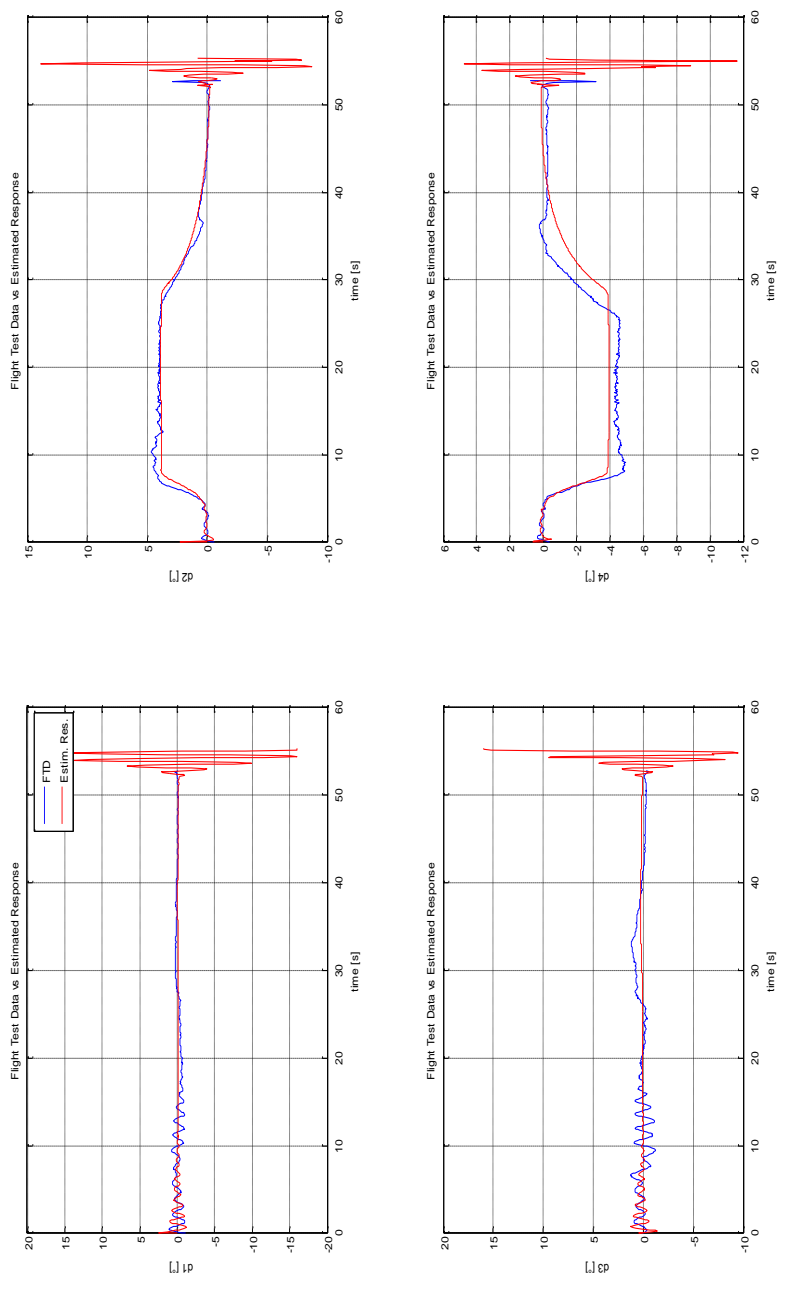


Figure 84. Deflections for test case 3 (attempt 2)

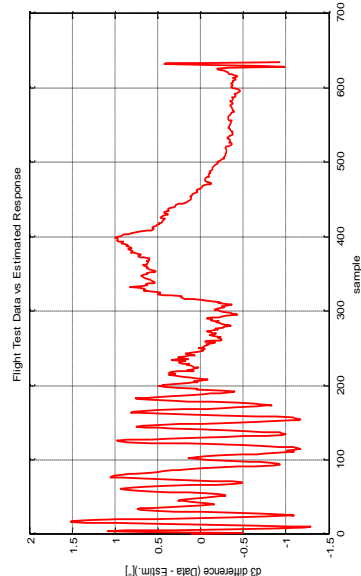
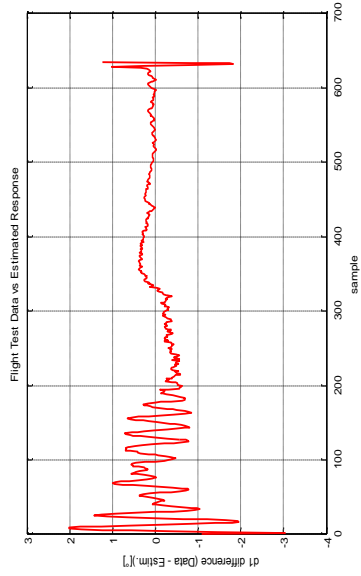
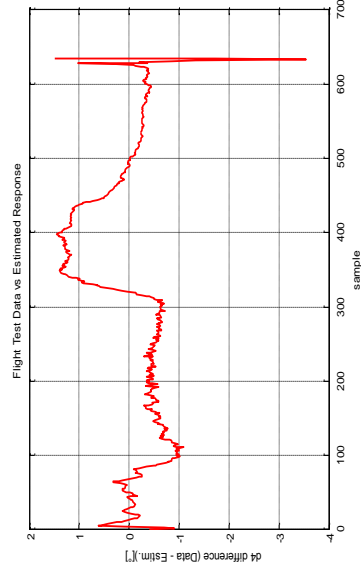
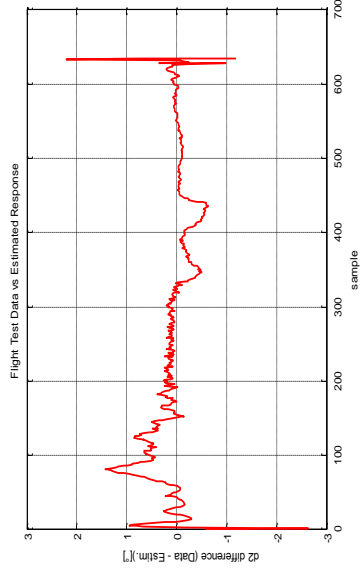


Figure 85. Error in deflections for test case 3 (attempt 2)

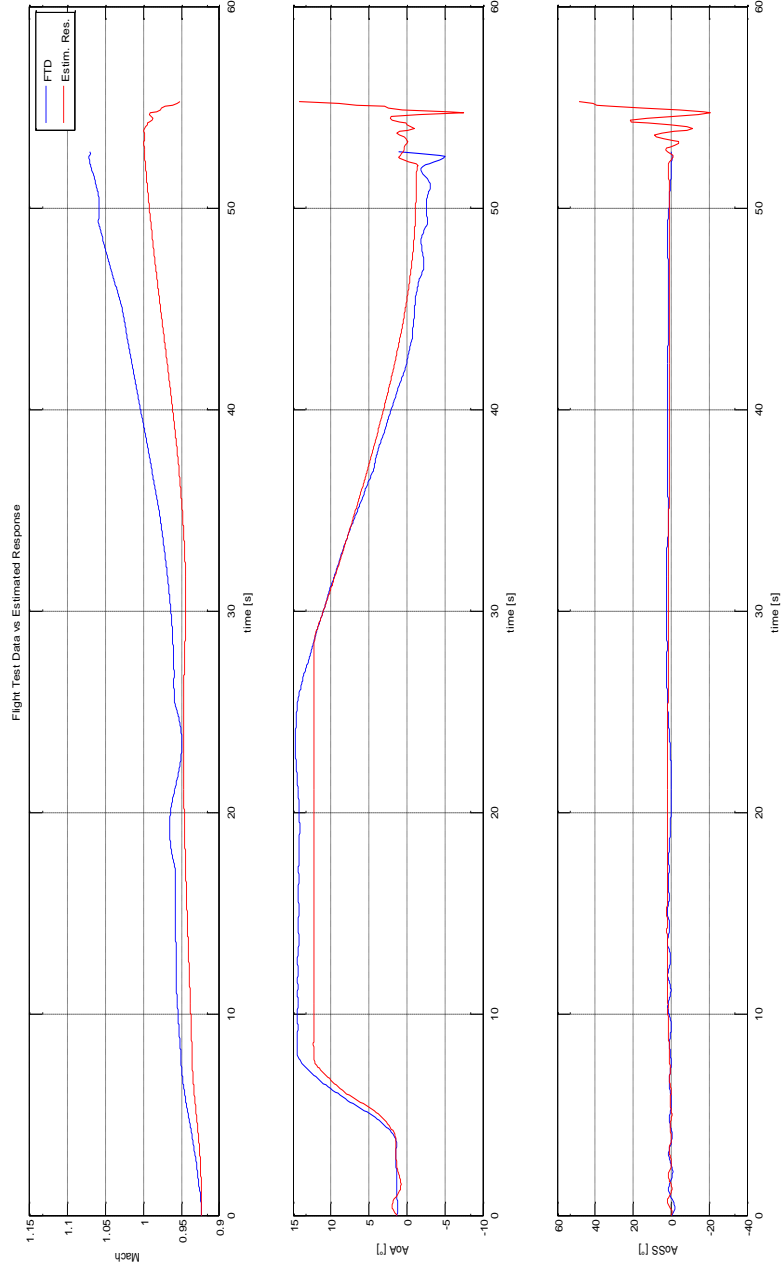


Figure 86. Flight parameters for test case 3 (attempt 2)

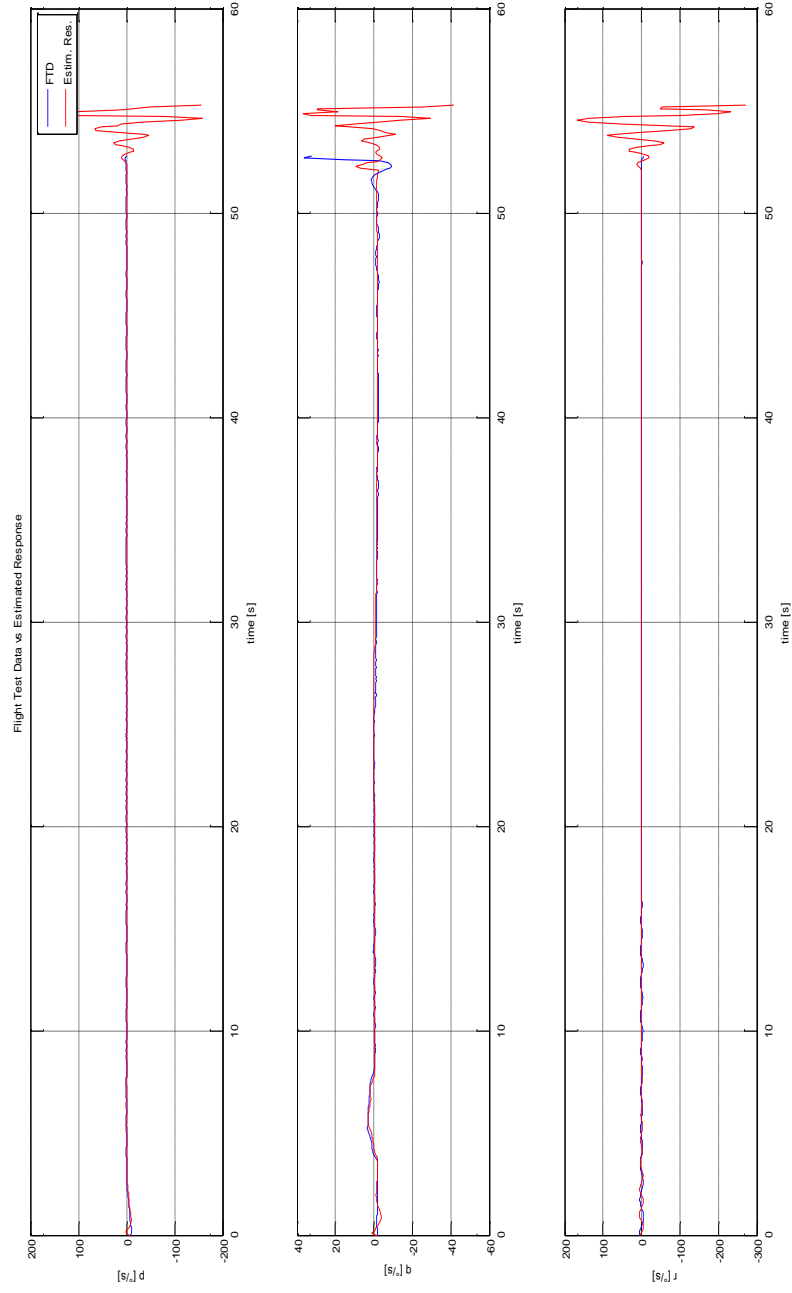


Figure 87. Rates for test case 3 (attempt 2)

When Figure 74 through Figure 77 and Figure 84 through Figure 87 are compared, it is seen that the responses of the both models are close. Table 28 through Table 33 show the estimated parameter values for the dominant terms in each case.

Table 28. Estimated values for dominant parameters C_x

CX	Attempt 1 value	Attempt 2 value	% Difference
Static Term	2.5547	1.7754	30.5
alpha2	-4.5582	-2.1848	52.1
Mach2	1.7396	1.3343	23.3
Mach	-4.7575	-3.6335	23.6

Table 29. Estimated values for dominant parameters C_y

CY	Attempt 1 value	Attempt 2 value	% Difference
Static Term	-0.0011	-0.0012	9.1
beta3	-30.3538	-42.7200	40.7
beta	-7.3629	-7.6874	4.4
dr	3.7774	4.6233	22.4
alpha2dr	-3.0820	-3.4697	12.6
Machdr	-1.6944	-1.5666	7.5

Table 30. Estimated values for dominant parameters C_z

CZ	Attempt 1 value	Attempt 2 value	% Difference
Static Term	0.2986	0.2917	2.3
alpha3	-36.6254	-41.2270	12.6
alpha	-7.6275	-8.2602	8.3
beta	0.1083	0.1073	0.9
de	5.1912	6.9567	34.0
beta2de	-2.9351	-1.6404	44.1
Machde	-1.8991	-2.2301	17.4

Table 31. Estimated values for dominant parameters C_i

CI	Attempt 1 value	Attempt 2 value	% Difference
Static Term	-0.0018	-0.0010	44.4
alpha	-0.0390	-0.0275	29.5
da	12.4932	10.6670	14.6
alpha2da	1.3938	1.1796	15.4
Mach3da	-8.6646	-7.6543	11.7
Mach2da	19.3724	19.3333	0.2
Machda	-21.6548	-21.6370	0.1

Table 32. Estimated values for dominant parameters C_m

Cm	Attempt 1 value	Attempt 2 value	% Difference
Static Term	1.1504	0.9665	16.0
alpha3	-23.3502	-47.2120	102.2
alpha	-1.8269	-2.3939	31.0
de	19.3917	24.1500	24.5
beta2de	-6.5630	-13.5200	106.0
betade	0.4971	0.3486	29.9
Machde	-8.3964	-7.9114	5.8

Table 33. Estimated values for dominant parameters C_n

Cn	Attempt 1 value	Attempt 2 value	% Difference
Static Term	-0.0217	-0.0207	4.6
beta3	33.5934	20.9890	37.5
beta2	0.8333	0.9708	16.5
beta	-0.4474	-0.4139	7.5
dr	-18.9279	-16.9240	10.6
alpha2dr	18.9451	17.7560	6.3
Machdr	2.7988	6.1914	121.2

The percent differences in Table 28 through Table 33 confirm the relation of parameter estimation with parameter dominance: The values for most dominant parameters are estimated with small differences in two different model runs.

CHAPTER 6

DISCUSSION, CONCLUSION AND FUTURE WORK

This study aimed to devise a methodology that can be used for the identification of aerodynamic models and estimation of parameters for different types of autonomous flight vehicles using actual flight test data.

To obtain an adequate aerodynamic model, a stepwise regression method is utilized. The method is based on selecting relevant parameters for the aerodynamic model based on their correlations with the aerodynamic behavior of the flight vehicle under consideration. The aerodynamic behavior of the flight vehicle is gathered from the inverse solution of six degrees of freedom force and moment equations using with actual flight conditions. If an existing a priori aerodynamic model is provided, then the information contained in that model is used and the aerodynamic behavior that is not foreseen by the a priori model is identified.

The objective of determining the model structure with a minimal intervention from the user is fulfilled by the utilization of

automated regressor generation algorithms and imposed run and stopping rules. In fact, practical considerations for the application of model structure determination methods to autonomous vehicles are not well defined in the literature and this doctoral study serves as a guide to these considerations.

Aside from the model structure determination, a closed loop optimization approach is also proposed for aerodynamic parameter estimation utilizing genetic algorithm as the kernel. Practical considerations and recommendations for the closed loop aerodynamic parameter estimation approach are given for autonomous flight vehicles.

Both methods are tested on different test cases of simulated and actual flight test data. The initial application of the stepwise regression/equation error method to the simulated flight test data of a guided flight vehicle demonstrated the inability of the identification algorithms to converge to relevant and adequate models, if low – quality flight test data, i.e., flight test data which lacks necessary and sufficient information about the dynamics of the vehicle, is supplied. However, when - even non-optimal - maneuver designs are implemented in simulations, the algorithms converged successfully.

This study also focused on the flight test data processing. Considerations on conditioning the actual flight test data for identification include decimating a higher sample rate data to save valuable time, filtering out noise using Global Fourier Smoother, and trimming data from different test runs into one to obtain a global aerodynamic model.

When the model identification algorithms are applied to the conditioned actual flight test data of the guided flight vehicle some reasonable models are obtained for all coefficients, except the axial force coefficient, even for a flight test data which was not designed for system identification purposes.

For the closed loop aerodynamic estimation algorithm, the trials with simulated flight test data once again demonstrated that the success of identification and estimation heavily relies on the content of the flight test data supplied. When the simulated data with no specific maneuvers is supplied, some of the parameters are estimated with large errors. However, adding even non-optimal maneuvers improved the parameter estimates.

When the closed loop estimation algorithm is tested on an actual flight test data of the guided vehicle, it is seen that the success of estimation is lower when compared to the simulated test data. Trying to estimate the parameters of a reduced model yielded

acceptable results and also speeded up the process since the method takes quite long to converge, even on fast computers. Unfortunately, the only flight test data in hand (for a guided flight vehicle) was not designed for system identification/parameter estimation purposes, so it was not possible to test the methods on high quality data.

During the course of this study, three conference papers have been published. Two of them, [12], [13], explain the practical considerations in flight test data processing of autonomous flight vehicles and aerodynamic model structure determination. The last one gives the results of closed loop aerodynamic parameter estimation using genetic algorithm for simulated flight test data of an autonomous flight vehicle, [14].

As follow-on studies, an effort should be directed on the validation of identified models and estimated parameters, trials with different optimization methods and comparisons of results with different estimation methods.

Validation is an important subject, since the results of the identification and estimation runs must be validated before they can be implemented on the aerodynamic models of actual flying vehicles.

Although the genetic algorithm has some advantages over the conventional gradient based optimization algorithms, the convergence takes quite so long for optimization using the flight test data. During this study, some run times up to 1 month were encountered, which are not acceptable during an actual flight test program. So, the utilization of different optimization algorithms can be tried to shorten the convergence time.

Another future work should be the comparison of the results of the closed loop aerodynamic parameter estimation method with other popular methods such as the output error method. Yet, to do this a high quality flight test data is required.

One of the most important results of this study is the understanding the importance of the quality of the flight test data. Any method in practice cannot succeed, unless a flight test data with sufficient information about the flight vehicle is supplied. This, in fact, shows that the system identification and parameter estimation starts before the actual flight test, with the design of maneuvers. The maneuver design was not in the scope of this study, however, it is shown that maneuver design is crucial for identification and estimation. Thus, it is recommended that the future work should focus on maneuver design and optimization, since:

“If it is not in the data, it cannot be estimated.”, [19].

REFERENCES

- [1] Hamel, P.G., Jategaonkar, R.V., "Evolution of Flight Vehicle System Identification", *Journal of Aircraft*, Vol. 33, No. 1, pp.9 – 28, January – February 1996.
- [2] Morelli, E.A., Klein, V., "Application of System Identification to Aircraft at NASA Langley Research Center", *Journal of Aircraft*, Vol. 42, No. 1, pp. 12 – 25, January – February 2005.
- [3] Aksteter, J.W., Parks, E.K., Bach Jr., R.E., "Parameter Identification and Modeling of Longitudinal Aerodynamics", *Journal of Aircraft*, Vol. 32, No.4, pp.726 – 731, July – August 1995.
- [4] Özger, E., "Aerodynamic Model Validation of Eurofighter Aircraft", AIAA-2007-6718, AIAA Atmospheric Flight Mechanics Conference and Exhibit, August 20 – 23, 2007, Hilton Head, SC, USA.
- [5] Paris, A.C., Alaverdi, O., "Nonlinear Aerodynamic Model Extraction from Flight Test Data for the S-3B Viking", *Journal of Aircraft*, Vol. 42, No. 1, pp. 26 – 32, January – February 2005.
- [6] Song, C., Jeon, I., Lee, S., Kwon, S., "Estimation of the Aerodynamic Parameters for a Flight Vehicle from Flight Test", AIAA-95-3497-CP, AIAA Atmospheric Flight Mechanics Conference, August 7 – 10, 1995, Baltimore, MD, USA.
- [7] Anderson, M.B., McCurdy, R.E., "Weapon Drag Coefficient Determination Using Genetic Algorithm", AIAA-94-3468-CP,

- AIAA Atmospheric Flight Mechanics Conference, August 1 – 3, 1994, Scottsdale, AZ, USA.
- [8] Anderson M.B., Lawrence, W.R., "Launch Conditions and Aerodynamic Data Extraction by an Elitist Pareto Genetic Algorithm", AIAA-96-3361-CP, AIAA Atmospheric Flight Mechanics Conference, July 29 – 31, 1996, San Diego, CA, USA.
- [9] Anderson, M.B., Lawrence W.R., Gebert G.A., "Using an Elitist Pareto Genetic Algorithm for Aerodynamic Data Extraction", AIAA-96-0514, Aerospace Sciences Meeting and Exhibit, January 15 – 18, 1996, Reno, NV, USA.
- [10] Gage, P.J., Stuckey, R.A., Drobik, J.S., "A Genetic Approach to Modeling Flight Dynamic Characteristics", AIAA-97-0536, Aerospace Sciences and Exhibit, January 6 – 9, 1997, Reno, NV, USA.
- [11] Mohammadi, A., Massoumnia, M.A., "Missile Aerodynamic Identification Using Mixed EKF and EBM", AIAA-2000-4288, AIAA Modeling and Simulation Technologies Conference, August 14 – 17, 2000, Denver, CO, USA.
- [12] Kutluay, Ü., Mahmutyazıcıoğlu G., Platin, B.E., "An Application of Equation Error Method to Aerodynamic Model Identification and Parameter Estimation of a Gliding Flight Vehicle", AIAA – 2009-5724, AIAA Atmospheric Flight Mechanics Conference and Exhibit, August 10 – 13, 2009, Chicago, IL, USA.
- [13] Kutluay, Ü., Mahmutyazıcıoğlu G., Platin, B.E., "An Application Of Equation Error Method To Aerodynamic Model Identification And Parameter Estimation For Gliding Flight",

AIAC-2009-050, Ankara International Aerospace Conference, August 17 – 19, 2009, Ankara, TURKEY.

- [14] Kutluay, Ü., Mahmutyazicioğlu G., Platin, B.E., "Closed Loop Aerodynamic Parameter Estimation For Autonomous Flight Vehicles Using Genetic Algorithm", AIAC – 2011 - 128, Ankara International Aerospace Conference, September 14 – 16 2011, Ankara, TURKEY.
- [15] Tobak, M., Schiff, L.B., "Aerodynamic Mathematical Modeling – Basic Concepts", AGARD LS – 114.
- [16] Klein, V., Morelli, E.A., "Aircraft System Identification: Theory and Practice", AIAA Education Series, AIAA, 2006
- [17] Phillips, Warren H., "Mechanics of Flight", John Wiley & Sons, 2004.
- [18] Klein, V., Batterson, J.G., "Determination of Airplane Model Structure from Flight Data Using Splines and Stepwise Regression", NASA TP 2126, NASA 1983.
- [19] Jategaonkar, R.V., "Flight Vehicle System Identification: A Time Domain Methodology", Progress in Astronautics and Aeronautics Volume 216, AIAA, 2006.
- [20] Morelli, E.A., Ward, D.G., "Automated Simulation Updates Based on Flight Data", AIAA 2007-6714, AIAA Atmospheric Flight Mechanics Conference and Exhibit, August 20 – 23, 2007, Hilton Head, SC, USA.
- [21] Morelli, E.A., "Estimating Noise Characteristics From Flight Test Data Using Optimal Fourier Smoothing", Journal of Aircraft, Vol.32, No.4, pp. 689 – 695, July – August 1995.
- [22] Knapp, T.B., Matts, J.A., "METGM Interpolation Methodology for the NATO Armaments Ballistic Kernel", US Army Tank – Automotive and Armament Command, Armament Research,

Development and Engineering Center, Fire Support Armaments Center, Fire Control and Software Engineering Division, Firing Tables and Ballistics Information Report No. 67, June 2002.

- [23] Whorton, M.S., "Closed Loop System Identification with Genetic Algorithms", AIAA-2004-4887, AIAA Guidance, Navigation and Control Conference and Exhibit, August 16 – 19, 2004, Providence, RI, USA.
- [24] Whorton, M.S., "Closed Loop System Identification with Genetic Algorithms", Journal of Aerospace Computing, Information and Communication, Vol. 5, pp. 161- 173, June 2008.
- [25] Van den Hof, P., "Closed Loop Issues in System Identification", Annual Reviews in Control, Vol. 22, pp.173 – 186, 1998.
- [26] Forssell, U., Ljung, L., "Closed-loop Identification Revisited", Automatica, Vol. 35, Issue 7, pp. 1215 – 1241, July 1999.
- [27] Hjalmarsson, H., et. Al., "For Model-based Control Design, Closed-loop Identification Gives Better Performance", Automatica, Vol. 32, Issue 12, pp. 1659 – 1673, Dec 1996.
- [28] Landau, I.D., Karimi, A., "An Output Error Recursive Algorithm for Unbiased Identification in Closed Loop", Automatica, Vol. 33, Issue 5, pp. 933 – 938, May 1997.
- [29] Wang, L., Cluett, W.R., "System Identification Based on Closed Loop Step Response Data", Control Theory and Applications, Vo. 141, Issue 2, IEEE Proceedings, Mar, 1994.
- [30] Global Optimization Toolbox 3 User Guide, Mathworks, 2011
- [31] Optimization Toolbox 6 User Guide, Mathworks, 2011.

CURRICULUM VITAE

Ümit KUTLUAY

Contact Information:

Work Address: TÜBİTAK – SAGE, Pk. 16, 06261,
Mamak/ANKARA/TURKEY

Telephone: +90 312 590 91 86

E-mail: ukutluay@gmail.com

Nationality: Turkish

Academic Background:

PhD in Mechanical Engineering: METU, 2011

MSc. in Mechanical Engineering: METU, 2004

BSc. in Aeronautical Engineering: METU, 2001

Professional Background:

Chief Research Engineer: TÜBİTAK – SAGE Flight Mechanics
Division, 2009 to date.

Senior Research Engineer: TÜBİTAK – SAGE Flight Mechanics Division, 2005 – 2009

Research Engineer: TÜBİTAK – SAGE Flight Mechanics Division, 2002 – 2005

Papers and Publications:

1. Kutluay, Ü., Mahmutyazıcıoğlu G., Platin, B.E., “Closed Loop Aerodynamic Parameter Estimation For Autonomous Flight Vehicles Using Genetic Algorithm”, AIAC – 2011 - 128, Ankara International Aerospace Conference, September 14 – 16, 2011, Ankara, TURKEY
2. Kutluay, Ü., Mahmutyazıcıoğlu G., Platin, B.E., “An Application Of Equation Error Method to Aerodynamic Model Identification And Parameter Estimation For Gliding Flight”, AIAC-2009-050, Ankara International Aerospace Conference, August 17 – 19, 2009, Ankara, TURKEY.
3. Kutluay, Ü., Mahmutyazıcıoğlu G., Platin, B.E., “An Application of Equation Error Method to Aerodynamic Model Identification and Parameter Estimation of a Gliding Flight Vehicle”, AIAA – 2009-5724, AIAA Atmospheric Flight Mechanics Conference and Exhibit, August 10 – 13, 2009, Chicago, IL, USA.
4. Kutluay, Ü., Karbancıoğlu, İ.M., Hasanoğlu, M.S., “External Geometry Optimization with Flight Mechanics Constraints Using Response Surfaces”, AIAA – 2008 – 6886, AIAA

Atmospheric Flight Mechanics Conference and Exhibit,
August 18 – 21, 2008, Honolulu, HI, USA.

5. Yazıcıoğlu Y., Martin B.A., Navarro-Castillo K., Kutluay Ü., Royston T.J., "Transverse Vibration of Pre-stressed Beams: An Experimental Technique for the Determination of Dynamic Viscoelastic Material Properties of Tissue Mimicking Materials", Acoustics 08, June 29 – July 4, 2008, Paris, FRANCE.
6. Kutluay Ü., Kafdağlı, K.E., "Evaluating Flight Performance During Conceptual Design", AIAC – 2007 – 074, Ankara International Aerospace Conference, September 10 – 12, 2007, Ankara, TURKEY.
7. Aytar Ortaç, S., Durak, U., Kutluay, Ü., Küçük, K., Candan, C., "NABK Based Next Generation Ballistic Table Toolkit", Poster Presentation, 23rd International Symposium on Ballistics, April 16 – 20, 2007, Taragona, SPAIN.
8. Aytar Ortaç, S., Durak U., Kutluay Ü., Küçük K., Candan C., "Implementation of Next Generation Ballistic Solver in Different Applications", SAVTEK 2006, June 29 – 30, 2006, Ankara, TURKEY.
9. Karbancıoğlu, İ.M., Katırcı, A., Kutluay, Ü., Kafdağlı, K.E., Ataç, S., "An Application of Photogrammetric Methods for the Analysis of Safe Separation", SAVTEK 2006, June 29 – 30, 2006, Ankara, TURKEY.

10. Kutluay Ü., "Design Scaling of Aeroballistic Range Models", M.Sc. Thesis, METU, 2004.
11. Kutluay, Ü., Aytar Ortaç, S., "Design Optimization for Aeroballistic Range Models of a Low Drag Aircraft Bomb", 55th Aeroballistic Range Association Meeting, September 27 – October 1, 2004, Freiburg, GERMANY.